Alma Mater Studiorum – Università di Bologna
Dipartimento di Medicina Specialistica, Diagnostica e Sperimentale
Dottorato di Ricerca in Oncologia, Ematologia e Patologia
Coordinatore Prof. Pier-Luigi Lollini
XXXI Ciclo

Settore Scientifico Disciplinare: MED/04 - Patologia Generale
Settore Concorsuale: 06/A2 – Patologia Generale e Patologia Clinica

Preclinical Development of novel therapeutic approaches in models resistant to targeted therapies in HER2-positive mammary breast cancer

Presentata da:
Dott.ssa Veronica Giusti

Supervisore:
Char.mo Prof. Pier-Luigi Lollini

Esame finale anno 2019

Index

Abstract

HER2 enriched mammary breast cancer represents 15-25% of mammary carcinomas and is associated to increased aggressiveness and worse prognosis. Advent of targeted therapies against HER2 has improved 5-year survival up to 75%, nevertheless receptor discordance, which is observed in 10.8% of metastasis, as well as resistance to targeted therapies render it a still challenging disease.

On the one hand, taking advange of a recently estabilished murine model of spontaneous loss of HER2 expression, we sought to understand the underlying mechanism, to evaluate role of trastuzumab and to identify identify druggable targets in HER2-negative metastasis or relapses of HER2-positive tumors. The study of transcriptome of cell lines with different HER2 expression has permitted us to identify pathways related to the modulation of this more malignant phenotype, which appeared to be promoted by trastuzumab. Some indications emerged for inhibition of PDGFR-B by sunitinib in tumours which have lost HER2 expression.

On the other hand, a recently established collection of patient derived xenografts (PDX) was used to obtain models of progression where to evaluate the effect of neratinib, a pan-HER tyrosine kinase inhibitor. No abrupt loss of HER2 expression was registered in these models. Collectively, our data, obtained in ER-/PR- HER2+ PDX, strongly indicate a great and long-lasting efficacy of neratinib even in trastuzumab-resistance and after progression and call for further evaluation of neratinib in advanced clinical settings. In our PDX diagnosed as luminal B expressing HER2 (score 2+), neratinib alone had no effect but synergized with tamoxifen and their combination tended to confer a little survival benefit *in vivo*, thus underscoring the possible relevance of dual blockade in tumors expressing both hormone receptors and HER2.

Introduction

Breast cancer is estimated to be the second leading tumour diagnosed world-wide for both sexes combined, with more than $2x10^6$ new cases world-wide (11.6% of newly diagnosed cancer). Worldwide, breast cancer is the most commonly diagnosed female cancer and about 2.1 million newly diagnosed breast cancer cases have been estimated for 2018, accounting for almost 1 in 4 cancer cases among women. Breast cancer is also the leading cause of cancer death in more than 100 countries (Bray et al., 2018). Over the past decades, breast cancer incidence has remained fairly stable, whereas mortality has dropped of 38% thanks to early diagnosis and improvements in therapy. Indeed, most breast cancer are local (>60%) or regional (>30%) at diagnosis, thanks to screening programs, and 5-year survival rates has been 80-90% in 2006-2012 (Picture 1) (Siegel et al., 2017). In Italy, breast cancer is the most frequently newly diagnosed cancer in women of any age as well (29%), with 52800 estimated new cases in 2018. Breast cancer represents the first oncological cause of death among women of all ages. 5- and 10-years survival both exceed 80% (I numeri del cancro in Italia, 2018).

Breast cancer is hence a vast clinical problem as it pertains to a big cut of female population all over the world. Breast cancer, though, is not a single entity but a multitude of diseases and different subtypes with extremely different molecular characteristics, response to therapies and prognosis (Yersal & Barutca, 2014).

Estimated New Cases

	Males				Females	
Prostate	164,690	19%		Breast	266,120	30%
Lung & bronchus	121,680	14%		Lung & bronchus	112,350	13%
Colon & rectum	75,610	9%		Colon & rectum	64,640	7%
Urinary bladder	62,380	7%		Uterine corpus	63,230	7%
Melanoma of the skin	55,150	6%		Thyroid	40,900	5%
Kidney & renal pelvis	42,680	5%		Melanoma of the skin	36,120	4%
Non-Hodgkin lymphoma	41,730	5%		Non-Hodgkin lymphoma	32,950	4%
Oral cavity & pharynx	37,160	4%		Pancreas	26,240	3%
Leukemia	35,030	4%		Leukemia	25,270	3%
Liver & intrahepatic bile duct	30,610	4%		Kidney & renal pelvis	22,660	3%
All Sites	856,370	100%		All Sites	878,980	100%

Estimated Deaths

	Males				Females	
Lung & bronchus	83,550	26%		Lung & bronchus	70,500	25%
Prostate	29,430	9%		Breast	40,920	14%
Colon & rectum	27,390	8%		Colon & rectum	23,240	8%
Pancreas	23,020	7%		Pancreas	21,310	7%
Liver & intrahepatic bile duct	20,540	6%		Ovary	14,070	5%
Leukemia	14,270	4%		Uterine corpus	11,350	4%
Esophagus	12,850	4%		Leukemia	10,100	4%
Urinary bladder	12,520	4%		Liver & intrahepatic bile duct	9,660	3%
Non-Hodgkin lymphoma	11,510	4%		Non-Hodgkin lymphoma	8,400	3%
Kidney & renal pelvis	10,010	3%		Brain & other nervous system	7,340	3%
All Sites	323,630	100%		All Sites	286,010	100%

Picture 1. Epidemiology of breast cancer

(A) Estimates (rounded to the nearest 10) of new cases and deaths by sex for 10 most wide-spread cancers in United States (US) for year 2017. Basal cell and squamous cell skin cancers and in situ carcinoma except urinary bladder are excluded from the analysis.

(B) Incidence (rate per 10^5 people) of 10 principal cancers in women between 1975 and 2013 in US.

(C) Stage at diagnosis of female breast cancer in US between 2006 and 2014.

(D) Percent relative survival rates of female breast cancer in US between 2006 and 2014.

(Siegel et al., Cancer Statistics 2017)

1.1 Breast cancer intrinsic subtypes

WHO (World Health Organization) offers a traditional classification of breast tumours based on morphology, which includes few molecular elements (Sinn & Kreipe, 2013). At present, grading and staging at diagnosis evaluate clinical parameters such as dimension, lympho-nodal invasion, presence of metastasis, patient's age and tumour grade; moreover, ER (oestrogen receptor), PR (progesterone receptor) and HER2 are assessed by immune-histochemical or molecular analysis as they are recognized as predictive and prognostic markers in breast cancer (Schmidt et al., 2016).

In the past decades, thanks to -omic technics, a great effort has been performed to classify breast cancer according to its molecular characteristics (Table 1).

The forefather paper by Sorlie and colleagues analysed gene expression of breast cancer tissues by hierarchical clustering. Tumours could be classified into two principal clusters according to ER expression. In ER negative cluster, tumours could be further classified in basal-like, normal breast-like and ERBB2 overexpressing; ER positive tumours, also defined luminal, could be distinguished in luminal A, B and C subtypes (Sorlie et al., 2001). Later on, some subclasses rearrangement occurred, and the final and current intrinsic subtypes were defined as luminal-A, luminal-B, HER2 enriched and basal-like. Since 2011, St. Gallen consensus has adopted this classification in its recommendations for adjuvant treatment of breast cancer. In the following decades, molecular profiling by PAM50 or other microarrays provided a more accurate and reproducible technic to identify intrinsic subtypes. Moreover, using the largest sample collection with extensive genomic, transcriptomic and clinical annotation in existence, a scheme for classifying breast tumours into 10 subtypes has been proposed, as well. This classification is based on the pattern of copy number alternations (CNAs) which exert a concordant effect on gene expression in cis (eQTLs). It is named IntClust owing to the clustering of tumours based on the integration of genomic and transcriptomic data to find probable driver events (Ali et al., 2014). Though more accurate and informative in patients' stratification, molecular profiling is expensive and not available for every patient. Hence, immune-histochemical analysis and clinical-pathological parameters are still used in clinical praxis as good surrogates for subtyping of breast cancer with a concordance of 80-90% to clustering based on multi-gene analysis (Prat et al., 2015).

Intrinsic subtype	IHC markers	Grading	Prognosis	Therapy	Gene expression	Mutations	Sites of metastasis
Luminal-A 50-60%	ER+ PgR+ HER2- Ki-67 low **HER2+ 6.3-7.8%**	**Low:** few nuclear pleomorphism and low mitotic activity	**Good:** low relapse rate	Endocrine therapy	**Cytokeratin** (CK8 and 18) **Luminal genes downstream to ER**: ER1, LIV1, X-BP1, ZIP6, SLC39A6, HGF3A, TFF3, FOXA1, BCL2, HER3 and HER4	TP53 12% MAP3K1 45% PI3KCA 13% GATA3 14% Low mutational burden	Brain 8% Liver 29% Lung 24% **Bone 67%** Visceral 28%
Luminal B 15-20%	ER+ PgR+/- HER2- Ki-67 high **HER2+ 16.4-20.8%**	**High:** ki-67 high, various aneuploidies	**Intermediate:** higher relapse rate and lower survival	Less responsive to endocrine therapy than luminal A; chemotherapy	**Proliferation-related genes**: v-MYB, GGH, LAPTMB4, NSEP1, CCNE1, AURKA	TP53 29% MAP3K1 29% PI3KCA 5% GATA3 15% Iper-methylation	Brain 11% Liver 32% Lung 24% **Bone 71%** Visceral 35%
HER2 enriched 15-25 %	ER- PgR- HER2 +	**High:** high proliferative index and genomic instability	**Poor,** in absence of targeted therapies	HER2 targeted therapies in (neo)adjuvant setting+ chemotherapy (doxorubicin)	**HER2 and pHER2** and downstream related genes **GRB7** and other genes on HER2 amplicon	TP53 72% PI3KCA 39%	**Brain 29%** Liver 44% Lung 37% **Bone 60%** Visceral 32%
Basal-like 8-37%	ER- PgR- HER2- **HER2+ 2.1-17.4%**	**High:** high proliferative index, poor tubule formation, presence of necrotic or fibrotic zones, pushing borders, abundant lymphocytic infiltration, medullary features	Poor: frequent metastasis, younger patients	Chemo- and radiotherapy	**Myoepithelial markers:** CK5, 14 and 17 Laminin, P-cadherin, fascin, caveolin 1-2, -crystallin and EGFR	BRCA-1 TP53 80% PI3KCA 9% Hypo-methylation	Brain 25% Liver 21% **Lung 43%** Bone 39% Visceral 30%

Table 1. Breast cancer intrinsic subtypes
The table reports histological, clinical and molecular features of breast cancer by intrinsic subtype (Modified from Sorlie et al., 2001; Kennecke et al., 2010; Yersal & Barutca, 2014; Hoadley et al., 2014; Prat et al., 2015; Iancu et al., 2017).

1.2 Luminal breast cancer

Luminal tumours are named according to their up-regulated expression of genes related to epithelial and luminal differentiation. Altogether, they represent 75% of breast cancers (Yersal & Barutca, 2014) and show a tendency to better prognosis with respect to non-luminal tumours.

Luminal A tumours are the most common intrinsic subtype of breast cancer (50-60%). The low ki-67 (mitotic index inferior to 14%) distinguishes them from luminal B subtype. Phenotypically, luminal A tumours are characterized by low histological grade, low degree of nuclear pleomorphism and low mitotic activity; they also express luminal cytokeratin 8 and 18. At molecular level, besides the expression of ER , they also express high levels of ER1, GATA binding protein 3, X-box binding protein 1, trefoil factor 3, hepatocyte growth factor 3 and oestrogen-regulated LIV1, BCL2, erbB3 and erbB4. At the DNA level, luminal A tumours show a low genomic instability which is mirrored by the low number mutations and chromosomal aberrations. TP53 is rarely found mutated (12%), whereas MAP3K1 and PI3KCA mutations are more common (45% and 13%, respectively). Clinically, patients with luminal A breast cancer have good prognosis and significantly lower relapse rates than other subtypes. Recurrences are to be found mainly in bone. Gold standard therapy for this subtype is endocrine therapy with either SERMs (selective oestrogen receptor modulators) such as tamoxifen, or inhibitors of aromatase which convert androgens in oestrogens, or up-stream block of ipothalamus-ipophysis axis with LH-RH analogues. Luminal A tumours are so responsive to endocrine therapy that adjuvant therapy does not require chemotherapy, but only tamoxifen given for 5-10 years (Sorlie et al, 2001; Yersal & Barutca, 2014; Hoadley et al., 2014; Prat et al., 2015; Iancu et al., 2017).

Luminal B tumours comprise 15-20% of breast cancers. They show lower expression of genes related to ER compared to luminal A tumours and higher proliferative index, accompanied by a higher expression of proliferation-related genes such as v-MYB, gamma glutamyl hydrolase, lysosome-associated transmembrane protein 4-beta, nuclease sensitive element binding protein 1 and cyclin E. AURKA (aurora kinase A) and genes related to signalling down-stream growth factor receptors are found up-regulated in this subtype, as well. At DNA level, conversely to what observed in luminal A, luminal B tumours are more frequently mutated in TP53 (29%) yet less frequent mutations are

detected in PI3KCA (5%) and MAP3KI (29%). Moreover, methylation pattern of luminal B cancers is altered, and hyper-methylation is registered in up to 8% of cases. Prognosis is worst for this subtype in the first 5 years after diagnosis. Metastasis are frequently found in bone, as in luminal A tumours. Luminal B tumours are less sensible to endocrine therapies but more to chemotherapy due to their increased mitotic index. Hence, in this subtype endocrine therapy is more often accompanied by chemotherapy (Sorlie et al, 2001; Yersal & Barutca, 2014; Hoadley et al., 2014; Prat et al., 2015; Iancu et al., 2017).

Of note, intrinsic subtypes in breast cancer are not to be intended as airtight compartments and exceptions exist. For example, a quote of luminal A (6.3-7.8%) and B tumours (16.4-20.8%) overexpress HER2 (Prat et al., 2015). It is still under scientific debate whether a new subtype of triple positive breast cancer, expressing both ER/PR and HER2 at high levels, actually exists. A peculiar behaviour of these tumours has indeed been noticed in clinical trials and in the clinic: triple positive tumours show an increased tendency to develop resistance to therapy. This could partly be explained by the fine interplay existing by ER/PR and HER2 signalling pathways, which are alternatively up-regulated when the other pathway is inhibited. Research is still ongoing to determine whether these tumours benefit from a dual approach with endocrine therapy combined with anti-HER2 agents (Iancu et al., 2017).

1.3 HER2-enriched

HER2 enriched tumours account for 20-25% of breast cancers. HER2 overexpression is an independent factor of worst prognosis by itself, conferring aggressiveness at both biological and clinical levels. Phenotypically, HER2-enriched tumours are characterized by HER2 amplification and overexpression and absent or low ER/PR, high proliferative index, nuclear and histological grade. Gene expression is dominated by genes linked to HER2 overexpression or found on the same amplicon on 17q21; luminal and basal-like typical genes are expressed at low to intermediate level. Genomic instability is observed in HER2-enriched tumours, probably due to up-regulation of APOBEC3B which encode a deaminase converting cytidine to uracil. TP53 is frequently found mutated (72%) as well as PI3KCA (39%). Without targeted therapies, prognosis of HER2 enriched tumours is extremely inauspicious, with high recurrences rate often in the brain. Therapy is primarily based on HER2-targeting agents; furthermore, HER2 enriched tumours show a marked sensibility to doxorubicin, due to presence of its target (TOPOIIA) in HER2

containing amplicon (Sorlie et al, 2001; Yersal & Barutca, 2014; Hoadley et al., 2014; Prat et al, 2015; Iancu et al., 2017).

As previously observed, a quote of HER2 overexpressing tumours may fall in other intrinsic subtypes. It should be noted that HER2 enriched subtype embraces tumours with very different levels of HER2 amplification and overexpression; this heterogeneity may affect prognosis as well as response to therapies. Moreover, not every up-regulation of HER2 detected by microarray is translated at protein level and in turn not every HER2 overexpressing tumour by immunohistochemistry will be assigned to HER2 enriched intrinsic subtype (Prat et al., 2015).

1.4 Basal-like

Basal-like tumours are extremely different in morphological and molecular characteristics from the other subtypes. Real proportion of basal-like tumours is difficult to calculate, as they are often diagnosed as big undifferentiated tumours and often fall out of breast cancer statistics; however, they are estimated 8-37% of all breast cancers. Phenotypically, basal-like cancers have high histological and nuclear grade together with high mitotic and proliferative indexes, poor tubule formation, presence of necrotic or fibrotic zones, pushing borders, abundant lymphocytic infiltration, medullary features. Their expression profile lacks luminal genes and is in turn enriched in basal genes, like cytokeratin 5, 14, 17, adhesion molecules such as laminin, P-cadherin, fascin, caveolin 1 and 2, -crystallin, and other membrane molecules (fatty acid binding protein 7 and epithelial growth factor receptor 1). Commonly deregulated pathways are integrin, MAPK, PI3K-Akt and NF-kB, but the landscape of basal-like breast cancers is extremely variegated. At DNA level, they show abundant genomic instability with frequent loss of function mutations in TP53 and Rb; moreover, BRCA1 mutated breast cancer often show a basal-like phenotype. Prognosis of these aggressive tumours is exceptionally poor, even worsen by lack of therapeutic targets. Metastasis in this subtype are common and target principally lung and brain (Sorlie et al., 2001; Yersal & Barutca, 2014; Hoadley et al., 2014; Prat et al., 2015; Iancu et al., 2017).

In the diagnosis praxis, basal-like tumours are recognized as triple negative tumours, since they express neither ER/PR nor HER2 receptors. It should be however noted that some basal-like tumours express HER2 (2.1-17.4%) and that not every triple negative tumour can be assigned to the basal-like subtype. At least two other sub-clusters are

reported in literature, such as claudin-low and normal-breast like. The former is an extremely aggressive subtype characterized by absence of adhesion molecules forming tight junctions such as claudin, occludin and E-cadherin, by features of epithelial-to-mesenchymal transition (EMT) and cancer stem cells. Normal breast-like cancers are still triple negative, but cluster together with normal and benign adenoma samples; their real occurrence and biological significance is still debated (Prat et al., 2015).

1.5 New insights in breast cancer aetiology

An open question is how different the 4 breast cancer subtypes are and more importantly whether all breast cancers stem from a single progenitor or not.

A principal component analysis revealed that transcription profiles of luminal and HER2 enriched subtypes are mutually similar. In contrast, basal-like tumours are more similar to squamous cell lung carcinomas than to the other breast cancer subtypes and should hence be regarded as a single molecular entity (Prat et al., 2015).

A bimodal distribution of breast cancer incidence has been noted with two peaks at 50 and 70 years. Dissecting this difference by intrinsic subtype, it was revealed that ER positive and ER negative tumours show an independent bimodal incidence with opposite trends. ER negative cancers had a major incidence peak at 50 years, whereas ER positive tumours had more frequently a later onset (Anderson et al., 2014).

Following these and other observations, Anderson and colleagues suggested a major division between basal-like and luminal breast cancers, with HER2 enriched tumours being luminal cancers with HER2 expression as a plus. In this model, a transformation event can occur either in a progenitor cell committed to luminal differentiation giving rise to a luminal tumour (A, B or HER2 enriched) or in a basal/myoepithelial committed cell originating a basal-like tumour (Picture 2).
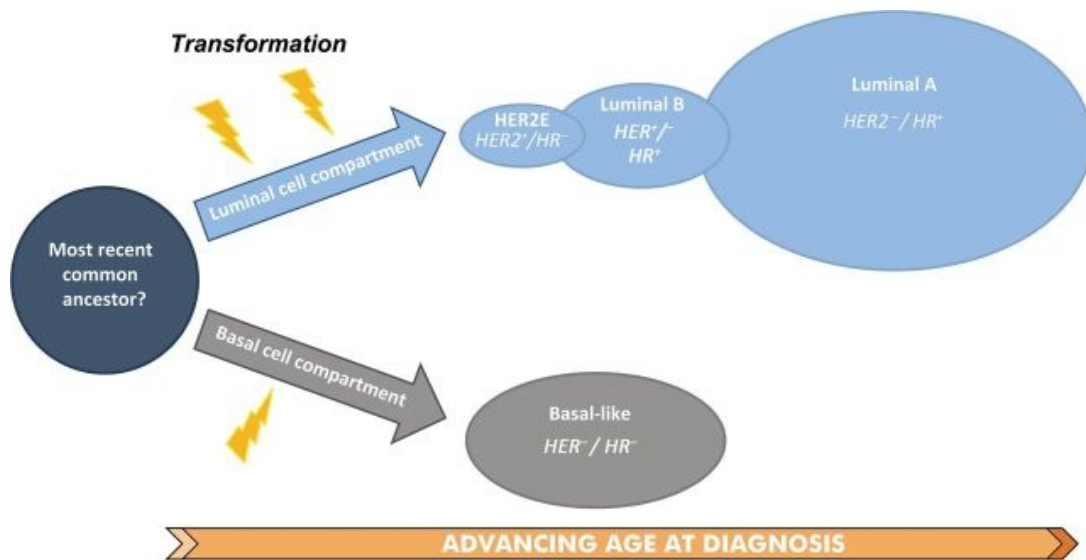
Picture 2. Aetiology of breast cancer

The cartoon illustrates the hypothesis of breast cancer of luminal (A, B or HER2-positive) and non-luminal (basal-like) cancer originating by transformation event (lightning bolts) in differently committed cells (Anderson et al., 2014). HER2E= HER2 enriched

2. Role of HER2 in breast cancer

HER2 enriched tumours account for 15-25% of breast cancers. HER2 was first identified as a proto-oncogene whose amplification was an independent factor of worse prognosis, namely shorter relapse-free and overall survival, in 1987 in a cohort of 189 breast cancer patients (Slamon et al., 1987; Menard et al., 2004). Since then, extensive research has deepened our knowledge of the mechanistic role of HER2 in oncogenesis and numerous targeted therapies against HER2 have been developed, ameliorating prognosis. Currently, life expectance for metastatic HER2-positive breast cancer is 5 years and 75% of newly diagnosed patients achieve a pathological complete response (Loibl & Gianni, 2017). Still, HER2-positive breast cancer presents challenges for clinicians and researcher, mainly due to high rates of intrinsic and acquired resistance to HER2 targeted therapies and metastasis to the brain.

2.1 Biology of ErbB-HER receptor family

The HER family (also called ErbB or epidermal growth factor receptor family) comprises four transmembrane receptor tyrosine kinases, EGFR (or HER1), HER2, HER3, and HER4 (Eccles, 2011; Nuciforo et al., 2015; Hsu & Hung, 2016). As many other receptor tyrosine kinases, these receptors are involved in many essential developmental processes such as differentiation, cell proliferation, motility, wound healing, tissue regeneration and apoptosis.

All receptors in HER family are membrane-anchored proteins and share a similar structure, made up of 4 domains. An extra-cellular (ECD) domain responsible for ligand binding (LD1 and LD2) and dimerization (CR1 and CR2), a membrane-spanning domain and an intracellular domain (ICD) responsible for auto-phosphorylation and triggering of down-stream signalling cascade (Roskoski, 2014; Bazley & Gullick, 2005).

In absence of a ligand, receptors lay interspersed in the plasma membrane in close conformation, with the dimerization domain blocking ligand binding domain in the receptor monomers. Upon ligand binding, receptors switch to an open conformation where dimerization domain is accessible for homo- or hetero-dimerization with other HER receptor monomers (Bazley & Gullick, 2005). Active receptors cluster in the membrane in complexes involving up to 10^6 receptors. Moreover, HER receptors have been demonstrated to interact with other receptor tyrosine kinases such as IGF-1R (insulin growth factor receptor 1) and c-MET as well as adhesion molecules, i.e. integrins

and tetraspanins (Eccles, 2011). These cross-links between receptor tyrosine kinases belonging to different families may also provide a ligand-independent way of activation of HER receptors (Stern, 2008).

HER2 and HER3 represent exceptions to this model. HER2 indeed is not able to assume a close conformation and shows a very low affinity for ligands: this receptor is therefore always accessible for dimerization with other HER receptors, regardless of ligand. HER3, in turn, lacks tyrosine kinase activity and is therefore obliged to form heterodimers upon ligand binding. Hence, HER2 and HER3 homo-dimers are not active and these receptors are preferred partner of dimerization of the other HER receptors.

Up to date, 10 different ligands of HER receptors have been identified, which are produced by protease cleavage of membrane-anchored precursors by ADAM protease. EGF (epithelial growth factor), TNF (tumour necrosis factor), amphiregulin (AR) and epithelial mitogen (EPGN) bind only to HER1; betacellulin (BCN), heparin binding epithelial growth factor (HB-EGF) and epiregulin (EPR) bind both HER1 and HER4; lastly, heregulins or neuregulins (NRG) bind both HER3 and HER4 (NRG-1 and -2) or HER3 only (NRG-3 and -4) (Moasser et al., 2007). Upon ligand binding, HER receptor monomers could theoretically form 10 different dimers, but not all of them are equally active (Eccles, 2011). Heterodimers involving HER2 and HER3 result the most active because of high affinity binding to dimerization partner and to ligand (HER3 only). They are followed by other heterodimers containing HER2, non-HER2 heterodimers and lastly homodimers of HER1 (the only one active homodimers) (Eccles et al., 2011).

Other than signalling mediated by their tyrosine kinase activity (see paragraph 2.4), all ErbB-HER receptors can translocate to the nucleus and directly control transcription of target genes, interact with other transcription factors and alter DNA structure (Hsu & Hung, 2016).

HER family signalling may appear redundant, but the variety of ligands and possible dimerization partners leads to unique and specific signalling pathway down-stream. The type and amplitude of activated downstream signalling cascades are a co-function of which receptors are expressed by a particular cell, the number of receptors expressed, and the amount and type of ligand that stimulates the cell (Harari and Yarden, 2000): HER1 and HER4 have 100 different molecular interactors, whereas HER2 and HER3, being mock receptors, show fewer interactors mostly linked to their tyrosine kinase activity (i.e.

HER3 present copious docking sites for Akt activating subunit, p85) (Moasser, 2007; Sergina & Moasser, 2007; Hynes & MacDonald, 2009).

Signalling of HER receptors is terminated by ligand-dependent endocytosis, regulated by c-Cbl (Cbl proto-oncogene, E3 ubiquitin protein ligase) which has greater affinity for HER1 rather than HER2 and no affinity for HER3 and HER4 (Yarden, 2001).

2.2 ErbB-HER receptors in cancer

Given their role in cell proliferation, differentiation and motility, it is self-evident that an aberrant expression of ErbB-HER receptors may lead to cancer and in the last decades a leading role has been proposed for many of these receptors in initiating and promoting solid tumours' growth (Bazley & Gullick, 2005; Arteaga & Engelmann, 2014).

Overexpression of EGFR has been observed in breast, lung, colorectal, oesophageal cancers, and glioblastomas. Its up-regulation can be due to amplification, as in some triple negative breast cancers. Another mechanism of HER1 activation is represented by deletion of some exons in its ECD, which leads to an always open and signalling conformation: deletions of exons 2-7 are found in 40% of glioblastomas (Arteaga & Engelmann, 2014). Moreover, EGFR can harbour gain-of-function mutations, which are reported in 10–35% of lung cancers. In breast cancer, EGFR is rarely mutated, but its overexpression is observed in 15–30% of patients, primarily in basal-like and triple negative tumours, where it associates with large tumour size and poor clinical outcomes (Hsu & Hung, 2016). Targeted therapies against HER1 include monoclonal antibodies (cetuximab) and tyrosine-kinase inhibitors (afatinib, erlotinib and gefinitib). These drugs are in current clinical praxis for lung tumours and glioblastomas showing overexpression of EGFR; their implementation in triple-negative breast cancer is under evaluation.

Other than in breast cancer, HER2 is found amplified in gastric and oesophageal tumours. HER2 mutations in breast cancer are rare (2.8%), but they can be detected in other carcinomas such as ovary, endometrium, lung, head&neck, colon, liver, bladder and glioblastomas (Yan et al., 2014; Connell and Doherty, 2017). Target therapies against HER2 comprise trastuzumab, trastuzumab-DM1, pertuzumab, lapatinib and neratinib and will be discussed later (see paragraph 3).

HER3 has no oncogenic potential by itself because of lack of tyrosine kinase activity, but it is required for oncogenesis driven by other HER receptors: HER3 knock-out mice fail

to develop mammary tumours despite HER2 overexpression (Mujoo et al., 2014). It is often co-expressed with HER2 and alterations in its copy number have been reported in 28% of HER2-positive breast cancers. Its mutations are rare and sporadically observed in breast and gastric cancer (Arteaga & Engelmann, 2014; Hsu & Hung, 2016).

HER4 has a controversial role in breast cancer, where some authors report its tumour-suppressing activity and others its oncogenic potential. Mutations of HER4 have been found in melanomas, medulloblastomas, lung and non-small cell lung carcinomas (Arteaga & Engelmann, 2014; Hsu & Hung, 2016).

A further mechanism explaining oncogenic potential of ErbB-HER receptors is represented by excessive production of their ligands due to mutations or aberrant trafficking (Arteaga & Engelmann, 2014).

2.3 HER2 patho-physiological role

HER2 is principally involved in development and maintenance of cardiac and nervous epithelia, other than of the mammary gland. HER2 knock-out mice face a premature *intra-uterus* death, highlighting HER2 crucial role in embryogenesis: HER2-HER4 dimers activated by neuregulins are involved in development of cardiac *trabeculae*, HER2-HER3 dimers are in turn involved in correct differentiation of Schwann cells and formation of peripheral ganglia (Emde et al., 2012). After birth HER receptors assume a prominent role in normal development of the mammary gland. During puberty, signalling from HER1-HER2 dimers promote invasion of fat pad by out-branching mammary tubes. In the mature mammary gland, HER2 controls mammary ducts morphology and density orchestrating formation of terminal end buds. During pregnancy, HER2 promotes formation of alveolar tubes (Eccles, 2011).

As demonstrated in mice transgenic for human HER2 expression and in cell lines transduced with this gene, HER2 amplification is a necessary and sufficient condition to induce tumorigenic transformation (Moasser et al., 2007). Amplification occurs at DNA level, where 25-50 copies of the oncogene can be found in transformed cells, and exponentially augments both expression at RNA level (40-100 times with respect to normal cells) and number of receptor monomers on cell surface (up to $2x10^6$ receptors per cell). It is self-evident that this amplification not only increases tyrosine kinase activity of HER2 as a point mutation would, but also provokes structural changes in the membrane

and alters signalling downstream all ErbB-HER receptors which concur together in oncogenesis.

HER2 is the preferred dimerization partner of all other HER receptors and forms stronger and more persistent dimers. High density of HER2 monomers promotes formation of HER2-containing homo- and heterodimers, thus intensifying signalling down-stream all HER receptors. Increased homo-dimerization and dimers' clustering disrupt membrane structure, especially at tight junctions, causing a loss of cell polarization and unordered proliferation of epithelial cells. Moreover, HER1-HER2 dimers promote cell motility by signalling down-stream of Akt, Ras and protein lipase C (PLC). Hence, HER2 amplification completely disrupts tissue architecture (Moasser et al., 2007).

HER2 exists not only as full-length protein but also as isoforms, lacking C-terminus, N-terminus or internal exons. These isoforms, like 16 and p95HER2, have often been linked to increased aggressiveness and resistance to targeted therapies (Castiglioni et al., 2006; Sperinde et al., 2010; Arribas et al., 2011; Marchini et al., 2011; Castagnoli et al., 2017; Palladini et al., 2017). HER2 amplification leads to a parallel increase in the expression of these isoforms, as well.

HER2 can translocate to the nucleus and directly regulate target genes, such as COX2 (cycle-oxygenase 2), VEGF-A (vascular-endothelial growth factor A), Stat3 (signal transducer and activator of transcription 3) and CXCR4 (chemokine C-X-C motif receptor 4). As observed for trans-membrane isoforms, nuclear HER2 is increased due to amplification as well and results in increased expression of target genes (Moasser et al., 2007).

HER2 amplification, moreover, affects the rate of ligand release from active dimers and slows down receptor recycling and internalization, making signalling even more persistent (Harari & Yarden, 2000; Prenzel et al., 2011).

HER2 is not the only amplified gene, but part of a bigger amplicon conserved among HER2 enriched tumours and centred on HER2. This amplicon (17q12-21; minimum size 280 Kb) comprises 10 transcribed genes, such as GRB7 (growth factor receptor-bound protein 7) directly linked to HER2 function, MLN64 involved in cholesterol trafficking, TOPO II A (topoisomerase II A), PNMT, MGC9753 and MGC14832 which are all amplified together with HER2.

2.4 Alterations in HER down-stream signalling pathways

Physiologically, the principal signalling pathways activated by HER dimers are phosphatidylinositol 3-kinase (PI3K), Ras, phospholipase C (PLC), and Janus-activated kinase (JAK) (Picture 3).

Signalling through PI3K is generally due to hetero-dimerization of any HER receptor with HER3, which harbours 6 docking sites for the activating subunit of PI3K, p85. This pathway is mostly activated by HER2-HER3 heterodimers though, since HER3 represents the preferred HER2 ligand. The catalytic subunit of PI3K, p110 converts PIP_2 (phosphatidylinositol 4,5 -bisphosphate) in IP_3 (inositol 1,4,5 trisphosphate), which in turn activates Akt leading to cell survival and inhibition of apoptosis. Indeed, Akt inhibits BAD (BCL2-associated antagonist of cell death), FKHR and p27 which would stop cell cycle and induce apoptosis. In turn, Akt activates mTOR, NF-kB, FOXO and GSK3 which mediate further proliferative and anti-angiogenic effects (Eccles, 2011).

Ras signalling activation is mediated by docking of the adapter proteins Grb2 (Growth factor receptor-bound protein 2) and guanine exchange factor, Sos (Son of seven less), directly or through other Shc (Src homology domain) adaptor to the docking sites on HER1 or HER2 ICD. Binding of these adaptor proteins recruits Ras GTP-binding protein and results in Ras activation, which triggers the kinase cascade that activates Raf, MEK, and ERK. As a final result, transcriptional factors are phosphorylated and translocate to the nucleus, where they regulate cell proliferation and motility through up-regulation of ELK1 and, MYC and Jun/Fos (Emde et al., 2012).

PLC is activated by heterodimers comprising HER1 only. Once docked at phosphorylated receptors and activated, the enzyme breaks PIP_2 to yield IP_3, which induces transient increase in intracellular calcium and DAG (1,2-diacylglycerol), which functions as a co-activator of protein kinase C. Activation of this pathway results in transcriptional activation of Jun/Fos (Eccles, 2011).

HER1 and HER4 can bind to and directly activate signal transducer and activator of transcription (STAT) proteins via the Sh2 domain. Once active, STAT proteins homo- and hetero-dimerize and translocate into the nucleus to drive expression of specific target genes involved in proliferation, differentiation, and survival.

Since HER2 is the preferential partner of other HER receptors, it is self-evident that all pathways down-stream to HER family are up-regulated in HER2 enriched breast cancer.

HER2 and HER3 form the strongest dimers, hence HER2 amplification in breast cancer primarily results in activation of PI3K pathway down-stream HER3. Activation of PI3K-Akt pathway aberrantly controls cell survival, dimension, response to nutrients, glucose metabolism, epithelial to mesenchymal transition (EMT), motility, genome stability and angiogenesis (Moasser, 2007).

HER receptors are rich in docking sites for adaptor proteins containing PTB (phophoproteinase binding) or Sh2 domains, leading to Src protein activation down-stream. Their role in mammary carcinogenesis still needs to be clarified. Their inhibition in a human HER2-positive cell lines blocks aggressive clones with metastatic potential, leading to hypothesize a role of Src proteins in loss of cell polarity and cell-cell adhesion with consequent anchorage-independent growth. Moreover, Src proteins can phosphorylate HER2 in Tyr877 increasing its affinity to HER3 (Moasser et al., 2007).

Signalling down-stream PI3K phosphorylates p27^{kip1}, sequestering it in the cytoplasm, and HER2 further modulates its action through MAPK signalling pathway; HER2 overexpression thus alters cell cycle control at G1/S checkpoint. Moreover, cyclin D1, E and cdk6 (cyclin dependent kinase 6) are often hyper-expressed in HER2 enriched tumours. Indeed, transgenic mice for HER2 expression and knock out for cyclin D1 or cdk4 or p16 fail to develop mammary tumours (Moasser et al., 2007).

Many other pathways down-stream HER receptors result altered in HER2 overexpressing cancer, many of them promoting a metastatic phenotype. They include modulation of PKC- , FAk (Focal Adhesion kinase), TGF- , integrin 4 and , and of metalloproteinases 2 and 9 (MMP-2 and -9) all contribute to this phenotype (Moasser et al., 2007).

Last but not least, overexpression of HER2 aberrantly modulates angiogenesis, leading to formation of scarcely organized and often fenestrated vessels. Indeed, HER2 directly up-regulates transcription of VEGF-A and HIF- ; moreover, it enhances their translation through P706K kinase, down-stream to Akt signalling. COX-2 is also up-regulated by nuclear HER2: it again enhances secretion of VEGF and of eicosanoids, which activate endothelial cells protecting them from apoptosis (Alameddine et al., 2013).
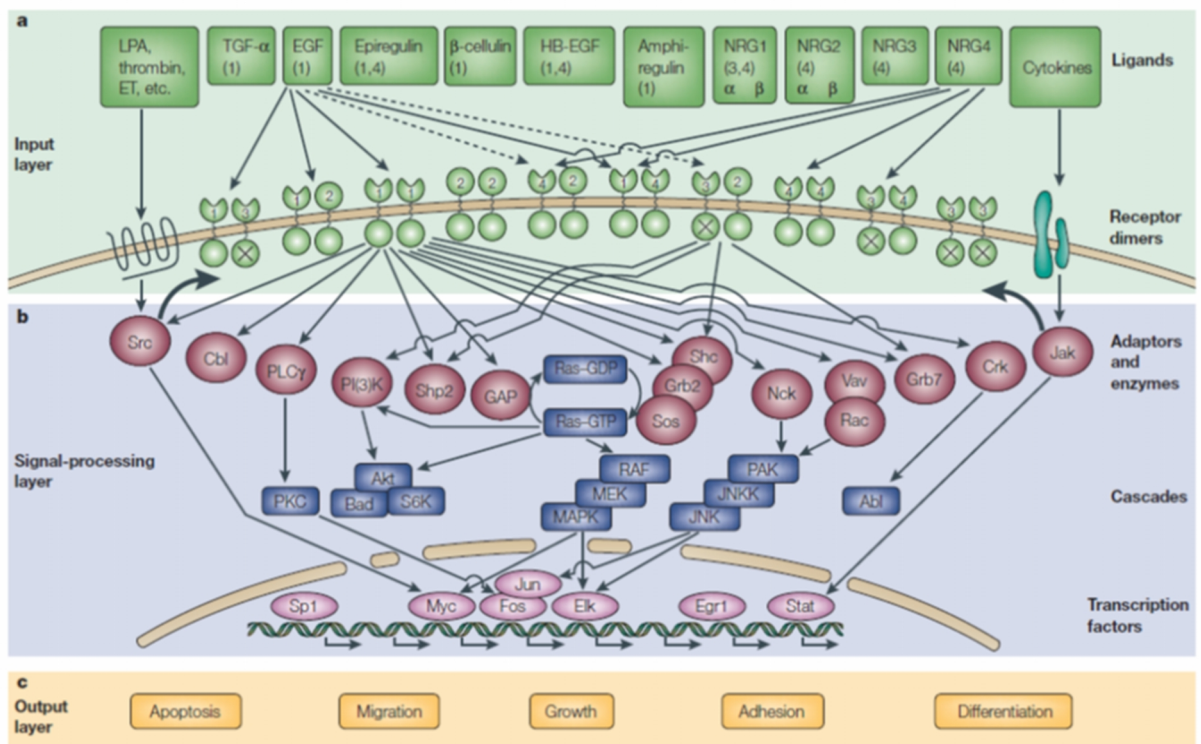
Picture 3. Signalling of HER2 receptor family

Figure shows HER receptor interactions upon ligand binding and elicited down-stream pathways (Yarden & Sliwkowski, 2001).

3. HER2 targeted therapies

HER2 targeted therapies are offered as standard of care to all patients diagnosed with HER2-positive breast cancer. According to St. Gallen consensus and ASCO/CAP recommendations 2013, HER2-positive cancers are defined as 1) evidence of HER2 protein overexpression measured by immunohistochemistry IHC3+ status and complete staining in at least 10% of cells, or 2) by fluorescence in-situ hybridisation (FISH) measurement of a HER2 gene copy number of six or more or a HER2/CEP17 ratio of 2·0 or greater (Loibl and Gianni, 2017). HER2 targeted agents exploit two different mechanisms of action: on the one hand, HER2 is used as a target to convey molecules with cytotoxic properties (antibodies or antibody-drug conjugates) specifically to the tumour; on the other hand, tyrosine kinase inhibitors directly dampen oncogenic signalling downstream HER2 (Escrìvia-de-Romani et al., 2018). Clinicians currently dispone of 5 drugs targeted against HER2, trastuzumab, the forefather of anti-HER2 agents, trastuzumab-DM1, pertuzumab, lapatinib and neratinib to be used in different clinical settings (table 2).

3.1 Trastuzumab: mechanism of action and resistance

The current standard of care for HER2-positive early breast cancer includes trastuzumab (with or without pertuzumab) and chemotherapy given either before or after surgery (Loibl and Gianni, 2017). Trastuzumab is a humanized monoclonal antibody which targets HER2 ECD in domain IV (the nearest domain to the membrane); year 2018 marks 20 years since consent to its commercialization by FDA. Approval of trastuzumab was granted following several trials determining a benefit of adding trastuzumab to chemotherapy both in neoadjuvant and adjuvant setting. HERA trial showed 1 year of adjuvant trastuzumab was associated with significant improvements in both 10-year disease-free survival (DFS; 69% vs 63%; HR 0.76) and 12-year of overall survival (OS 79% vs 73%; HR 0.74) compared to observation (Baselga et al., 2017). Other trial demonstrated no additional benefit in prolonging treatment with trastuzumab for 2 years. NOAH trial confirmed these results in neoadjuvant setting, where addition of trastuzumab to chemotherapy significantly improved rate of pathologic complete response (pCR) and 5-year event-free-survival (EFS 58% vs 43%; HR 0.64) (Baselga et al., 2017).

Albeit its wide-spread use in clinical practice, trastuzumab mechanisms of action still need to be completely understood. Known effects of trastuzumab are reported below (Wong & Lee, 2012):

- As an antibody, trastuzumab elicits antibody-dependent cell-mediated cytotoxicity (ADCC) through binding to Fc R on effector NK (natural killer) cells, which lysate cells bound to trastuzumab;

- Trastuzumab inhibits HER2 shedding and decreases blood levels of p95^{HER2}, which have been linked to a more aggressive tumoral phenotype;

- Trastuzumab inhibits down-stream signalling and progression through cell cycle by up-regulation of PTEN and p27^{kip1} and simultaneous down-regulation of PI3K and Akt;

- Trastuzumab inhibits hetero-dimerization of HER2 creating a steric hindrance and induces apoptosis;

- Trastuzumab normalizes intra-tumour vasculature enabling a better drug delivery;

Trastuzumab has demonstrated efficacy in early breast cancer, but still a significant proportion of patients will eventually progress. Phase III trials evaluating trastuzumab reported different rates of progression, varying from 28.8% at 10-years follow-up in HERA trial to 42% at only 5 years follow-up in NOAH trial. More recent trials have registered and improvement up to 5-year DFS of over 85%. Even if it is difficult to correctly estimate proportion of patient relapsing after first-line trastuzumab, these data clearly indicate an unmet need to understand mechanisms of acquired resistance to trastuzumab. Moreover, heterogeneity in HER2-positive tumours should be considered as some patients show an intrinsic resistance to trastuzumab despite being diagnosed with an HER2-positive disease. Research is thus ongoing to identify predictive markers of response to therapy other than HER2 and alternative therapeutic approaches in trastuzumab-resistant patients (Baselga et al., 2017).

Acquired resistance to trastuzumab can be due to factors intrinsic to the target, activation of compensatory pathways or to host-related factors.

It is self-evident that alterations such as mutations of HER2 can prevent trastuzumab binding, thus limiting its efficacy. Mutations are rare in HER2, but emergence of isoforms lacking epitope bound by trastuzumab also frustrate or limit treatment efficacy. Moreover, trastuzumab binding to HER2 can be sterically hindered by up-regulation of mucin-1 or -4. Up-stream up-regulation of HER ligands can also outweigh trastuzumab-mediated inhibition.

Once signalling through HER2 ECD is pharmacologically inhibited, cells try to counteract this by intracellular pathways of ligand-independent activation of HER2. This receptor can indeed be trans activated by hetero-dimerization with any other activated HER receptor, as well as IGF-1R, MET and EphA2. Moreover, TGF can mediate resistance to trastuzumab by up-regulating ADAM17 protease, which cleaves HER ligands from the membrane, and thus augmenting their local concentrations. Activating mutations in pathways down-stream HER2 or re-activation of ER pathway can counterbalance trastuzumab action as well.

Lastly, resistance to trastuzumab can be due to alteration of tumoral microenvironment. One hallmark of cancer is deregulation of apoptosis machinery, which is required for trastuzumab inhibitory action: alterations in BIM, survivin, cyclins or $p27^{kip1}$, frequently found in HER2-positive tumours, can allow cells to escape apoptosis again impeding trastuzumab action. Trastuzumab enhances receptor degradation; thus, any miss-regulation of endocytosis can dampen its efficacy. Trastuzumab action is also mediated by ADCC, so any down-modulation of immune system due to tumour immune-suppressive properties or to host polymorphisms or mutations in ADCC machinery can cause resistance to trastuzumab (Rexer & Arteaga, 2012; Escrìvia-de-Romani et al., 2018).

Of note, trastuzumab displays a well-known cardio-toxicity which limits its usage in patients with high cardiac risk.

Trastuzumab patent has expired with the consequence of many biosimilar being tested in clinical trials. Results appear favourable and trastuzumab-biosimilar are expected soon to enter in the clinical praxis, providing an alternative and hopefully less expensive choice of treatment.

Research is ongoing to improve trastuzumab, as well. It has been reported that polymorphisms in Fc R can influence trastuzumab binding and the magnitude of ADCC elicited. Margetuximab was designed to improve trastuzumab binding to low-affinity receptors and contemporarily decrease trastuzumab affinity for inhibitory receptor Fc RIIB. Combination of margetuximab and chemotherapy is now being directly compared to trastuzumab plus chemotherapy in the pivotal phase III trial SOPHIA (Escrìvia-de-Romani et al., 2018) (Table 3).

3.2 Trastuzumab-DM1, Pertuzumab and other antibodies

Trastuzumab-DM1 conjugates the antibody with emtansine, a potent inhibitor of microtubule polymerization, which is driven to the tumour cells by trastuzumab. Thus, this drug improves therapeutic index minimizing exposure of normal tissues (Loibl and Gianni, 2017). T-DM1 was tested in the two phase III TH3RESA and EMILIA trials enrolling patients with advanced breast cancer progressed after trastuzumab; both trials reported a statistically significant benefit in progression free survival (PFS) with respect to lapatinib+capecitabine or treatment of physician's choice. MARIANNE trial was designed to test T-DM1 action alone or combined with pertuzumab in neoadjuvant setting; unfortunately, the two drugs did not show additive action nor improvement in PFS with respect to trastuzumab and a taxane. So, despite its favourable safety profile and better quality of life of patients treated with T-DM1, this drug is currently approved only in metastatic breast cancer patients pre-treated with trastuzumab and taxane. Of note, despite involving a big antibody-drug complex, some activity of T-DM1 on brain metastasis has repeatedly been reported (Loibl and Gianni, 2017; Hurvitz et al., 2017).

Pertuzumab is a second monoclonal antibody targeting HER2 in the dimerization domain; indeed, HER2-driven transformation and signalling requires hetero-dimerization. Its activity has been documented in first line setting by CLEOPATRA phase II and NeoSphere phase III trial. Both of them showed superiority in terms of response rates and overall as well as progression free survival of regimens adding pertuzumab to trastuzumab and docetaxel and minimal increase in toxicity, with respect to either single drug. These trials granted approval for pertuzumab in first line treatment in HER2-positive breast cancer. There are currently no indications for a prosecution of treatment with pertuzumab beyond progression (Loibl and Gianni, 2017; Hurvitz et al., 2017).

Bi-specific antibodies target multiple epitopes in order to simultaneously affect different molecules. ZW25 targets two distinct epitopes on HER2 and appears to improve binding affinity and receptor degradation. MCLA-128 targets both HER2 and HER3 and has shown promising activity in a phase I trial. Simultaneous targeting HER2 and CD3 with ertumaxomab appears promising as it has demonstrated both immune-stimulatory and anti-tumour activity in a trial, enrolling patients with HER2-expressing advanced solid tumours. Moreover, encouraging data on a new bispecific antibody simultaneously targeting p95^{HER2} and CD3 have recently been reported in a preclinical study on

mammary patient derived xenografts (Ruiz et al., 2018; Hurvitz et al., 2017; Escrìvia-de-Romani et al., 2018) (Table 3).

New antibody-drug conjugates are in the pipe-line, as well. SYD 985 combines trastuzumab with a prodrug, DUPA SYD 986, which is activated by proteasomal cleavage in lysosomes or in the tumoral microenvironment becoming a potent alkylating agent. Its efficacy in second-line is being evaluated in TULIP phase III trial. DS-8201 combines trastuzumab with a topoisomerase II inhibitor and is showing promising activity in phase I and II trials (Escrìvia-de-Romani et al., 2018).

Other strategies to deliver chemotherapy to HER2-positive cells are being explored. MM302 is an HER2-targeting nanoparticle combined with doxorubicin, a chemotherapeutic agent particularly active in HER2-positive breast cancer. Unfortunately, HERMIONE trial, comparing MM302 plus trastuzumab *versus* physician's choice *plus* trastuzumab in HER2-positive breast cancer progressed after pertuzumab, was recently closed due to unfavourable futility analysis (Hurvitz et al., 2017) (Table 3).

3.3 Inhibitors of tyrosine kinase

Tyrosine kinase inhibitors (TKIs) were studied in breast cancer to overcome trastuzumab issues. Being smaller molecules than antibodies, they should be able to cross brain-blood barrier for treating of cerebral metastasis. They can be administered orally improving compliance to therapy and reducing hospitalization. TKIs also induce less cardiac adverse effects than trastuzumab, thus they can be employed in heart-suffering patients. Moreover, TKIs show a broader specificity than trastuzumab, targeting for example HER2 isoforms lacking ECD o trastuzumab binding site (Hurvitz et al. 2017).

Lapatinib was the first TKI to be introduced in the clinical practice. It reversibly binds tyrosine kinase domain of HER1 and HER2. Direct comparison of lapatinib to trastuzumab and taxane in first-line setting did not show any superiority of lapatinib neither in survival nor in the safety profile of the drug. On the contrary, in the adjuvant setting this inhibitor showed benefit in combination with chemotherapy or with chemotherapy and trastuzumab in terms of progression-free and/or overall survival. An action on brain metastasis was not clearly shown in specifically designed trials CEREBREL and EMILIA. Following these results and emergence of newer and more effective agents such as T-DM1, lapatinib use is now limited to advanced breast cancer as

a second and further-line of treatment (Loibl and Gianni, 2017; Hurvitz et al., 2017; Baselga et al., 2017).

Neratinib is an irreversible pan-HER2 inhibitor targeting tyrosine kinase domain of HER1, HER2 and HER4. Initial studies *in vitro* demonstrated specificity and superiority to lapatinib in HER2-positive cell lines. Its action was shown to be mediated by a reduction in pHER2, pAkt and pErk in treated cell lines. Combination of trastuzumab and neratinib further inhibited growth of HER2-positive human cell lines *in vitro*, impeding reactivation of pHER3 as a compensatory mechanism. *In vivo*, volumes and weight of tumours induced by HER2-positive human cell line BT474 were diminished by treatment with neratinib alone or in combination with trastuzumab. Its action was again mediated by down-regulation of HER2, pHER2, pHER3, pAkt and pErk which, although not statistically significant, was even stronger in mice treated with the combination of neratinib and trastuzumab (Canonici et al., 2013). Clinical efficacy of neratinib has been evaluated in first- and second-line and on brain metastasis. In the NefERT-T trial, Neratinib combined with paclitaxel did not show any superiority with respect to trastuzumab+paclitaxel in early metastatic breast cancer; however, the tyrosine kinase inhibitor significantly delayed and reduced incidence of brain recurrences. In ExteNet trial neratinib ameliorated 2-year progression free survival of 2.3% with respect to placebo in women with grade I-III HER2-positive breast cancer who had completed 1-year adjuvant trastuzumab (Baselga et al., 2017; Unni et al., 2018). This result granted its approval in advanced breast cancer by FDA (Food and Drug Administration) in 2017. EMA (European Medicines Agency) was in turn more cautious and initially refused permit for neratinib commercialization in Europe; the small improvement in progression free survival was judged not to outweigh the increased frequency of adverse effects observed in the neratinib treated arm. Grade 3/4 adverse effects of diarrhoea were indeed often observed in both trials and prophylaxis with loperamide was requested to prevent these adverse effects. After re-examination of results, EMA granted neratinib approval (2018) only in a subset of patients with ER+/PR+/HER2+ disease (triple positive), where neratinib appeared to elicit a more significant protective effect. Neratinib efficacy is currently being assessed with respect to lapatinib, both in combination with capecitabine, in metastatic breast cancer previously treated with two HER2-targeted agents.

Novel tyrosine kinase agents are currently in the pipe-line of clinical development, such as ONT-380 with an expected improved activity against brain metastasis, tucatinib which

selectively inhibits HER2 and not HER1 thus reducing adverse effects such as diarrhoea and skin rush, poziotinib and pyrotinib which show promising activity on tumours harbouring HER2 mutations. All of them are being evaluated in phase II trials (Escrìvia-de-Romani et al., 2018) (Table 3).

3.4 Other strategies

Most of HER2 targeted treatments involve antibodies, thus it can be expected that checkpoint inhibitors could positively modulate activity of the immune system potentiating trastuzumab action. Thus, various combinations of checkpoint inhibitors, such as atelimizumab and pembrolizumab, with current standard of care are being investigated in HER2-positive breast cancer.

Abundant preclinical evidence has demonstrated a role of cyclin D1 and E and cdk4/6 in HER2-positive breast cancer. Hence, cdk4/6 inhibitors such as palbociclib, ribociclib and abemaciclib are being evaluated both in neoadjuvant and adjuvant setting (Table 3).

Lastly, barely 40% of HER2-positive breast cancer harbour mutations in PI3K pathway which may lead to resistance to HER2 targeted therapies; so, it is not surprising that many inhibitors of PI3K are being developed for use as single agents or in combination with HER2 targeted therapies. Among them, buparlisib, pilaralisib and copanlisib, apelisib and tapelisib are being evaluated in phase I or II clinical trials (Escrìvia-de-Romani et al., 2018) (Table 3).

	Trastuzumab	Lapatinib	T-DM1	Pertuzumab	Neratinib
Class Mechanism of action	Monoclonal antibody Recombinant humanized monoclonal antibody that inhibits ligand-independent HER2 and HER3 signaling, inhibits the shedding from the extracellular domain, and might trigger antibody-dependent cellular cytotoxicity	Tyrosine kinase inhibitor Dual tyrosine kinase inhibitor of HER2	Antibody-drug conjugate Monoclonal antibody directed at the dimerization domain of HER2	Monoclonal antibody Antibody–drug conjugate in which trastuzumab is stably linked to a potent microtubule inhibitor that is a derivative of maytansine	Tyrosine kinase inhibitor Tyrosine kinase inhibitor of HER1, HER2, and HER4
Route of administration and half-life	Endovenous, weeks	Oral, 24 hours	Endovenous, 4 days	Endovenous, weeks	Oral, 24 hours
Adverse effects	Rare cardiotoxicity and diarrhea	Rare cardiotoxicity; skin rush; dose-limiting toxicity causing diarrhea	No cardiotoxicity; rare diarrhea	Rare cardiotoxicity; dose-limiting toxicity causing diarrhea	No cardiotoxicity; dose-limiting toxicity causing diarrhea
Indication	HER2-positive early breast cancer; HER2-positive metastatic breast cancer	HER2-positive metastatic breast cancer in combination with capecitabine, trastuzumab, or an aromatase inhibitor	HER2-positive metastatic breast cancer that has not already been treated with chemotherapy medicines, or treated together with trastuzumab and docetaxel for non-operable HER2-positive breast cancer	HER2-positive advanced or metastatic breast cancer in adults who previously received trastuzumab and a taxane	In development for the treatment of HER2-positive early breast cancer and metastatic breast cancer

Table 2. Pharmacological characteristics of approved anti-HER2 agents.
The table sums up principal pharmacological characteristic of currently approved targeted drugs against HER2. (Modified from Garret & Arteaga, 2011; Loibl & Gianni, 2017).

Agent	Mechanism of action	Reported results	Further Development
NOVEL ANTI-HER2 ANTIBODIES			
Margetuximab (MGAH22)	Optimized Fc domain for enhanced binding To the activating low-affinity Fc receptor, Fc RIIIA	Phase I monotherapy clinical trial, 12% pts. with PR; PFS of 5.5 months	Phase III trial (NCT02492711) margetuximab + chemotherapy vs. trastuzumab+ chemotherapy
MCLA-128	IgG1 bispecificfic antibody with enhanced ADCC activity targeting both HER2 and HER3 receptors	Phase I/II monotherapy clinical trial 70% CBR.	Further exploration of MCLA-128 based combinations with chemotherapy or trastuzumab is planned
ZW-25	Bispecific antibody directed against two distinct epitopes of HER2	Phase I preliminary results: 8 BC pts: 2 PR, 2 SD, 3 PD.	Phase I (NCT02892123)
ANTIBODY-DRUG CONJUGATES (ADC)			
SYD 985	Trastuzumab with an alkylant prodrug DUBA (Duocarmicin derivate) payload	Phase I monotherapy ORR 34% in HER2-positive and HER2 low breast cancer	Phase III trial (TULIP) with a 2:1 randomization of SYD 985 vs physician treatment's choice (NCT03262935)
DS- 8201	HER2 antibody attached to a topoisomerase I inhibitor (DXd) payload	Phase I ORR 40.2%, DCR (disease control rate) 91.8%	Phase II trial in patients resistant or refractory to T-DM1 (NCT03248492)
TYROSINE KINASE INHIBITORS (TKIS)			
Tucatinib	ATP competitive, selectively inhibits HER2 relative to EGF	Phase Ib: Capecitabine+Trastuzumab+ Tucatinib: RR 61%; CBR 74%	Capecitabine+ Trastuzumab ± Tucatinib/placebo
Poziotinib	Irreversible pan-HER kinase inhibitor	Phase II monotherapy: PFS of 4.04 months: DCR of 75.49%.	Phase II trial monotherapy: HER2-positive (NCT02659514) Phase II trial monotherapy: HER2 or EGFR mutation or activated AR or EGFR pathway (NCT02544997)
Pyrotinib	Irreversible TKI pan-HER kinase inhibitor	Phase I: RR 50%, CBR 61%, PFS 35.4 weeks.	Phase III Trial (NCT02973737): Pyrotinib+ Capecitabine vs. Placebo+ Capecitabine
CHECKPOINT INHIBITORS			
Atezolizumab	Anti-PD-L1 antibody	NR	Phase II KATE2 (NCT02924883): T-DM1+ Atezolizumab/Placebo Phase 2 single arm (NCT03125928): Paclitaxel+ Trastuzumab + Pertuzumab+Atezolizumab
Pembrolizumab	anti-PD-L1	NR	Phase Ib (NCT03032107): Pembolizumab+T-DM1

		antibody	
CDK4/6 INHIBITORS			
Palbociclib	CDK4/6 inhibitor	NR	Phase II PATRICIA (NCT02448420): Palbocilib+ trastuzumab±Letrozol. Phase III PATINA (NCT02947685): Palbociclib+Trastuzumab±Pertuzumab
Abemaciclib	CDK4/6 inhibitor	NR	Phase II trial MonarcHER (NCT02675231): Abemaciclib+Trastuzumab±Fulvestrant vs. Chemotherapy+Trastuzumab
Ribociclib	CDK4/6 inhibitor	NR	Phase Ib/II trial (NCT02675231): Ribociclib+Trastuzumab or T-DM1
PI3K INHIBITORS			
Alpelisib	- specific PI3K inhibitor	Phase I: Alpelisib+ T-DM1: All pts. PFS 6 months, PFS in 6 pts with prior T-DM1 10.6 months.	Phase I trial (NCT02167854). Alpelisib+Trastuzumab for pretreated pts. requiring a PI3K mutation
Copanlisib	Pan-class PI3K inhibitor	NR	Phase Ib/II Panther trial (NCT02705859): Copanlisib+Trastuzumab
Taselisib	- sparring PI3K inhibitor	Phase Ib (NCT02390427): Arm A: Taselisib+ T-DM1: 4% CR, 29% PR, 50% SD.	Phase Ib (NCT02390427): Arm A: Taselisib+T-DM1; Arm B: Taselisib+T-DM1+Pertuzumab; Arm C: Taselisib+Pertuzumab+Trastuzumab; Arm D: Taselisib+Pertuzumab+Trastuzumab+Placlitaxel

Table 3. Novel anti-HER2 agents and combinations

The table reports new anti-HER2 agents by mechanism of action, reported clinical results and further development. Abbreviations: pts. patients; PR. Partial response; PFS. Progression free survival; vs. versus; ADCC Antibody-dependent cell-mediated cytotoxicity; CBR. Clinical benefit rate; ORR. Overall response rate; NR. Not reported; DCR. Disease control rate (Modified from Escriva-de-Romani et al., 2018).

4. Tumour as heterogeneous society

4.1 The concept of oncogene-addiction and intra-tumour heterogeneity

HER2 expression is not always homogenous and wide-spread in every cell in a tumour. Clinically, 10% of cells overexpressing HER2 at membrane level or a HER2: CEP ratio 2 or a HER2 copy number >6 are enough to classify a breast cancer as HER2-positive (Loibl & Gianni, 2017). As a consequence, different HER2-positive tumours do not show the same level of HER2 expression and the same percentage of cells overexpressing HER2. In 1-40% of HER2-positive breast cancers, indeed, different clones can be identified with different HER2 expression. These phenomena are known as inter-tumour and intra-tumour heterogeneity. Moreover, they represent a clinical issue and heterogeneous tumours for HER2 expression show a shorter overall survival when compared to homogeneous tumours (Ng et al., 2015).

Cancer cells contain multiple genetic and epigenetic abnormalities. Despite this complexity, their growth and survival can often be impaired by the inactivation of a single oncogene. This phenomenon, called "oncogene addiction," provides a rationale for molecular targeted therapy (Weinstein & Joe, 2008). It is of main importance for the success of HER2 targeted therapies to ensure that the vast majority of tumour cells are indeed addicted to HER2 expression for the maintenance of malignant phenotype (Escrìvia-de-Romani et al., 2018). In some cases, HER2 could represent a passenger mutation found in a minority of cells rather than the driver mutation of the tumour sustaining its proliferation. When HER2 is therapeutically targeted, if the tumour is addicted to HER2 expression for maintenance of malignant phenotype, cells will undergo apoptosis, senescence or at least will stop growing. On the contrary, if the tumour is not addicted to HER2, targeted therapies will not eradicate the disease and may select clones which show no HER2 overexpression.

4.2 Receptor discordance and loss of HER2 expression

Expression of ER, PR and HER2 has for a long time been considered an intrinsic property of breast cancer. Nevertheless, receptor discordance between primary tumour and loco-regional or distant metastases is non-rarely observed and affects not only HER2, but ER and PR.

ER was found differently expressed in primary tumours and metastasis in percentages ranging from 7.3% to 51.2% of analysed patients, with metastasis acquiring expression of

this receiver in 21.5% of and losing it in 22.5% of cases. Alterations in expression of PR were detected in meta-analytic pooled percentage of 30.9%. Expression of this receptor was more frequently lost (49.4%) than acquired (15.9%) in the metastasis (Schrjiver et al., 2018). HER2 discordance percentage between primary tumours and metastasis was reported between 0% and 34%, with a pooled meta-analysis percentage of 10.8%. HER2 changed twice as often from positive to negative (21.3%) than vice versa (9.5%) (Schrjiver et al., 2018) (Picture 4).

The role of adjuvant therapy with endocrine inhibitors or trastuzumab is currently under investigation and literature reports contrasting data. Endocrine therapy is reported to trigger conversion to ER negative disease in brain metastasis, whereas trastuzumab does not promote HER2 loss in the same setting (Timmer et al., 2017). In a different study, trastuzumab in turn appears to increase the rate of loss of HER2 in metastasis (19.8%) with respect to patients treated with chemotherapy only (9.4%) (Wang et al., 2017).

Effect of receptor conversion on prognosis is controversial, as well. BRITS and DESTINY clinical trials did not show significant effects of receptor conversion on patients' survival (Amir et al., 2012), whereas other studies reported a decreased time to progression and survival in patients losing HER2 expression in metastasis (Niikura et al., 2012; Dieci et al., 2013; Wang et al., 2017).

Receptor conversion is a recognized clinical issue and entails a risk of treatment failure in discordant metastasis. Up-to-date guidelines therefore recommend new assessment of receptor in any metastasis or recurrences. If a receptor is gained, targeted therapy already exists and can be promptly administered. On the contrary, when either HER2 or ER expression is lost, tumours lose their oncogene-addiction and depend on a different pathway for maintenance of their malignant phenotype. Extensive research is ongoing to identify oncogenic drivers and therapeutic targets in tumours losing HER2 and ER expression. Clinical data are not mature yet, to determine whether therapeutic changes upon receptor conversion actually improve patients' prognosis (Schrjiver et al., 2018).

Importantly, loss of HER2 expression has been detected in HER2-positive gastric and gastroesophageal cancer, as well (Pietrantonio et al., 2016).
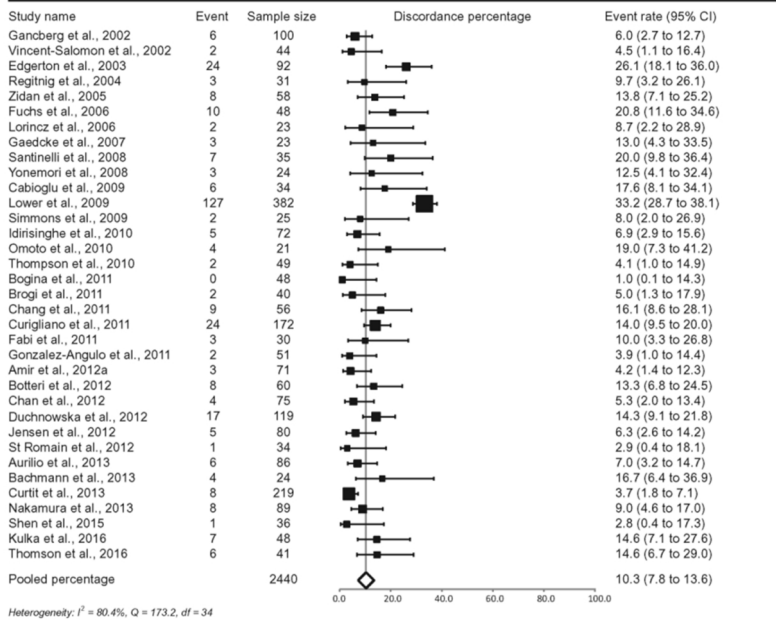
Picture 4. Meta-analysis of HER2 discordance

The tables report discordance percentages for HER2 of single studies and the pooled estimate discordance in primary breast tumors and paired distant metastases. Discordance percentages are shown for total conversion (A), conversion from positive to negative (B), and conversion from negative to positive (C). Error bars indicate confidence intervals. Heterogeneity was assessed using I2 and Cochran's Q. CI ¼ confidence interval; df ¼ degrees of freedom (Schjiver et al., 2018).
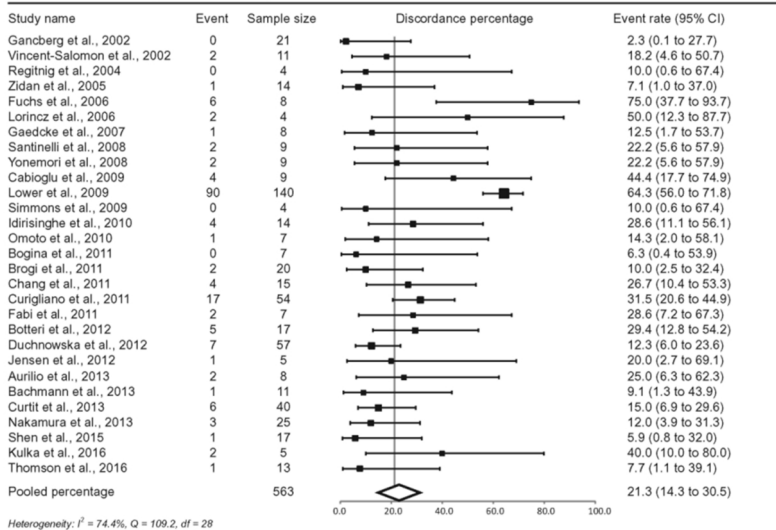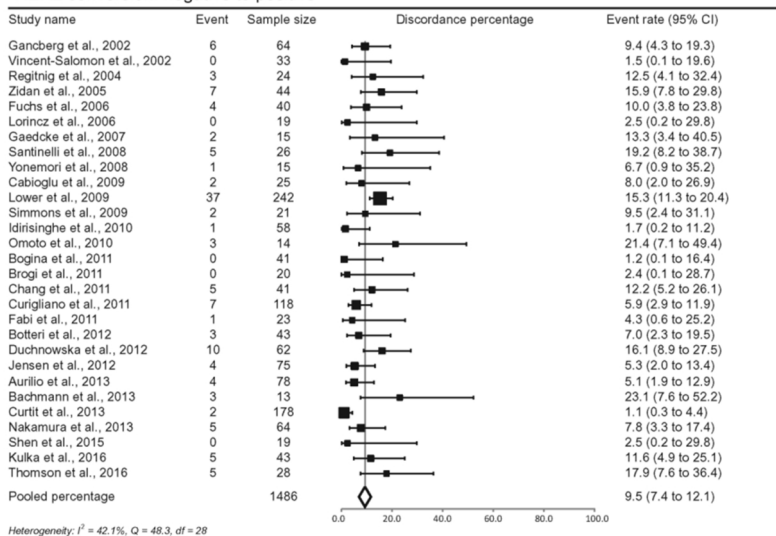
4.3 Breast Cancer Stem Cells and Plasticity

Cancer stem cell concept supports a hierarchical organization of the tumour cells and predicts that only a specific sub-population with stem cell-like properties, such as the capacity to self-renew and generate the heterogeneous lineages of cancer cells, is able to initiate tumorigenesis (Duru et al., 2013). These cells were firstly identified in breast cancer as a sub-population (1-5%) able to give rise to colonies *in vitro* and to tumours, even if extremely diluted, *in vivo* (Al-Haji et al., 2003). These multipotent cells are characterized by plasticity, an altered balance between self-renewal and differentiation, and an active program of EMT, which allow them to sustain tumour growth at different levels: support of primary tumour, relapse, metastasis and resistance to chemo- and radiotherapy (Nigam et al., 2012; Kotiyal and Battarchaya, 2014).

At molecular level, breast cancer stem cells (BCSC) are identified by cytofluorimetric analysis as CD44+/CD24-/low/Lin-; other markers which help characterizing BSCS are Cd49f, CD29, Sca-1, ESA/EpCAM, cytokeratins 5 and 14, ALDH enzymes, IL1a, IL-6, IL-8, and urokinase plasminogen activator (UPA) (Al-Haji et al., 2003; Nigam et al., 2012; Duru et al., 2013). Active pathways sustaining BCSCs are TGF- , NOTCH, SonicHedgog, NFkb, Dach-1, p21, cyclin D1 and MAPK/ERK (Velasco-Velasquez et al., 2013).

EMT is a physiological process essential during embryogenesis, tissue repair and fibrosis. During metastasis of carcinomas, epithelial cancer cells are believed to undergo EMT in order to acquire migratory abilities, necessary for metastasis. EMT reprogramming occurs at transcriptional level and leads to loss of cell polarity and cell-cell adherent junctions, and gain of mesenchymal stem cells properties with ability to migrate. Master regulators of EMT are Snail, Slug, Zinc finger E-box-binding homeobox-1 (ZEB1), ZEB2, Forkhead box protein 1 (FOXC1), FOXC2, Transcription factor 3 (TCF3) and homeobox protein Goosecoid (GSC). Down-stream pathways activated during EMT are represented by a network of several stemness signalling pathways such as TGF- , Wnt/ -catenin, Notch, JAK/STAT, Hedgehog, inflammatory pathways such as NF- B, extracellular and intracellular growth factors such as Epidermal growth factors (EGFs), Insulin-like growth factor 1 (IGF1), Fibroblast growth factors (FGFs), Platelet-derived growth factor (PDGF) and interleukins (IL6 and IL8), cell adhesion transmembrane proteins such as E- and N-cadherins and filament protein vimentin. Altogether, these processes reprogram epithelial cells to transit to the mesenchymal phenotype (Nami and Wang, 2017).

BSCSs display a mesenchymal phenotype and localize at tumour expanding periphery. Although BCSCs are generally negative for both luminal marker and HER2, the latter has been proposed as a novel regulator of BCSCs. Indeed, it has been found to increase staminal properties of BCSCs and anti-HER2 targeted therapies have in turn been associated to a decrease in staminal properties of tumours. An active and supportive role of HER2 has been reported in all signalling pathways sustaining stemness, such as TGF- /Smad, Notch, Wnt/ -catenin and JAK/STAT (Picture 5). However, HER2 appears to promote EMT as well through structure disruption of the tight junction which leads to loss of cell poarity; during this process, metalloproteases result up-regulated and cleave HER2 itself besides many proteins involved in cell-cell and cell-ECM adhesion. Cleavage of HER2 produces p95HER2 fragment, which lacking the ECD is not recognized by trastuzumab, but retains signalling activity, leading to resistance (Nami and Wang, 2017).
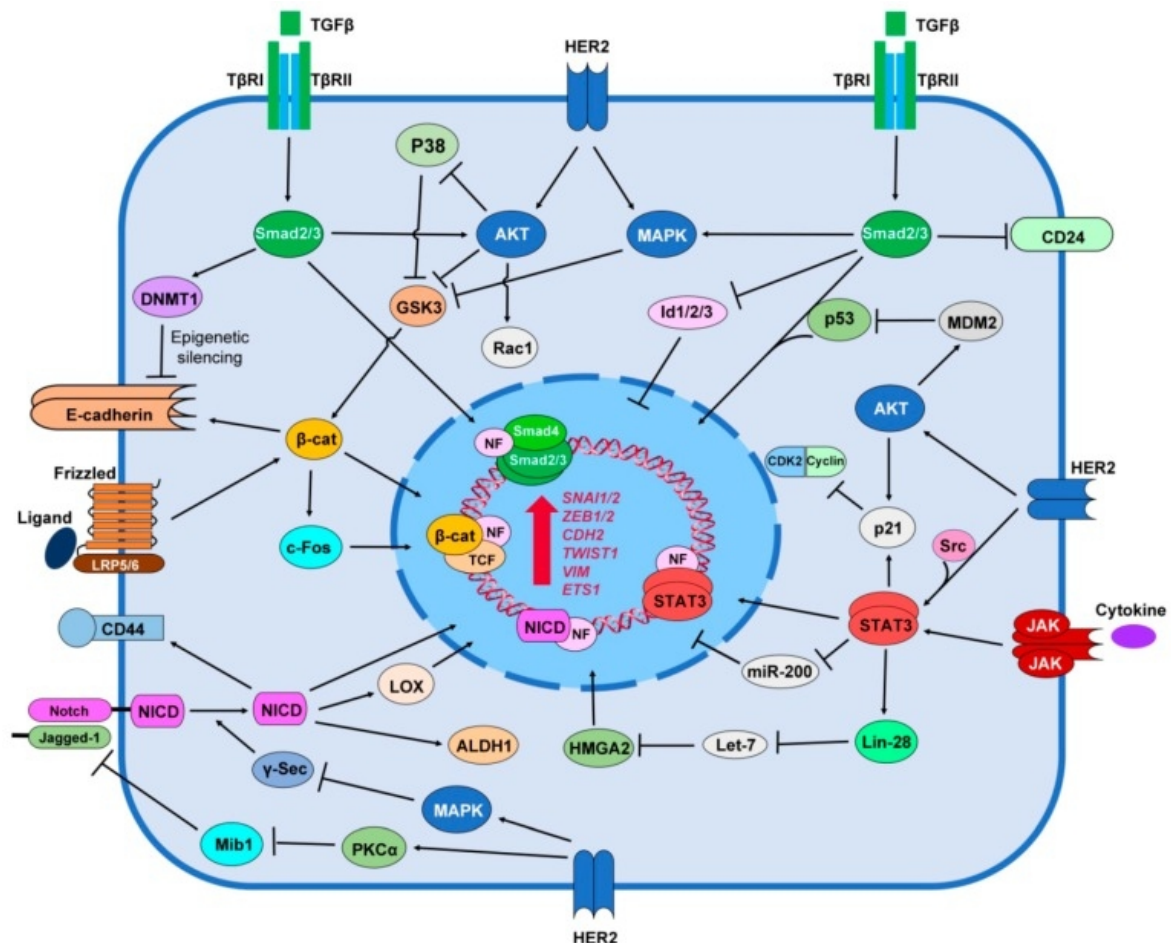
Picture 5. Cross-talk between HER2 and BCSC signalling pathways
The cartoon describes interaction between HER2 and pathways sustaining cancer stem cells in breast cancer (Nami & Wang, 2017).

5. Preclinical models of breast cancer

5.1 Murine models of HER2/neu driven mammary carcinogenesis

Most of our knowledge of the role of HER2 in mammary carcinogenesis is derived from preclinical models.

Initially, a mutation of neu, the HER2 homolog in rat, was identified in a chemically induced model of breast cancer and later validated as able to transform NHI 3T3 murine fibroblast cell line. Mutated oncogene, neuT, harbours a point mutation (V664E) which triggers dimerization and signalling of neu receptor. Hence, the first preclinical models of neu driven mammary carcinogenesis were represented by mice transgenic for neuT under control of MMTV (mouse mammary tumour virus), which restrains expression of the transgene to mammary epithelium. These mice develop mammary tumours with low latency and high incidence. Transgenic mice harbouring the proto- oncogene neu still develop mammary tumours with high incidence, but much longer latency due to time required for accumulation of tumorigenic mutations (Guy et al., 1992; Muller et al., 1988; Bose et al., 2013). Different promoters have been used up-stream neu and neuT transgenes with different phenotypes (Boggio et al., 2000; Andrecheck et al., 2000; Weinstein et al., 2000; Freudenberg et al., 2009;)

In human tumours, HER2 is not often mutated but amplified and hence overexpressed in the vast majority of HER2 enriched breast cancers; consequences of this difference have already been discussed in paragraph 2.3 of this introduction. To better mimic human carcinogenesis and to yield model for the study of anti-human HER2 targeted therapies, a murine model has been developed harbouring multiple copies of human HER2 wild-type gene under MMTV promoter: HER2 is thus overexpressed preferentially in mammary epithelium. FISH and PCR analysis have revealed 30-50 copies on the transgene inserted in chromosome 6. HER2 overexpression is tumorigenic in 76% of female mice with a mean latency of 28.2 weeks (Finkle et al, 2004; De Giovanni et al., 2014). Histopathological analysis of tumours evidenced solid, papillary and tubular growth accompanied by high mitotic index and aberrant cellular shape. HER2 expression at membrane level is high, yet heterogeneous. Spontaneous lung metastasis is found in 23% of mice (Finkle et al, 2004; De Giovanni et al., 2014).

Full-length HER2 oncoprotein and splice variant   16 are co-expressed in human breast cancer. Therefore, transgenic mice harboring   16 have been developed and crossed with

animals transgenic for the full-length HER2, obtaining F1 mice harboring both isoforms (Castiglioni et al., 2006; Marchini et al., 2011; Castagnoli et al., 2017; Palladini et al., 2017).

5.2 Mammary patient derived xenograft models (PDX)

With respect to basic and translational research, breast cancer inter- and intra-tumoral heterogeneity present significant challenges to generation and use of relevant pre-clinical models that represent the full spectrum of breast disease (Dobrolecki et al., 2017). Patient-derived xenografts (PDXs) are an extremely useful tool in the perspective. Available human breast cancer cell lines and cell lines derived from preclinical models of mammary carcinogenesis are representative of a limited subset of breast tumors. Moreover, not all of them are tumorigenic *in vivo*. PDXs recapitulate and stably maintain over time the characteristics of originating tumor at genomic, phenotypic, histological, molecular and metabolic level. A collection of mammary PDXs could hence be representative of a wider variety of human breast cancers.

Mammary tumors graft in immunocompromised mice with very high rates (40%), but only 10% of implanted tumors actually give rise to a stable PDX, i.e. transplantable for at least three passages *in vivo*, with a bias towards more aggressive tumors being more represented into PDX collections (Dobrolecki et al., 2017).

Recently, a consortium of academic institutions has gathered 537 PDX models, representative of 500 individual specimen. Implanted samples derived from primary tumors (79%), pleural effusions (6%), ascites (3%) or metastasis (15%). The vast majority of PDX in this collection originated from triple negative tumors (56%). Despite representing 10-15% of all mammary carcinomas, this subtype shows a very high take. 36% of PDXs represent patients with ER+ disease, which is under-represented with respect to clinical occurrence, since low malignancy of luminal tumors makes it difficult to obtain PDX of this subtype. Only the remaining 8% represent HER2-positive breast cancers, due to low take rate and stable PDX yields from this subtype (Dobrolecki et al., 2017).

PDX are an always renewable resource of tumor tissue, which is useful for in depth and repeated analysis and for in parallel or subsequent testing of different drugs (Dobrolecki et al., 2017). Indeed, the US National Cancer Institute (NCI) has replaced their NCI-60 cell line resource (a panel of 60 mammary cell lines used for drug screening) with PDX

samples, highlighting the importance and acceptance of this resource (Holen et al., 2017). However, when using PDXs for testing drugs it should be kept in mind that the bias towards aggressive tumors may falsely infer therapeutic benefit (or indeed not). Moreover, study of the tumor microenvironment is compromised due to intrinsic species differences and the lack of immune cells in tolerant hosts (Holen et al., 2017).

It is still under scientific debate, whether PDXs recapitulate metastatic pattern of tumors of origin. The latter are indeed obtained at the time of surgery and long observation time may be requested to understand whether PDX metastasize at the same organs of derivative tumors in patients. However, metastasis in PDX are often observed in lymph nodes and lungs, whereas breast tumors preferentially disseminate to bone and brain (Holen et al., 2017).

Initially, the possibility was conceived to exploit PDX models as mouse 'avatars' for personalizing treatment to individual patients. However, clinical decision-making is quick (weeks), compared with the time taken to establish a PDX (even a year) and low take rates and high costs further limit use of PDX models as avatar. Hence, currently the potential of these models is limited to cohort-based preclinical studies (Holen et al., 2017).

5.3 Models of HER2 loss

Various strategies have been employed to transiently knock-down HER2 expression *in vitro* and *in vivo*, at different stages of tumour development.

HER2 silencing with siRNA, ribozymes on antisense RNA resulted in inhibiting tumour cell growth both *in vitro* and in vivo. Cell lines used appear hence to be oncogene-addicted to HER2, since the stop growing once HER2 expression in down-modulated. In MMTV-neuT mice, where transgene expression was inducible by tetracycline or doxycycline, once neuT expression was knockdown, tumours regressed as well (Moasser et al., 2007).

Sometimes, though, emergence of HER2-neu negative or mesenchymal populations out of HER2-neu positive or polygonal mammary cell lines has been reported either spontaneously or in concomitance with drug-resistance.

Cell lines derived from p185(neu)-positive tumours arisen in FVB-NeuN mice (N202) bearing the rat neu protooncogene driven by the mouse mammary tumour virus

promoter/enhancer gave rise to p185(neu)-positive and p185(neu)-negative clones. In vitro, analysis of anchorage-independent growth in soft agar revealed colony formation from p185(neu)-positive but not p185(neu)-negative cells. Upon in vivo injection, p185(neu)-positive cells gave rise to fast-growing tumours with a short latency, while p185(neu)-negative cells required a very long latency time, and the resulting tumours were invariably p185(neu)-positive (Nanni et al., 2000).

TUBO-P2J is a variant of TUBO cell line. TUBO derive from the tumour of a mice transgenic for neuT expression (see paragraph 5.1). Cells injected in mice treated with anti-neu antibody eventually gave rise to lung metastasis, whose cells had lost neu expression (TUBO-P2J). In this cell line, loss of neu expression was associated with mesenchymal morphology, resistance to chemotherapy, increased migration and metastasis and characteristics of EMT, such as loss of epithelial markers and acquisition of mesenchymal markers both at transcript and at protein level (Song et al., 2014).

SkBr3 and BT474 were kept long-term in increasing concentrations of lapatinib or AZD8931 (a different tyrosine kinase inhibitor) giving rise to resistant cells lines, which displayed a decreased expression and phosphorylation of HER2 and HER3. Drug-resistant cell lines acquired an EMT profile, increased proliferation and migration ability (Creedon et al., 2016).

Materials and Methods

1. Mice

The experiments reported in this thesis were performed in three different murine strains:

- Breeders for the two immunodeficient strains, NOD-SCID-Il2rg$^{-/-}$ (NSG) and BALB/c Rag2$^{-/-}$Il2rg$^{-/-}$ were received from Jackson Laboratories (USA) and Drs T. Nomura and M. Ito (Central Institute for Experimental Animals, CIEA, Kawasaki, Japan), respectively. Animals were inbred at our animal facility and kept under sterile conditions.
- FVB MMTV.f.huHER2 mice (Finkle et al., 2004) were received from Genentech Inc. (South San Francisco, CA, USA). In our animal facility human HER2 was maintained in heterozygosis by crossing male transgenic mice with non-transgenic FVB female mice purchased from Charles River (Calco, Italy). Mice were routinely genotyped by PCR analysis (Finke et al., 2004). In this thesis, these mice will be further referred to as FVBhuHER2.

All experiments were approved by the institutional review board of the University of Bologna, authorized by the Italian Ministry of Health and performed according to Italian and European legislation and guide-lines.

2. Cell lines

Cell lines derived from mammary tumors spontaneously arisen in FVBhuHER2 mice and all their derivatives were previously obtained and characterized in the Laboratory of Biology and Immunology of Metastasis. Cells were cultured in DMEM (Dulbecco's Modified Eagles' Medium; Life Technologies, Milan) supplemented with penicillin 100 U/ml and streptomycin 100 µg/ml (Life Technologies, Milan), 20% Fetal Calf Serum (FCS, Life Technologies, Milan) and growth factors, such as Bovine Pituitary Extract (30 µg/ml, BD Biosciences, USA) and MITO Serum Extender (0.5% v/v, BD Biosciences, USA). Mammary murine cell lines TS/A, obtained at Laboratory of Biology and Immunology of Metastasis, and its derivative overexpressing mIL-6, TS/A IL-6 (Di Carlo et al., 1997), were cultured in DMEM supplemented with antibiotics 10% FCS only; TS/A IL-6 was kept under selection by geneticin 500 µg/ml.

Human mammary cell lines, BT474, MDA-MB 453, SkBr3, MCF7, kindly given to the Laboratory of Biology and Immunology of Metastasis by Dr. Serenella M. Pupa (Istituto Nazionale dei Tumori, Milan, Italy), MDA-MB 231 and HCC1954, purchased by ATCC,

were cultured in RPMI (Roswell Park Memorial Institute; Life Technologies, Milan) supplemented with antibiotics and 10% FCS only.

Cells were cultured at 37°C in humidified atmosphere at 5% CO_2. Cell were split once or twice a week according to density using trypsin-0.05% EDTA (Life Technologies, Milan) for detachment. Whenever needed, cells were counted on Neubauer's hemocytometer using the vital colorant erythrosine (Sigma, Milan) and harvested for cytofluorimetric or molecular analysis.

2.1 Long term colture with trastuzumab

HER2^{stable}, HER2^{labile} and HER2^{loss} cells were kept in colture with trastuzumab 30 μg/ml for two months.

HER2^{stable} and HER2^{loss} cells were harvested twice a week and seeded in medium with or without trastuzumab. After 28 days, HER2 as well as expression of staminal marker (CD24 and CD44) was assessed by citofluorimetric analysis and samples were collected for molecular analysis. Afterwards trastuzumab was either maintained in medium (TRNT cell lines) or removed (TRT cell lines) for 28 days. Again, HER2 as well as expression of staminal marker (CD24 and CD44) was assessed by citofluorimetric analysis. At this time-point samples for RNASequencing were collected as well.

HER2^{labile} cells followed the same protocol with the exception of being splitted once a week. Every time cells were counted and seeded at a concentration of either 1.6×10^5 cells/cm^2 or 4×10^4 cells/cm^2. Citofluorimetric analysis was performed weekly.

2.2 Sensitivity to demethylating agent

HER2^{labile} and HER2^{loss} cells were seeded at 8×10^4 cells/cm^2. 24 hours after seeding, cells where treated with vehicle (DMSO 0.02%), 5' aza-2-deoxycytidine (Sigma) 0.5 μM or 5 μM. Treatment was renewed after 72 hours of treatment. Cells were harvested after 48, 72 and 144 hours of treatment and counted. HER2 expression was determined by cytofluorimetric analysis.

2.3 Sensitivity to sunitinib *in vitro*

Sensitivity to sunitinib *in vitro* was determined under different conditions of culture.

For the experiment under 2D adherent conditions HER2^{loss} cells were plated at 3.125×10^3 cells/cm^2 in 96-well plates (Corning Life Sciences, USA) in medium. After 24 hours from seeding, cells were treated with Sunitinib 0.1, 0.5, 1, 5 and 10 μM (LC Laboratories, MA,

USA), or DMSO 0.2% (Sigma) or fresh medium. Each treatment was evaluated in triplicate. After 72 hours of treatment, WST-1 reagent (Sigma) was added to each well and absorbance at 450/620 nm was measured 60 minutes thereafter with an ELISA microreader (Tecan Systems).

For the experiment under 3D non-adherent conditions, HER2^{loss} cells (0.5×10^3 cells/cm^2) were suspended in a solution of agarose 0.33% (Sea Plaque Agarose; Cambrex Bioscience Rockland, ME, USA) in medium containing DMSO 0.02% (Sigma) or sunitinib 1 or 5 µM (LC Laboratories, MA, USA) or no drug. On 24-well plates (Corning Life Sciences, USA), this overlayer was stratified on a jellified underlayer of 0.5% agarose in medium containing DMSO 0.02% (Sigma) or sunitinib 1 or 5 µM (LC Laboratories, MA, USA) or no drug. Colonies were counted after 14-22 days.

Evaluation of long-term sensitivity to sunitinib was performed seeding HER2^{loss} cells (8×10^4 cells/cm^2) in medium containing sunitinib 5 µM (LC Laboratories, MA, USA) or DMSO 0.05% (Sigma). Cells were split after 4 days; some samples and supernates were collected for further molecular analysis. Cells were cultured further on and split according to density in medium containing sunitinib, DMSO or no drug.

2.4 Tube Formation Assay
HER2^{loss} cells were seeded 8×10^4 cells/cm^2. After 24 hours, medium was replaced with fresh medium containing either sunitinib 5 µM (LC Laboratories, MA, USA) or DMSO 0.05% (Sigma). After 24 hours of treatment cells were harvested and seeded dropwise 6.3×10^4 cell/cm^2 in 24-well plate (Corning Life Sciences, USA), on a base of Matrigel diluted 10 mg/ml in DMEM basal medium (Corning, NY, USA) and let solidify 1 hour at 4°C. Plates were incubated at 37°C, 5% CO$_2$ over-night and the formation of vessel-like channels was observed 16-18 hours after seeding.

2.5 mIL-6 production
Cells were seeded 8×10^4 cells/cm^2 in medium containing either sunitinib 5 µM (LC Laboratories, MA, USA) or DMSO 0.05% (Sigma) or trastuzumab 30 µg/ml or no drug. After 4 days, supernates were collected, measured, centrifuged (2000 RCF, 20 min, 4°C) and filtered through 45 µm filters (Millipore) to eliminate cell debris. Aliquots were frozen and kept at -20°C.

mIL-6 production was analyzed with Mouse IL-6 Quantikine ELISA Kit (R&D Systems) according to manufacturer's protocol. Briefly, supernates were diluted in assay buffer and distributed on wells pre-coated with a specific anti-mouse IL-6 antibody. After 2 hours' incubation at room temperature, wells were washed three times with wash buffer and incubated again for two hours at room temperature with an enzyme-linked anti-mouse IL-6 antibody. After 3 washes, wells were incubated with the enzymatic substrate for 30 min at room temperature. Absorbance 450/620 nm was read on an ELISA microplate reader (Tecan Systems). Concentration of each sample was calculated interpolating values on a standard curve.

3. Murine mammary cell lines xenografts

HER2^{labile} and HER2^{loss} cells were subcutaneously (s.c.) injected in FVBhuHER2 or Balb/c Rag2$^{-/-}$ Il2rg$^{-/-}$ virgin female mice in the right posterior leg. Cells were diluted in 0.2 ml PBS (Phosphate Buffered Saline). Mice were palped and tumors measured with a caliper at least once a week. Tumor volumes were calculated as $\frac{\pi}{6}\left(\sqrt{a} \times b\right)^{3}$, where a represents tumor's major diameter and b tumor diameter perpendicular to a. At necropsy, tumors were harvested and disaggregated with trypsin-0.05% EDTA for cytofluorimetric analysis.

3.1 Treatment with trastuzumab *in vivo*

10^{6} HER2^{labile} cells were subcutaneously (s.c.) injected in FVBhuHER2 virgin female mice and treated intraperitoneally (ip.) with saline or trastuzumab 4 mg/kg twice a week starting from day 3 after cell injection. At necropsy, tumors were harvested and disaggregated with trypsin-0.05% EDTA for cytofluorimetric analysis.

3.2 Treatment with sunitinib *in vivo*

FVBhuHER2 mice harboring tumors induced by HER2^{labile} or HER2^{loss} cells were treated with sunitinib 60 mg/kg (LC Laboratories, MA, USA) *per os* by gavage. Animals in the vehicle group received METOCELL 0.5%+TWEEN80 0.4% (Sigma).

10^{6} HER2^{labile} cells were subcutaneously injected in the posterior leg of FVBhuHER2 mice treated starting 3 days after cell injection. Treatment in this group was originally planned on daily basis, but had to be discontinued due to weigh loss in treated mice; treatment was then continued every second day.

10^5 HER2^{loss} cells were subcutaneously injected in the posterior leg of FVBhuHER2 mice treated daily (7/7) starting the day after cell injection.

4. Patient Derived Xenografts (PDX)

Tumor fragments of BBR-4, SBR-45 or SBR-18, with a diameter of 3-4 mm, were serially implanted in the fourth left mammary intact fat pad, in anaesthetized 5-10-week-old NOD-SCID-Il2rg$^{-/-}$ (NSG) or BALB/c Rag2$^{-/-}$Il2rg$^{-/-}$ female mice. Mice were inspected weekly for tumor growth. Tumor volume was measured as previously described. At necropsy, tumors were harvested for molecular analysis, disaggregated with trypsin-0.05% EDTA for cytofluorimetric analysis or fixed in 10% buffered formalin solution (Sigma-Aldrich) for histological and immunohistochemical analysis.

For detection of metastatic dissemination, lungs, brain and femoral bone marrow were collected in cold phosphate buffered saline (PBS) and dissociated, both mechanically and with trypsin-0.05% EDTA, obtaining single cell suspensions. Defined fractions were used to obtain cellular pellets of each organ for quantitative comparison. Ovaries were frozen directly in vials, in liquid nitrogen, for nucleic acids extraction. In some cases, half of the lung and brain, one ovary, one femoral bone and the liver were fixed in 10% neutral buffered formalin solution for histological examination.

For experimental metastasis, BBR-4 PDX tumors of progressed and non-progressed sub-lines were dissociated to single cell suspensions and counted. 10^6 viable cells were diluted in 0.4 ml PBS and injected in a caudal lateral vein of female virgin immunodeficient mice.

4.1 Histological and immunohistochemical analysis

Histological and immunohistochemical analysis were conducted by pathologists at Bellaria or Sant'Orsola Hospital; we report the protocol for completeness. Primary or xenografted human neoplastic tissues were fixed in 10% buffered formalin (Sigma) for 12-24 hours at room temperature and afterwards processed using the Formalin/Ethanol/Isopropanol/Paraffin protocol by a hybrid tissue processor (Logos, Milestone Srl, Sorisole IT) to obtain paraffin blocks. Serial sections of Formalin-Fixed, Paraffin-Embedded (FFPE) tissue were cut, collected on adhesive glass slides (Tom-11, Matsunami Glass Ind., Ltd Osaka Japan) and air dried for at least 30 min at room temperature. Immunostaining was performed on FFPE sections in an automated

Benchmark Ultra Autostainer (Ventana Medical Systems, Inc., Tucson, Arizona, USA) with the following primary antibodies: anti-Bcl-2 (clone SP66), anti-ER (clone SP1), anti-PR (clone 1E2), anti-Ki-67 (clone 30-9), anti-HER2 (Pathway clone 4B5), anti-EGFR (clone EP38Y); anti-p53 (clone DO7). All antibodies were purchased from Ventana, except anti-EGFR (Thermo Fisher Scientific, Fremont USA or Abcam, Cambridge, UK). The immunologic reaction was visualized using the Ventana UltraView DAB Detection kit according to the manufacturer's instructions. Nuclear immunostaining for ER, PGR, Ki-67 and p53 was quantified using a semi-automated image analysis system (Image-Pro plus v.5.0.1, Media Cybernetics Inc., Rockville, USA) on at least 30 randomly selected 200× microscopic fields (2.000 cells) and expressed as percentage of immunostained neoplastic population. ER and PR were considered positive if $\geq$10% of neoplastic population was immunostained; Ki-67 values were classified as low $\leq$ 20%, intermediate 20<ki-67$\leq$30%, high > 30% of immunostained cells, according to St Gallen consensus 2015 suggestions HER2 expression was evaluated following ASCO/CAP 2013 recommendations. EGFR and Bcl-2 expression were semi-quantitatively evaluated by examining all the neoplastic population at 100x and classified as negative <10%, intermediate 10% x<30%, positive $\geq$30% of immunostained neoplastic cells.

4.2 FISH analysis

Histological and immunohistochemical analysis were conducted by pathologists at Bellaria or Sant'Orsola Hospital; we report the protocol for completeness. Dual-color FISH was employed to analyze HER2 amplification. Standard 4- to 5-µm sections of FFPE tissues were incubated at 56°C for 2 hours in a dry oven, deparaffinized by washing (3×15 min) in Bioclear (Natural terpenes-based clearing agent; Bio-Optica, Milan), dehydrated (2×5 min Dehyol absolute (Bio-Optica) and air dried at room temperature. After incubation in 2× Saline Sodium Citrate buffer (2× SSC; pH 7.0) at 75°C for 12 minutes, the sections were digested with proteinase K (0.25 mg/mL in 2× SSC; pH 7.0) at 45°C for 12 minutes, rinsed in 2× SSC (pH 7.0) at room temperature for 5 minutes, and dehydrated using ethanol in increasing concentrations (70%, 85%, and 100%). According to the manufacturer's instructions, the probe HER-2/CEP17 dual color (KREATECH Diagnostics, Amsterdam, The Netherlands) was applied on a selected area of immunohistochemically detectable cells. The hybridization area was covered with a coverslip and sealed with rubber cement. The slides were incubated at 75°C for 10 minutes for denaturation of both chromosomal and probe DNA and then at 37°C for 20-

24 hours to allow hybridization. Post-hybridization washes were performed in NP40 0.5%/SSC 2× (pH 7.0- 7.5) at 75°C for 2 minutes and in 2× SSC for 2 minutes at room temperature. Afterwards, the samples were dehydrated in ethanol as above, and 4,6 - diamidino-2-phenylindole 1 µg/ml suspended in anti-fade diluents (KREATECH Diagnostics, Amsterdam, The Netherlands) was applied for chromatin counterstaining. FISH analysis was carried out using an Olympus BX61 epifluorescence microscope (Olympus, Melville, NY).

4.3 Sensitivity to neratinib and tamoxifen

PDX bearing mice at XII and XXII passage *in vivo* were treated with neratinib (kindly received from Puma Biotechnology, USA) 40mg/kg, dissolved in methyl-cellulose 0.5%- tween80 0.4%, 5 times a week *per os* by gavage. SBR-18 was treated with tamoxifen (Innovative Research of America, Sarasota, FL, USA) alone or in combination with neratinib; tamoxifen was administered by subcutaneous implantation of a pellet releasing 0.5 mg of tamoxifen over 60 days. BBR-4 was treated with trastuzumab (Herceptin, Roche) 4mg/kg, diluted in physiological solution, twice a week, through intraperitoneal injection (ip.). Treatment began when tumors reached a volume of 0.01 cm^3 and were performed for at least 13-15 weeks or until sacrifice. Control groups did not receive any treatment.

To evaluate alterations in signal transduction downstream HER receptors, short-term treatment was performed. In this case, mice bearing PDX tumors of at least 1cm^3 were treated for 4 consecutive days with neratinib (40 mg/kg *per os*), or 7 consecutive days with tamoxifen (administered as described above) or tamoxifen and neratinib. 1 hour after the last treatment with neratinib mice were sacrificed and tumor samples were collected as described for further molecular analysis.

5. Cytofluorimetric analysis

Harvested cells and tumor samples, previously dissociated as described above to yield single-cell suspensions, were analyzed by immunofluorescence and cytofluorometric analysis (CyFlow Space, Sysmex Partec, Germany). Prior to incubation with primary antibodies, tumor cells were briefly (10 min) incubated with rat anti-mouse CD16-CD32 antibody Fc block (clone 2.4G2; 1:100 dilution; BD, Pharmingen, CA, USA). Primary antibodies used were mouse anti-human HER2 (MGR2, Alexis Biochemical, Enzo Life Sciences, Lansen, Swisse) and rat anti-mouse CD140b (PDGRB, APB5, 1:100 dilution;

Bio-Legend, CA, USA). Anti-mouse IgG AF488 (1:100 dilution; Invitrogen, UK) or anti-rat IgG (1:40; KPL 02-16-12) were used as secondary antibodies. For direct immunofluorescence anti-mouse-CD24AF488 (clone M1/69; dilution 1:10; Bio-Legend, CA, USA) and anti-mouse-CD44PE (clone IM7; dilution 1:10; Bio-Legend, CA, USA) (Biolegend) were used.

6. Molecular analysis

6.1 Real-Time PCR
DNA was extracted from cellular pellets of murine ($8x10^4$ cells/cm^2) and human ($4x10^4$ cells/cm^2) cells harvested 4 days after seeding; 10 ng of DNA per sample were analyzed.

DNA from lung, brain, bone marrow cellular pellets and frozen ovaries of PDX was extracted over-night at 56°C in an extraction buffer containing 50 mM KCl, 2.5 mM MgCl2, 0.01% gelatin, 0.45% igepal, 0.45% tween 20 and 120 mg/ml proteinase K in 10 mM Tris-HCl buffer pH 8.3 (all reagents from Sigma, Milan, Italy); proteinase K was inactivated by 30 min incubation at 95°C. DNA was quantified by Qubit Assay Kit (Invitrogen) and 1 ng of each sample were analyzed.

RNA was extracted from cellular pellets or frozen tissue sample, which were mechanically dissociated by gentleMACS Octo Dissociator (Milteny Biotech GmbH, Bergisch Gladbach, Germany). Extraction was performed according to the TRIzol protocol (Total RNA Isolation Reagent; Life Technologies, Milan). RNA was quantified by Qubit Assay Kit (Life Technologies). 1 µg was reverse transcribed with iScript cDNA Synthesis Kit (Bio-Rad Laboratories, CA, USA). 10 ng of cDNA were analyzed for each sample.

According to reaction type, DNA or cDNA was amplified using Sso Advanced SyBR Green Supermix or SsoAdvanced Universal Probes Supermix (Bio-Rad Laboratories, CA, USA) reagents. Reactions were performed by Thermal Cycler CFX96 (Bio-Rad Laboratories, CA, USA).

Analysis was performed using Bio-Rad CFX Manager 3.1 Software and relative quantification was calculated as $Ct = Ct_{gene} - Ct_{housekeeping}$.

HER2 in genomic DNA was amplified with primer qHsaCEP0052301 (Bio-Rad Laboratories) normalizing over human/mouse PTGER2 (dir

TACCTGCAGCTGTACGCCAC; rev GCCAGGAGAATGAGGTGGTC; probe AGAAGCCGCTGCGGA). Copy number of human and murine cell lines was inferred considering MCF7 and MDA-MB231 to harbor 2 copies of HER2 in the genome.

Disseminated cells in each organ were detected by amplification of a sequence in the ⍺-satellite region of the human chromosome 17. Primer and probe sequences were derived from Becker et al., with the sole alteration that the probe carried the non-fluorescent quencher dye TAMRA at the 39-end (Dir GGGATAATTTCAGCTGACTAAACAG; Rev AAACGTCCACTTGCAGATTCTAG; Probe CACGTTTGAAACACTCTTTTTGCAGGATC). To quantify human cells, a standard curve was constructed by adding scalar amounts of MDA-MB-453 human cells to a constant quantity of mouse cells. Ct (threshold cycle) of experimental samples were interpolated in the standard curve and final number of disseminated tumor cells per organ was obtained considering the fraction analyzed for each organ (Nanni et al., 2012).

HER2 gene-expression in PDX was analyzed using TATA binding protein (TBP) total, human and mouse genes as housekeeping (Bieche et al., 2014).

Gene expression of HER2, IL-6 and genes linked to EMT profile in FVBhuHER2 cell lines was quantified considering murine TBP as housekeeping. Primers for this part are listed in the next page.

Target gene	Primer	Conditions
HER2 (Mitra et al., 2009)	*Forward* GTGTGGACCTGGATGACAAGGG *Reverse* GCTCCACCAGCTCCGTTTCCTG	200 nM Annealing 60°C
Cdh1	qMmuCID0006332 (Bio-Rad Laboratories, USA)	
Col3a1	qMmuCID0006332 (Bio-Rad Laboratories, USA)	
Col5a2	qMmuCID0011413 (Bio-Rad Laboratories, USA)	
Dsp	qMmuCID0019458 (Bio-Rad Laboratories, USA)	
Fgfbp1	qMmuCID0007813 (Bio-Rad Laboratories, USA)	
Igfbp4	qMmuCID0006155 (Bio-Rad Laboratories, USA)	
Il1rn	qMmuCID0009153 (Bio-Rad Laboratories, USA)	1× According to manifacturer
IL6	qMmuCID0005613 (Bio-Rad Laboratories, USA)	
Mmp2	qMmuCID00021124 (Bio-Rad Laboratories, USA)	
Ocln	qMmuCID0005446 (Bio-Rad Laboratories, USA)	
Pdgfrb	qMmuCID0025167 (Bio-Rad Laboratories, USA)	
Sparc	qMmuCID0023536 (Bio-Rad Laboratories, USA)	
Vcan	qMmuCID0005235 (Bio-Rad Laboratories, USA)	
mTBP (Bieche et al., 2014)	*Forward* CCCTTGTACCCTTCACCAATGAC *Reverse* TCACGGTAGATACAATATTTTGAAGCTG	200 nM Annealing 60°C
huTBP (Bieche et al., 2014)	*Forward* AGAACAACAGCCTGCCACCTTAC *Reverse* GGGAGTCATGGCACCCTGAG	

6.2 HER2 copy number analysis

DNA was extracted from cellular pellets obtained as described in paragraph 6.1 by PureLink^TM Genomic DNA Mini kit (Life Technologies) according to manufacturer's protocol and quantified by Qubit Assay Kit (Life Technologies). HER2 copy number was quantified by RT-PCR and normalized over human/mouse PTGER2.

6.3 RNASequencing

Samples detailed in figure 10 were sequenced in collaboration with the equipe of prof. Calogero. Protocol is reported for the sake of completeness. Pellets were homogenized and total RNA was isolated by Trizol® reagent (Life Science Technologies, Italy) following the manufacturer's specifications. RNAs were quantified using a Nanodrop ND-100 Spectrophotometer (Nanodrop Technologies, Wilmington, USA) and a 2100 Bioanalyzer (Agilent RNA 6000 Nano Kit, Waldbronn, Germany); RNAs with a 260:280 ratio of 1.5 and an RNA integrity number of 8 were subjected to deep sequencing. Sequencing libraries were prepared with the Illumina TruSeq Stranded RNA Library Prep, version 2, Protocol D, using 500-ng total RNA (Illumina). Qualities of sequencing libraries were assessed by 2100 Bioanalyzer with a DNA1000 assay. Libraries were quantified by qPCR using the KAPA Library Quantification kit for Illumina sequencing platforms (KAPA Biosystems); RNA processing was carried out using Illumina NextSeq. 500 Sequencing. FastQ files were generated via Illumina bcl2fastq2 (Version 2.17.1.14 - http://support.illumina.com/downloads/bcl2fastq-conversion-software-v217.html) starting from raw sequencing reads produced by Illumina NextSeq sequencer. Gene and transcript intensities were computed using STAR/RSEM software52 using Gencode Release 19 (GRCh37.p13) as a reference, using the "stranded" option. Differential expression analysis for mRNA was performed using R package EBSeq53.

We performed various analyses on differentially expressed genes. Clusterization of genes according to their molecular function and biological process was performed through PANTHER web tool (www.pantherdb.org). Protein-protein interactions were investigated using the STRING database (www.strind-db.org). Gene enrichment analysis was performed on coding genes. We performed a Gene Ontology (GO) analysis for biological processes and molecular function and a Kegg pathway analysis (Kyoto Encyclopedia of Genes and Genomes http://www.genome.ad.jp/kegg) via enrichR web tool (www.amp.pharm.mssm.edu/Enrichr).

7. Western blot analysis

Proteins were extracted from cellular pellets or frozen tissue samples, which were mechanically dissociated by gentleMACS Octo Dissociator (Milteny Biotech GmbH, Bergisch Gladbach, Germany). Extraction was performed in lysis buffer, i.e. PhosphoSafe

Extraction Reagent (Novagen) supplemented with protease inhibitors (Protease Inhibitor Cocktail, Sigma 100x). After 10 min incubation, suspensions were centrifuged (12800xg, 15 min, 4°C) and proteins harvested at -80°C for further analysis.

After quantification with DC™ Protein Assay (Bio-Rad Laboratories), proteins were separated on an 8% polyacrylamide gel and then transferred to polyvinylidene difluoride membranes (Bio-Rad Laboratories). After blocking in TBST+5% Milk (Bio-Rad Laboratories), membranes were incubated overnight at 4°C with primary antibodies detailed in the table below. After 3 washes in TBST, membranes were incubated with polyclonal horse-radish-peroxidase conjugated anti-rat IgG antibody (1:3000. Bio-Rad Laboratories) or anti-mouse IgG antibody (sc-2005; 1:1000. Santa Cruz Biotechnology). Protein presence was detected by chemiluminescent reaction (Bio-Rad Laboratories) before film exposure. Densitometric analysis was performed using TotalLab software.

Primary antibody	Clone	Dilution	Molecular weight
-HER2	3B5	1:1000	185 kDa
-pHER2	Polyclonal	1:1000	185 kDa
-HER1	D38B1	1:1000	185 kDa
-pHER1	D7A5	1:1000	185 kDa
-HER3	D22C5	1:1000	185 kDa
-pHER3	21D3	1:1000	185 kDa
-HER4	111B2	1:1000	185 kDa
-pHER4	21A9	1:1000	185 kDa
-IGF1R	C-20	1:1000	100 and 200 kDa
-Stat3	124H6	1:1000	86-91 kDa
-pStat3	D3A7	1:2000	86-91 kDa
-Akt	Polyclonal	1:1000	60 kDa
-pAkt (Ser473)	D9E	1:1000	60 kDa
-MAPK	137F5	1:1000	42-44 kDa
-pMAPK	E10	1:1000	42-44 kDa
-actin	Polyclonal	1:1000	42 kDa

8. Statistical Analysis

Comparisons of growth rate, sensitivity to target drugs, signaling pathways upon pharmacological treatment were based on Student's t test. Comparison of survival rates to $1cm^3$ tumors were based on Mantel-Cox test. Calculation of IC50 (half maximal Inhibitory Concentration) of sunitinib was based on interpolation of percentages with a sigmoid dose-response curve. All statistical analyses were performed Prism 5, GraphPad software, La Jolla, CA, USA).

Results

1. Overcoming HER2-loss mediated resistance to targeted therapies

Recently, a murine model of HER2 loss in mammary tumors has been developed and characterized in the Laboratory of Biology and Immunology of Metastasis directed by Professor Pier-Luigi Lollini. The model is made up of cell lines, derived from either spontaneous or induced tumors in transgenic FVBhuHER2 mice, which display a different dynamic of HER2 expression *in vitro* and *in vivo*. HER2^{stable} cell line derives from a spontaneous mammary tumor and displays a high and stable HER2 expression (median fluorescence intensity, MFI, 1033 arbitrary units of fluorescence), which is not lost neither upon *in vivo* injection nor upon cloning *in vitro* (i.e. HER2^{stable} AG3 clone with MFI 875). HER2^{labile} cell line derives from inoculation *in vivo* of a cell line bimodal for HER2 expression (26% HER2-negative cells), which was in turn derived from a spontaneous mammary tumor. HER2^{labile} line displays a high expression of HER2 *in vitro* (MFI 558); nevertheless, it gives rise to HER2-negative tumors *in vivo* as well as HER2-negative clones *in vitro* (i.e. L2 clone MFI 4). HER2^{loss} cell line was eventually derived from a tumor induced *in vivo* by HER2^{labile} cell line and does not express HER2 neither on cell surface (MFI 4) nor at intracellular level. Table recapitulates the characteristics of HER2^{stable}, HER2^{labile} and HER2^{loss} cell lines, which were already reported extensively elsewhere (Master degree thesis of the candidate, Giusti Veronica, Perdita di HER2 e sensibilità a terapie mirate nel carcinoma mammario, 2015).

Briefly, HER2^{stable} and HER2^{labile} cell lines grew *in vitro* as a monolayer of polygonal cells, whereas HER2^{loss} cell line was constituted by multilayered spindle-like cells. HER2^{loss} cell line displayed the highest capacity of forming mammospheres *in vitro* and its population showed highly staminal characteristics: over 95% of cells were CD24^{low}/CD44^{high}. All the cell lines were tumorigenic, but HER2^{loss} cells displayed the shortest latency and time to sacrifice when compared to the other cell lines. Moreover, when injected intravenously HER2^{stable} and HER2^{labile} cell lines basically did not give rise to lung metastasis which in turn substituted lung lobes in animals injected with HER2^{loss} cell line. Lastly, when vascular properties were analyzed *in vitro*, a tube formation assay revealed that HER2^{loss} cell line formed more and bigger vascular-like structures *in vitro*. *In vivo,* pericytes were not detectable in the vasculature of tumors arisen upon injection of HER2^{labile} and HER2^{loss} cell lines, i.e. in HER2-negative tumors.

To sum up, loss of HER2 expression in HER2^{loss} cell line was accompanied by a spindle-like morphology, an increased stemness, a greater aggressiveness and superior vasculogenic activity in *vitro*; pericytes lack in vasculature of HER2-negative tumors *in vivo*.

	HER2^{stable}	HER2^{labile}	HER2^{loss}
Morphology	Monolayer of polygonal cells	Monolayer of polygonal cells	Multilayered spindle-like cells
Stemness (CD24^{low}/CD44^{high})	3%	1%	96%
Mammospheres (cells per sphere)	23±1 (806)	17±1 ND	69±9 (5100)
Median latency *in vivo* (weeks)	4	3	1
Median time to sacrifice (weeks)	13	9	3
Experimental metastasis	0-4	0-0	>200
***In vitro* vascular tube formation**	12	5	115
Presence of pericytes in vascular structures of tumors induced by	Yes	No	No

Table 1. Characteristics of HER2^{stable}, HER2^{labile} and HER2^{loss} cell lines
The table reports morphology of cell lines in adherence; percentage of CD24^{low}/CD44^{high} determined by FACS analysis; number of mammospheres formed when seeded in ultra-low adherence conditions and number of cells per mammosphere upon disaggregation; median latency and time to sacrifice upon intra-mammary inoculation of 10^6 cells in FVBhuHER2 mice; range of lung metastasis induced by intravenous injection of 10^5 cells in FVBhuHER2 mice; number of tubes formed in matrigel 16-18 hours after seeding (12×10^3 cells/cm^2); presence of pericytes, determined by immunohistochemistry as cells positive for NG-2 expression, surrounding blood vessels in tumors induced by either cell line *in vivo*. ND= not determinable

1.1 Trastuzumab promotes HER2-loss *in vitro*

HER2 loss is a clinical issue and occurs in up to 25% of metastasis (Loibl and Gianni, 2017). Literature reports contrasting data about the role of trastuzumab adjuvant therapy in promoting HER2 loss in metastasis and recurrences. We set out to understand if and how trastuzumab could affect loss of HER2 expression in HER2^{labile} cell line. Previous preliminary experiments (Master degree thesis of the candidate, Giusti Veronica, Perdita di HER2 e sensibilità a terapie mirate nel carcinoma mammario 2015) had shown that trastuzumab 10 µg/ml inhibited growth of colonies of HER2^{labile} cell line under non-adherent 3D culture conditions *in vitro*: the number of colonies was decreased of 79% with respect to untreated control. Under adherent 2D culture conditions, trastuzumab had a much lower, yet still significant, efficacy in inhibiting growth of HER2^{labile} cell line (<25% inhibition with respect to untreated control). FACS analysis of cells treated for 120 h with trastuzumab 10 µg/ml revealed an increased HER2-negative population in treated cells (19%) with respect to untreated control (7%).

Hence, we set up a long-term culture with trastuzumab 30 µg/ml for 2 months to verify whether prolonged treatment with trastuzumab could induce loss of HER2 expression in HER2^{labile} cell line. HER2^{labile} cells were seeded at high dose (1.6x10^5 cells/cm^2) and low dose (4x10^4 cells/cm^2). HER2 expression and stemness of treated cells were monitored over time (fig. 1 and fig. 2).

From day 21 cells at both doses treated with trastuzumab began to acquire some kind of spindle-like morphology. At day 28 trastuzumab treated low dose seeded cells were completely spindle-like and maintained this morphology over the next month (fig. 2A and 2D). High dose seeded cells were still mainly polygonal at day 28, but bunches of spindle-like cells were clearly visible (fig. 1A); afterwards, spindle-like cells took over and no polygonal cells could be observed with the exception of very little islets interspersed in the spindle-like multilayer (fig. 1D).

HER2 expression and stemness changed in parallel with morphology. In HER2^{labile} high and low dose cells treated with trastuzumab, HER2 expression was always almost completely lost when cells began to acquire a spindle-like morphology (day 28) (fig. 1B and 2B). HER2^{labile} cells in culture have an extremely limited staminal population (1%). In high-dose seeded trastuzumab treated cells, staminal population got gradually expanded from 35% of cells having lost CD24 expression at day 28 till 65% of cell being

staminal at day 56 (fig. 1C and 1F). HER2^{labile} cells seeded at low dose and treated with trastuzumab quickly acquired staminal properties with 46% of cells being staminal at day 28 and 70% at day 56 (fig. 2C and 2F).

Spontaneous changes of morphology, HER2 expression and staminal properties were observed in untreated populations of cells seeded at low dose, as well. Untreated HER2^{labile} cells at low dose began to acquire a spindle-like morphology at day 35, hence slower than trastuzumab treated cells. Change in morphology was accompanied by a gradual loss of HER2 expression, which was expressed in less than 25% cells at day 56 (fig. 2E), and a gradual increase in staminal population: loss of CD24 expression was already evidencable in 10% of cells at day 28 (fig. 2C) and staminal population accounted for 70% at day 56 (fig. 2F). High dose seeded untreated cells remained polygonal in shape, positive for HER2 expression and staminal population remained limited to 5% throughout long-term culture (fig. 1D, 1E and 1F).

Of note, removal of trastuzumab from cell culture medium did not restore neither polygonal morphology, nor HER2 expression, nor CD24^{high}-CD44^{low} population in HER2^{labile} cells (data not shown).

Altogether, trastuzumab appears to accelerate a spontaneous tendency of HER2^{labile} cells, when seeded at low dose, to lose HER2 expressionand in parallel acquire a spindle-like morphology and an increased staminal sub-population.
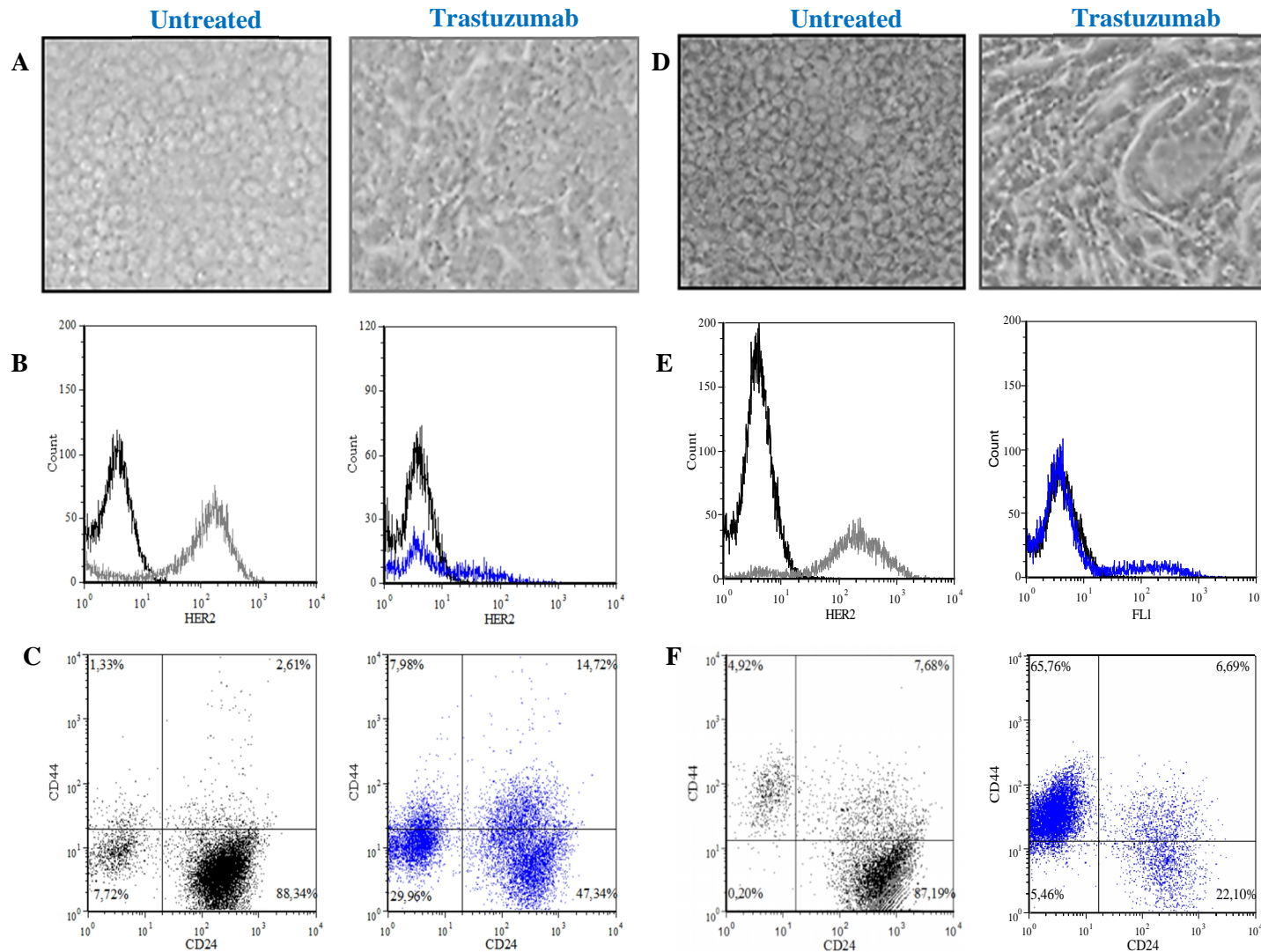
Fig. 1. Trastuzumab promotes HER2 loss *in vitro*_High dose
HER2^{labile} were seeded at high dose (1.6×10^5 cells/cm^2) and kept in long-term culture with normal medium (untreated; black) or trastuzumab 30 μg/ml (blue).

Photos were shot at Diavert microscope (250× magnification) at day 28 (A) and 56 (D).

HER2 expression was quantified by cytofluorimetric analysis at day 28 (B) and 56 (E). Histogram profiles show in black cells incubated only with secondary fluorescent antibody, in grey profile of untreated cells incubated with -huHER2 and in blue cells treated with trastuzumab incubated with -huHER2.

Dot blot of CD24 (x axis) and CD44 (y axis) analyzed by cytofluorimetric analysis at days 28 (C) and 56 (F). Dot blots show untreated cells in black and trastuzumab treated cells in blue.
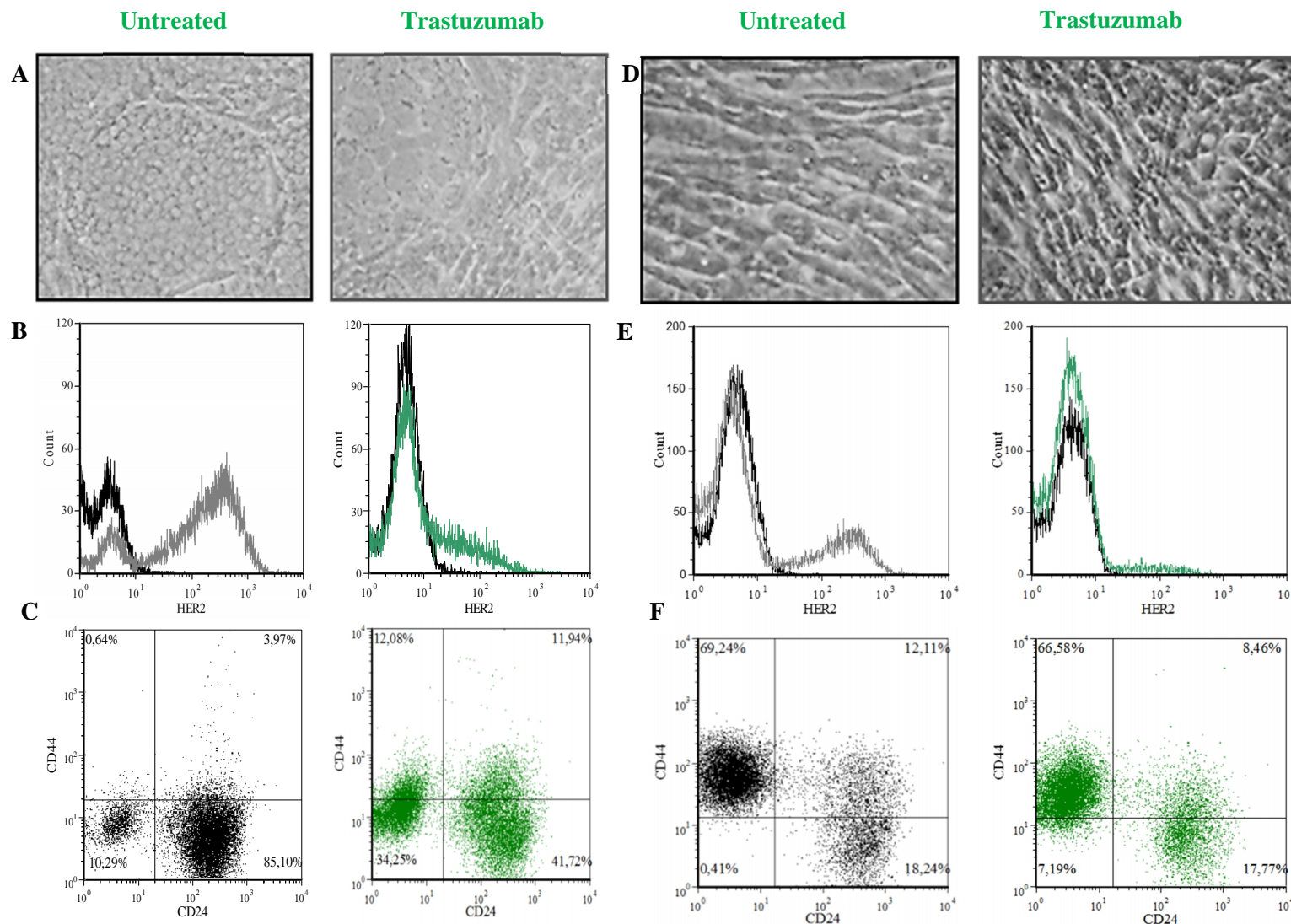
Fig. 2. Trastuzumab promotes HER2 loss *in vitro*_Low dose

HER2^{labile} were seeded at high dose (4×10^4 cells/cm^2) and kept in long-term culture with normal medium (untreated; black) or trastuzumab 30 µg/ml (green). Photos were shot at Diavert microscope (250× magnification) at day 28 (A) and 56 (D). HER2 expression was quantified by cytofluorimetric analysis at day 28 (B) and 56 (E). Histogram profiles show in black cells incubated only with secondary fluorescent antibody, in grey profile of untreated cells incubated with -huHER2 and in green cells treated with trastuzumab incubated with -huHER2. Dot blots of CD24 (x axis) and CD44 (y axis) analyzed by cytofluorimetric analysis at days 28 (C) and 56 (F). Dot blots show untreated cells in black and trastuzumab treated cells in green.

1.2 Trastuzumab accelerates growth of HER2-negative tumors *in vivo*

HER2^{labile} cells give rise to HER2-negative tumors when injected in FVBhuHER2 mice *in vivo*. We set out to understand the effect of trastuzumab treatment in such tumors. 10^6 HER2^{labile} cells were injected subcutaneously (s.c.) in the right posterior leg and mice were treated with either saline or trastuzumab twice a week starting from day 3 after cell injection. Animals treated with trastuzumab developed bigger tumors then ones treated with saline (control); differences in growth rate were statistically significant from day 25 after cell injection. No statistically significant difference was observed in latency between the two groups (fig. 3). All tumors were HER2-negative both in saline and trastuzumab treated groups and the vast majority of their populations displayed staminal features (75% CD24^{low}).

Overall, these data confirm *in vitro* observations: trastuzumab accelerates growth of HER2-negative tumors upon *in vivo* injection of HER2^{labile} cell line, as well.
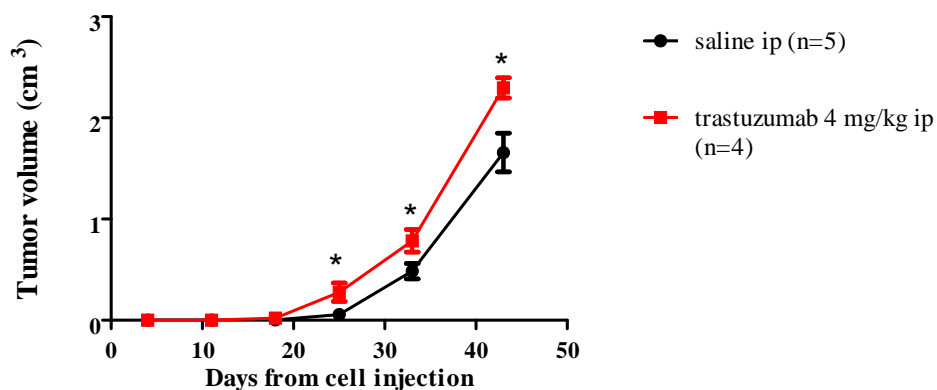
Figure 3. Effect of trastuzumab *in vivo* on HER2^{labile} induced tumors
Tumor growth curve of tumors arisen after s.c. injection of 10^6 HER2^{labile} cells and treated *intra-peritoneum* (ip) with saline (black round) or trastuzumab 4 mg/kg (red rectangle) twice a week from day 3 after cell injection. Each point represents the mean±s.e.m. volume of 4 or 5 mice. Statistical analysis: Student's *t* test, (*) p<0.05.

2. Unravelling HER2^{loss}

We performed some experiments to understand mechanisms underlying loss of HER2 expression in HER2^{labile} cell line. First of all, we determined whether number of injected cell or clearance by immune system could influence HER2 expression *in vivo*. Furthermore, we evaluated genetic and epigenetic alterations which could impair HER2 expression in HER2^{loss} cell line. Lastly, we performed analysis of transcriptomes and expression of genes associated to EMT was checked as well.

2.1 Effect of different injection doses

We primarily set out to verify whether and how dose of injected cells could influence tumor growth and HER2 expression in FVBhuHER2 mice. We injected either 10^6, or 10^7 or 2×10^7 HER2^{labile} cells: the more cells we injected the faster tumors grew (fig. 4A). Anyway, neither injection dose gave rise to HER2-positive tumors (fig. 4B).

Hence, high injection doses of HER2^{labile} cells do not give rise to HER2-positive tumors, strengthening the concept that close cell-cell contact is required for HER2^{labile} cells to maintain HER2 expression.
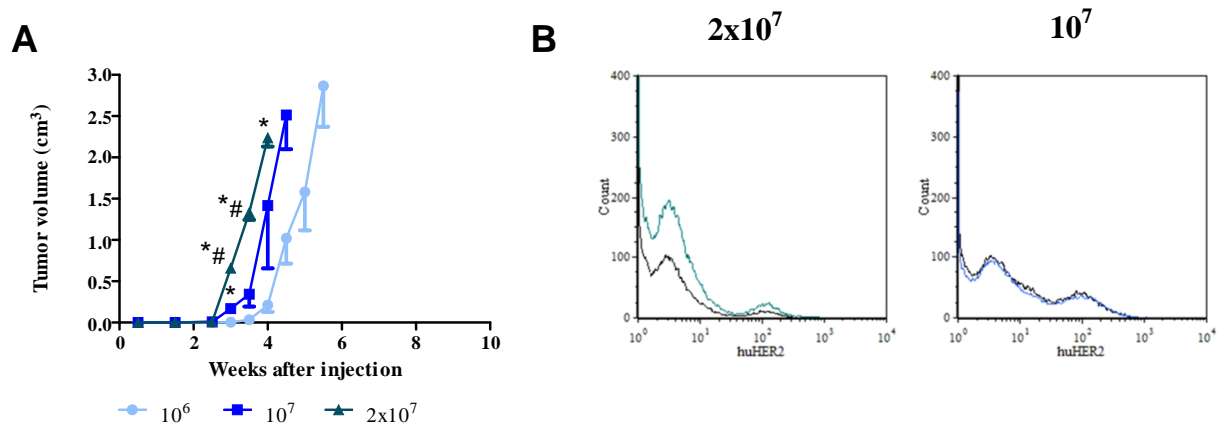
Figure 4. Different doses of HER2^{labile} *in vivo*

(A) Tumor growth curve of HER2^{labile} cells injected s.c. in FVBhuHER2 mice at different doses: 10^6 (round), 10^7 (square), 2×10^7 (triangle). Each point represents the mean±s.e.m. of 2 mice. Statistical analysis: Student's *t* test $p < 0.05$ *versus* 10^6 (*) or 10^7 (#).

(B) Histograms represent expression of huHER2 of one representative tumor for each indicated group; black profile refers to cells incubated with secondary antibody only, colored profiles indicate cell incubate with -huHER2.

2.2 Is HER2 loss due to immunological selection *in vivo*?

According to the theory of immune-surveillance, immune system can edit tumors eliminating highly immunogenic clones. Low immunogenic remaining cell have thus been selected for accumulating mutations which enable them to escape from immune-surveillance and are often more aggressive.

HER2^{loss} cell line was obtained from *in vivo* injection of HER2^{labile} cell line in FVBhuHER2 mice, i.e. immunocompetent mice tolerant to HER2 expression. Anyway, immune system could still react against and clear out HER2-positive clones selecting the more aggressive HER2-negative sub-population *in vivo*. To verify if this was the case, we inoculated HER2^{labile} cells in immunocompromised female mice (Balb Rag2$^{-/-}$; Il2rg$^{-/-}$). HER2^{labile} cells were tumorigenic with 100% incidence in immunocompromised mice; tumors grew even faster than in immunocompetent mice possibly due to absence of inhibitory effect of immune system (fig. 5A). Nevertheless, all tumors arisen in the immunocompromised mice were negative for HER2 expression, as well (fig. 5B).

From these results we can conclude that B, T and NK cells are not involved in clearance of HER2-positive cells from injected HER2^{labile} population.

A

B
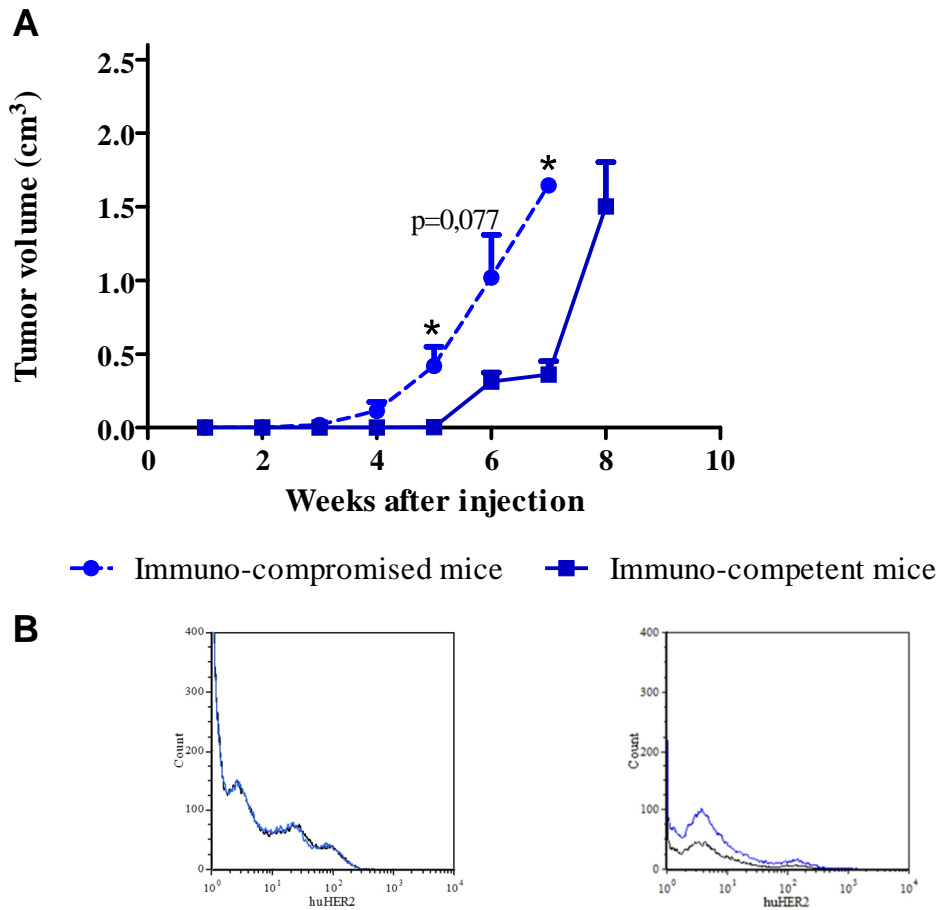
Figure 5. HER2^{labile} cells in immune-compromised mice

(A) Tumor growth curve of 10^5 HER2^{labile} cells injected s.c. in immunocompetent (FVBhuHER2) mice (solid square) or immunocompromised (Balb rag2$^{-/-}$; Il2rg $^{-/-}$) mice (solid round, dotted line). Each point represents the mean±s.e.m of 3 mice. Statistical analysis: Student's t test $p<0.05$ versus 10^6 or 10^7.

(B) Histograms represent expression of huHER2 of one representative tumor for each indicated group; black profile refers to cells incubated with secondary antibody only, blue profiles indicate cell incubate with -huHER2.

2.3 HER2 copy number analysis

We set out to verify whether HER2^{loss} cells had lost the transgene in their DNA. Copy number analysis was performed on HER2^{stable}, HER2^{labile} and HER2^{loss} cells. We also included a murine HER2-negative cell line derived from a mammary tumor (TS/A) and normal tissue from FVB non-transgenic mice as negative controls, normal tissue and spontaneously arisen tumors from FVBhuHER2 transgenic mice as positive controls and human mammary tumor cell lines with different known levels of HER2 expression. We considered MCF7 and MDA-MB-231, reported in literature as HER2-negative, as bearing 2 copies of HER2. Our analysis revealed 22±5 copies of HER2 in normal tissue from transgenic mice and 32±1 copies in tumors spontaneously arisen in such mice; this mirrors the 30-50 copies reported in literature (Finkle et al., 2004). HER2^{stable} cell line bore 51 copies of HER2 transgene and was thus comparable with human mammary cancer BT474 cell line (61 copies). HER2^{labile} and HER2^{loss} cell lines had 19 and 18 copies of HER2, respectively, being thus comparable to SkBr3 (13 copies) human mammary cancer cell line (fig. 6).

This result confirmed that HER2^{loss} cells actually harbor HER2 transgene and that its silencing must be due to other mechanisms at transcriptional or translational level.
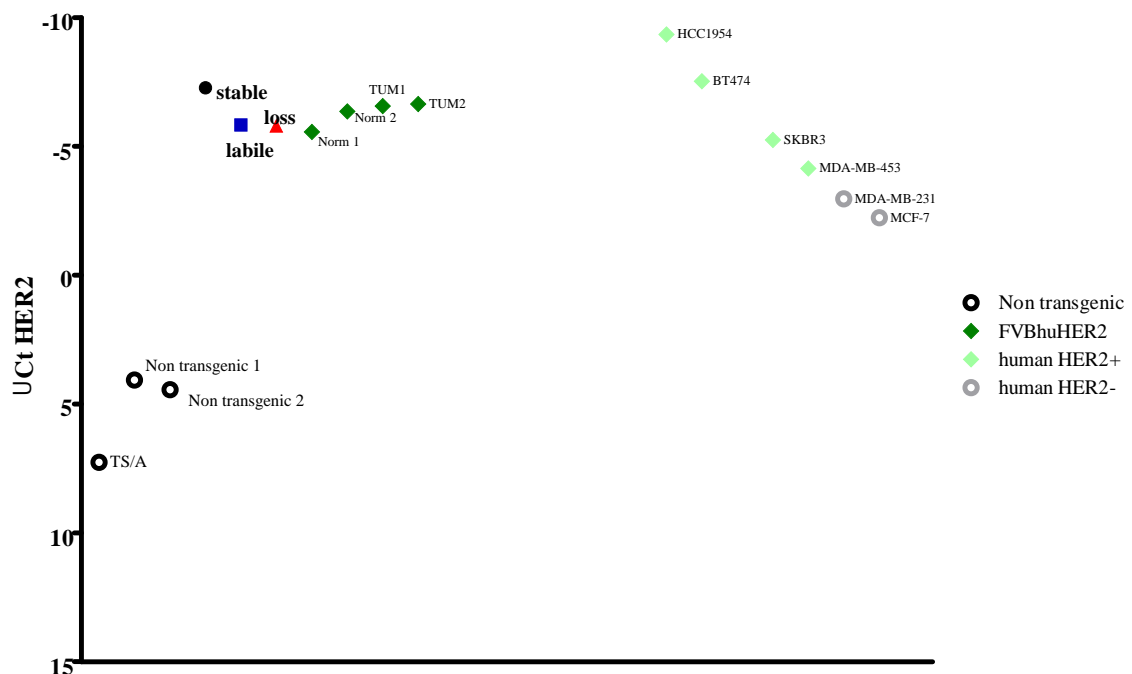
Figure 6. HER2 copy number
HER2 copy number was analyzed by RT-PCR on DNA extracted from HER2^{stable} (black solid round), HER2^{labile} (blue square) and HER2^{loss} (red triangle) cells, negative controls (black empty round), positive controls (green rhombus), human mammary cell lines known to be HER2-positive (light green rhombus) or HER2-negative (grey empty round). Each point represents the Ct of a sample, calculated as (Ct$_{HER2}$-Ct$_{h/m}$ $_{PTGER2}$). Copy number was calculated considering MCF-7 and MDA-MB-231 having 2 copies of HER2.

2.4 Is HER2-loss a matter of epigenetics?

To assess whether loss of HER2 expression was due to a hyper-methylation event determining its silencing, we treated HER2^{loss} cells with 5' aza-2-deoxycytidine (0.5 and 5 µM) for six consecutive days. In parallel, we conducted the same experiment on HER2^{labile} cells to verify if the demethylating agent could induce a switch to mesenchymal phenotype.

Treatment with 5' aza-2-deoxycytidine had a cytostatic effect on HER2^{loss} cell line and at each point we harvested as much cells as we had seeded ($2x10^6$ cells; $8x10^4$ cells/cm^2) (fig. 7A). No changes in HER2 expression were registered (fig. 7C).

On HER2^{labile} cell line, treatment with 5' aza-2-deoxycytidine 0.5 µM was cytostatic, whereas the higher dose was cytotoxic and cell yield kept decreasing over time (fig. 7B). No major changes in morphology and HER2 expression were observed in the lower dose of treatment. With 5' aza-2-deoxycytidine 5 µM, cells had a much lower HER2 expression (fig. 7D). Sporadically, some spindle-like cells were observed as well.

Thus, demethylation is not able neither to restore HER2 expression in HER2^{loss} cells nor to induce a complete switch to spindle-like phenotype in HER2^{labile} cells.
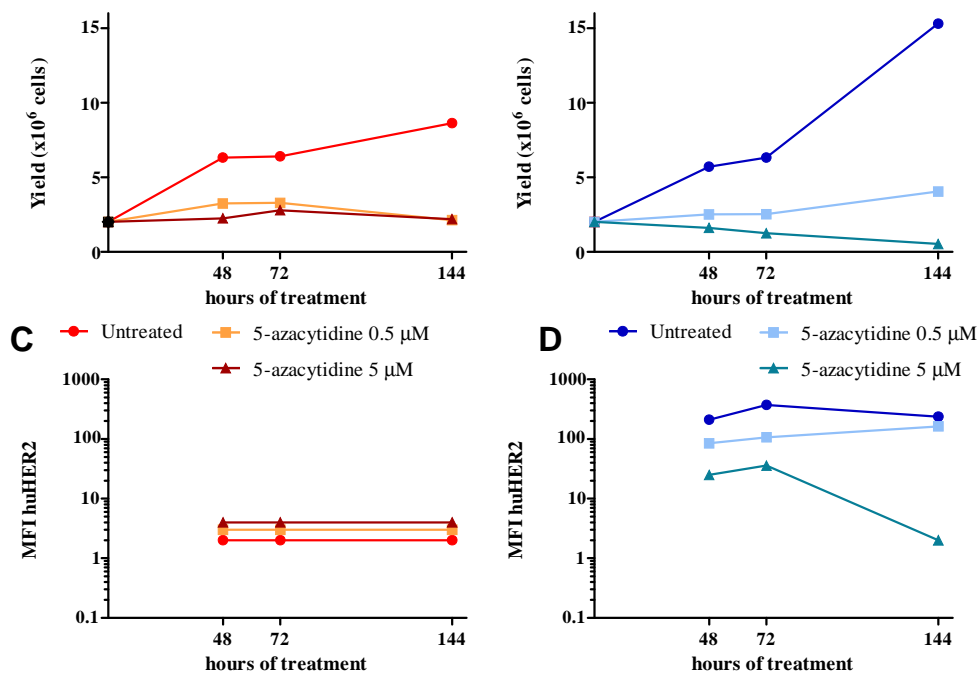
Figure 7. Effect of demethylation on HER2^{loss} and HER2^{labile} cells

Cells were seeded at $8x10^4$ cells/cm^2 and treated with 5' aza-2-deoxycytidine 0.5 µM (triangles) or 5 µM (squares) or medium only (round). Graphs (A) and (C) refer to HER2^{loss}, (B) and (D) to HER2^{labile} cell lines. (A) and (B) Cell counts at indicated time-points.
(C) and (D) HER2 expression evaluated by flow-cytometry and reported as fluorescence intensity (MFI).

2.5 Differential gene-expression of EMT genes in models of HER2^{loss}

Previous data from a PCR Array had demonstrated a differential expression of EMT-linked genes in HER2^{loss} cell line when compared to HER2^{stable} cell line. Up-regulated genes were **Col3a1, Col5a2,** Col1a2, **Pdgfrb, Igfbp4, Sparc, Versican, Mmp2**, Wnt5a, Itg5a, Nudt3, TCF4, ZEB-1, ZEB-2 and TGF- 1. Down-regulated genes were **Cadherin, Occludin,** Keratin 7 and 14, **Fgfbp1, Il1rn, Desmoplakin,** Desmocollin 2, F11r, Sox10. Wnt5b, Serpine1, Snai3, Notch1, Mmp9, Erbb3, EGFR, Tmeff and Bmp7. Genes **in bold** were validated in RT-PCR and their dynamic of expression was studied in HER2^{stable}, HER2^{labile}, HER2^{loss} and HER2^{labile} cells treated with trastuzumab (TRT).

Some polymorphisms in **Il1rn** have been linked to increased risk of breast cancer (Slattery et al., 2014). In our model Il1rn was found down-regulated in HER2^{loss} cell line, with respect to HER2^{stable} and HER2^{labile} cell lines. Il1rn was down-regulated in HER2^{labile} TRT cells, both at day 28 and 56 (fig. 8).

Fgfbp1 (fibroblast growth factor binding protein 1) is up-regulated in various adenocarcinomas and appears to have a proangiogenic activity (Tassi et al., 2007). In our model, it resulted down-regulated in HER2^{loss} cells and to a lesser extent in HER2^{labile} TRT cells at days 28 and 56 (fig. 8).

Cdh1 (E-cadherin 1), **Dsp** (desmoplakin) and **Ocln** (occludin) are molecules involved in different types of cell-cell adherence also known as markers of epithelial cells. Cdh1 is a transmembrane glycoprotein which connects cells together at adherent junction. A role for loss of E-cadherin expression causing EMT is often been proposed and its down-regulation has often been linked to poor prognosis and invasiveness (Velasco-Velasquez e al., 2013; Freundenberg et al., 2008; Ashaie et al., 2016; Prieto-Garcìa et al., 2017; Wong et al., 2018). Accordingly, in our model Cdh1 is down-regulated in HER2^{loss} cells and to lesser extent in HER2^{labile} cells treated with trastuzumab. Dsp is involved in cell adhesion at desmoplaques. Loss of its expression has been linked to invasiveness and progression in cancer (Pang et al., 2004). We observed a great inhibition of Dsp in HER2^{loss} cells and to a lesser extent in HER2^{labile} TRT cells, which is in accordance with highly tumorigenic and metastatic properties of HER2^{loss} cell line. Ocln is still involved in cell adhesion and particularly in regulation of cell membrane permeability at tight junctions. Ocln has been found down-regulated in HMLE (human primary epithelial breast cells immortalized through expression of T cell antigen SV40) cells transduced with Snail (a known driver of

EMT) or knocked-out for Cdh1 expression (Guen et al., 2017). Accordingly, Ocln was found down-regulated both in HER2^{loss} and HER2^{labile} TRT cells (fig. 8).

Col3a1 and **Col5a2** encode two different chains of fibrillary proto-collagen, an extracellular-matrix (ECM) component, which is abundant in extensible mesenchymal tissues. Col3a1 has been found up-regulated in TFG- 1 induced EMT in renal and lung carcinoma cell lines (Hosper et al., 2013). A down-regulation of Col5a2 has been in turn reported in pig fibroblasts facing mesenchymal-to-epithelial transition (MET), the opposite process to EMT (Shi et al., 2013). Accordingly, in our model both Col3a1 and Col5a2 are up-regulated in HER2^{loss} cell line with respect to HER2^{stable} cell line. HER2^{labile} cells displayed an intermediate expression of collagen, which was up-regulated in HER2^{labile} TRT cells to levels even higher than HER2^{loss} cell line (fig. 8).

Igfbp4 (insulin like growth factor binding protein 4) sequesters and down-modulates activity of IGF in blood and exerts therefore an inhibitory effect on cell growth. Nevertheless, it has been reported as up-regulated in glioblastoma U434 cell line, where it promotes EMT, invasiveness and is correlated to down-regulation of Cdh1 (Praaven et al., 2014). Our model mirrors U434 as Igbp4 is up-regulated in HER2^{loss} cell line with respect to HER2^{stable}. Again, HER2^{labile} expresses Igfbp4 at intermediate level and its expression is up-regulated after treatment with trastuzumab (fig. 8).

Vcan, Sparc and **Mmp2** are ECM molecules with a known role in proliferation, migration and angiogenesis. Their up-regulation is a common event in several carcinomas other than breast cancer and is often linked to EMT and poor prognosis. Vcan encodes the chondroitin-sulfate proteoglycan versican, whose down-regulation in MCF10A, stimulated by Snail, dampens their migratory properties (Zhang et al., 2017). Vcan is up-regulated in HER2^{loss} cells with respect to HER2^{stable}; HER2^{labile}, though minor variatons among samples, displays an intermediate expression which is augmented after trastuzumab treatment. Sparc (secreted protein acidic and rich in cysteine) has been shown as able to induce EMT together with an immunosuppressive microenvironment in murine breast cancer cell lines (Sangaletti et al., 2016). It results expressed at good levels in all the cell lines, with HER2^{labile} and HER2^{loss} cells expressing it slightly more than HER2^{stable} cell line. In HER2^{labile} TRT cells, Sparc expression was slightly enhanced. Mmp2 is a metalloproteinase whose expression has been reported down-regulated in a model where EMT was inhibited silencing STEAP1 (Xie et al., 2018). Its expression was

maximal in HER2^{loss} cells, followed by HER2^{labile} and eventually HER2^{stable} cell line and was up-regulated in HER2^{labile} TRT with respect to untreated cells (fig. 8).

Pdgfrb (platelet derived growth factor) encodes the receptor for a growth factor which stimulates proliferation of mesenchymal cells. It has been reported,together with PDGR- , as a down-stream target of Twist and Zeb1 and Foxq1 (fork-head box Q1), transcription factors inducing EMT (Meng et al., 2015). In our model it is up-regulated in HER2^{loss} cells and HER2^{labile} TRT cells, whereas it is overall down-regulated in the other cell lines, though minor variatons among samples occur in HER2^{labile} cells (fig. 8).

To sum up, Ilrn, Fgfbp1, Ocln, Dsp, Cdh1 are all down-regulated in HER2^{loss} and to a lesser extent in HER2^{labile} TRT cells. For these genes, HER2^{labile} cell expression resembles HER2^{stable} cell line. Col3a1, Col5a2, Igbp4, Sparc, Vcan, Mmp2 and Pdgfrb were in turn up-regulated in HER2^{loss} and HER2^{labile} TRT cells at similar levels. HER2^{labile} basal expression of these genes was intermediate between HER2^{stable} and HER2^{loss}. Of note, trastuzumab removal after switch to spindle-like morphology did not alter expression of above reported genes. Hence, trastuzumab removal was not able to restore basal expression of these genes, back to level of untreated HER2^{labile} cells (data not shown).
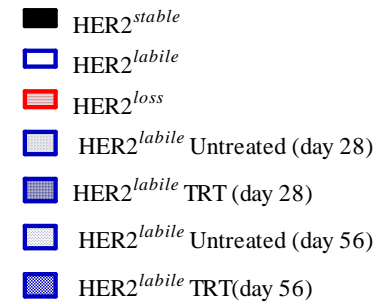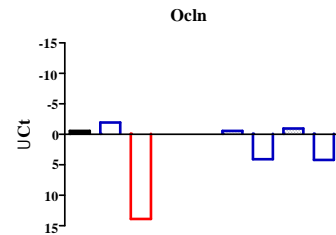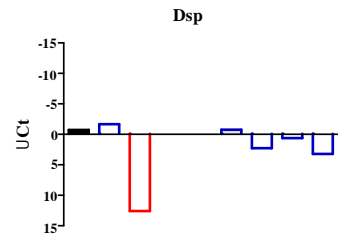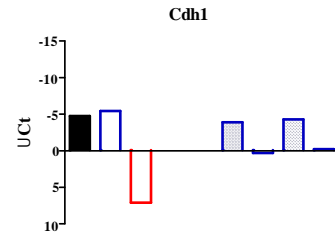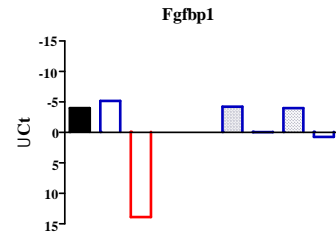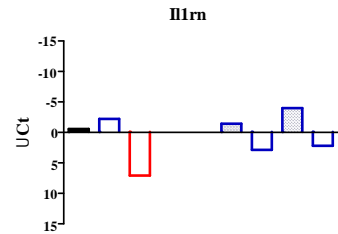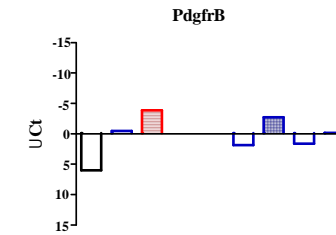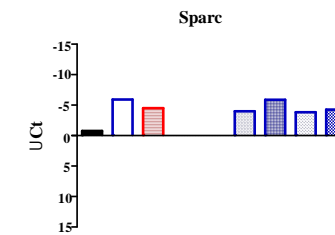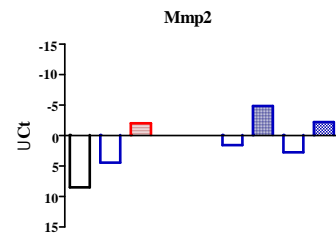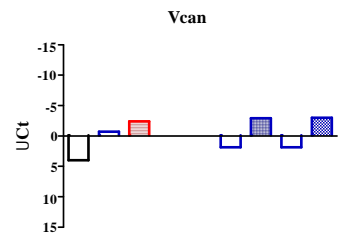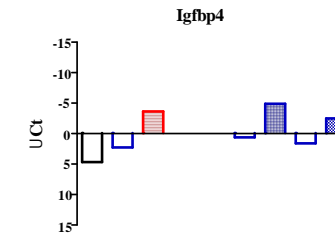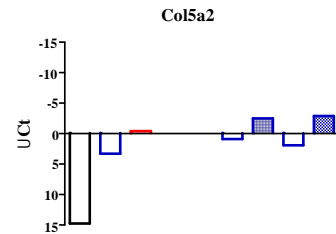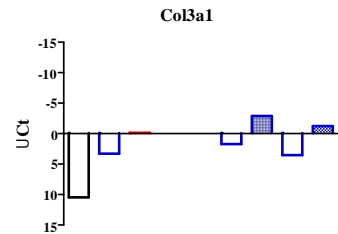
Figure 8. EMT expression profile in HER2^{stable}, HER2^{labile}, HER2^{loss} and HER2^{labile} TRT cells

Bar graphs represent expression of each indicated gene in HER2^{stable} (solid black), HER2^{labile} (empty blue) and HER2^{loss} (striped red). Right columns report expression in HER2^{labile} untreated cells (dotted blue) or TRT cells (checked blue) at 28 and 56 days of treatment. Expression was determined by RT-PCR analysis, normalized over TBP (total binding protein) expression (ΔCt=Ct$_{gene}$-Ct$_{TBP}$).

3. RNASequencing

Final aim of this study was not only to unravel mechanisms underlying HER2 loss, but also and primarily to identify new therapeutic targets in HER2-positive breast cancers having lost HER2 expression.

In collaboration with Prof. Federica Cavallo, Raffaele Calogero and Maddalena Arrigoni and Martina Olivero (Università di Torino), the transcriptomes of different cell lines were compared to highlight differences in gene expression and possibly identify therapeutic targets in HER2 loss. HER2^{stable}, HER2^{stable} AG3, HER2^{labile}, HER2^{labile} TRT, HER2^{labile} TRNT and HER2^{loss} cells were used for the analysis (see results paragraph 1 for detailed description of these cell lines). Moreover, HER2^{stable} and HER2^{loss} cell lines were treated with trastuzumab 30 µg/ml long-term for 30 days, as well as HER2^{labile}; afterwards, trastuzumab was removed (TRNT lines) or maintained for further 30 days (TRT lines). HER2^{labile} cell line lost HER2 expression in these conditions, as showed in paragraph 1.1 (fig. 1 and fig. 2). HER2^{stable} and HER2^{loss} cell lines did not undergo any changes in morphology, HER2 expression and stemness (fig. 9). Inclusion of HER2^{stable} TR(N)T cells and HER2^{loss} TR(N)T cells permit us on the one hand to identify genes not linked to lability of HER2 expression and on the other hand to identify those whose expression is modified upon trastuzumab binding to HER2. Figure 10 reports all cell lines included in this analysis and their derivation.
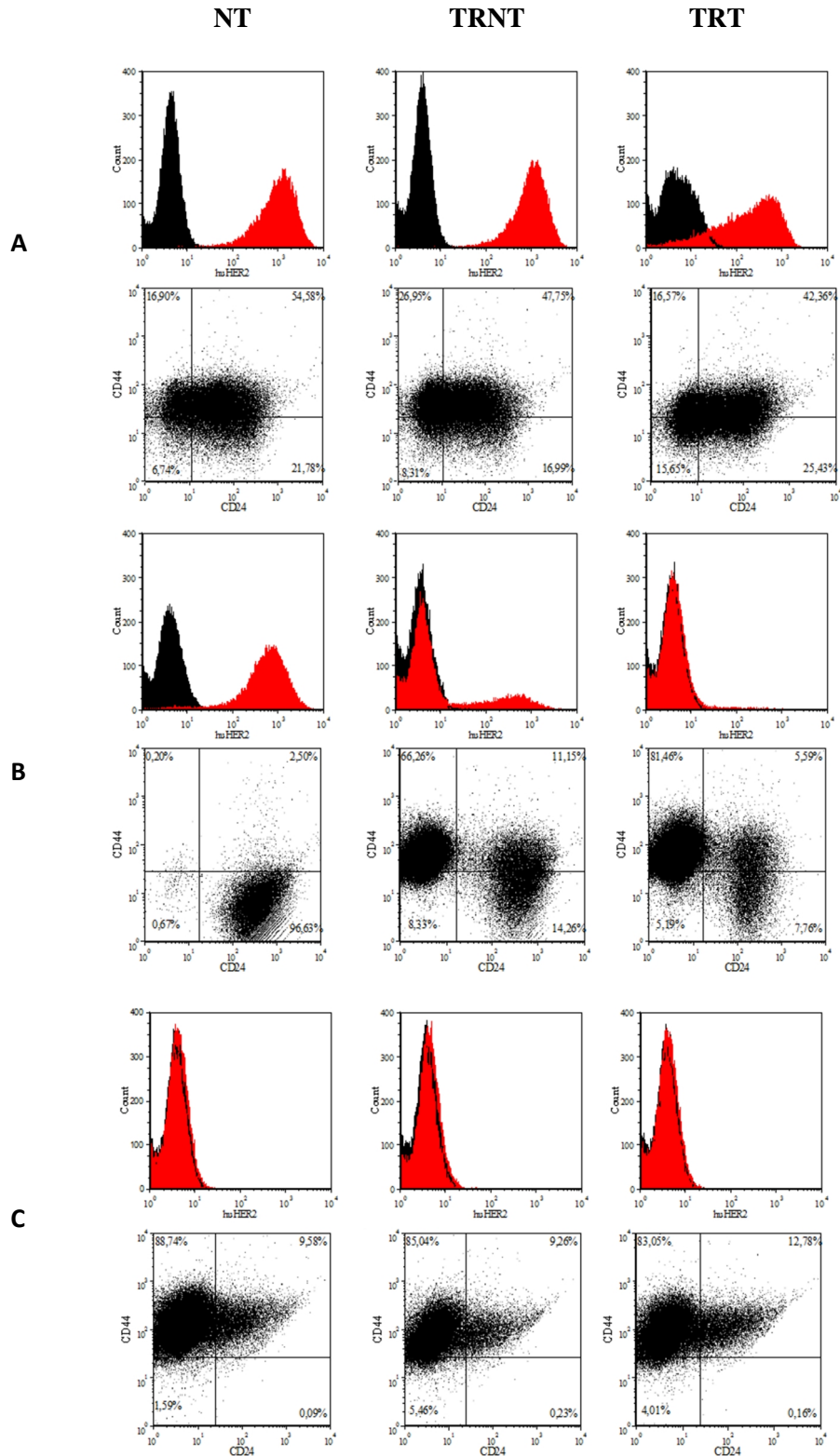
Figure 9. Long-term trastuzumab in HER2^{stable}, HER2^{labile} and HER2^{loss} cells

HER2^{stable} (A) HER2^{labile} (B) and HER2^{loss} (C) were kept in culture with trastuzumab 30 µg/ml for 30 days; afterwards, cells were treated for further 30 days (TRT cells) or trastuzumab was removed (TRNT cells). Histograms show HER2 expression by cytofluorimetric analysis with black profile referring to cells incubated with secondary fluorescinated antibody only and red profile to cells incubated with -huHER2. Dot blots report CD24 and CD44 expression, examined by cytofluorimetric analysis.
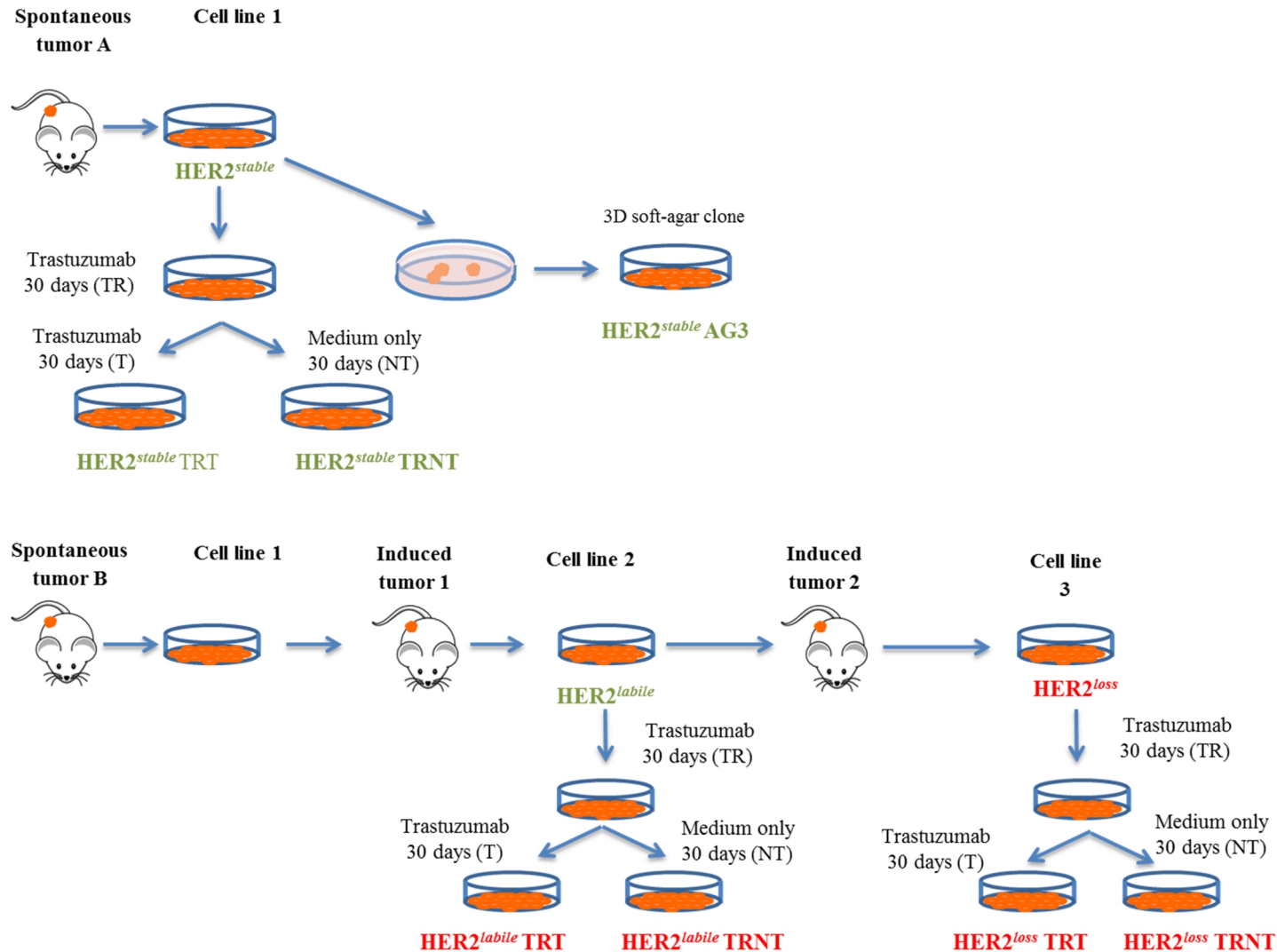
Figure 10. Cell lines included in RNASequencing
The figure illustrates cell lines whose transcriptomes were analyzed and their derivation. All cell lines in green are HER2-positive, show epithelial morphology and a reduced staminal population. All cell lines in red have no HER2 expression, spindle-like morphology and an increased staminal population.

3.1 HER2*labile versus* HER2*loss*

First of all, we compared transcriptomes of HER2*labile* and HER2*loss* cell lines. Stunningly, only 8 genes were differentially expressed between the two cell lines: 7 genes were down-regulated and only 1 was up-regulated in HER2*loss* cell line. Down-regulated genes were represented by Myh14, Wnt7b, Cdkn2b, Krt8, Ifitm 10, Postn and Krt7; Pla2g7 was in turn the only gene up-regulated in HER2*loss*.

The low number of genes detected by this comparison is maybe due to the low number of samples included in the analysis (3 replicates of HER2*labile vs* 3 replicates of HER2*loss*). The paucity of detected genes in turn did not permit any further clustering and analysis of pathway and we only performed a bibliographical research to understand how these genes and their products could be linked to phenotypic differences between HER2*labile* and HER2*loss* cell lines.

Mhy14 encodes a non-muscular myosin which has been found expressed in human mammary cell lines derived from luminal carcinomas, but not from basal-like carcinomas. EMT induction with TGF- in murine cell line NMuMG reduces expression of the myosin (Beach et al., 2011). Moreover, Mhy14 has been found down-regulated in a model of progression of tongue carcinoma; clinical data indicate a correlation between its low expression and lethality (Perez-Valentia et al., 2018). Accordingly, in our model Myh14 is down-regulated in HER2*loss* and correlates well with its aggressive and mesenchymal phenotype.

Cdkn2b encodes the inhibitor of cell cycle p15, which induces arrest of the cycle in G1/S binding and sequestering Cdk6, needed for subsequent cycle steps. This tumor-suppressor gene has been found hyper-methylated and hence down-regulated in breast cancer (Buyru et al., 2009) and in particular in the triple-negative subtype (Ansems et al., 2014). In our model, its down-regulation in HER2*loss* cell line is in accordance with its decreased doubling time with respect to HER2*labile* cell line.

Cytokeratin are biological marker of a luminal or at least epithelial commitment. **Krt7** and **Krt8** encode K7 and K8, respectively, which have been found expressed in 94% of a breast cancer cohort and associated to a better prognosis (El-Rehim et al., 2004). In particular, K8 is associated to low invasiveness in human mammary cell lines and in turn its absence correlates with a migratory and undifferentiated phenotype (Iyer et al., 2013).

As expected, due to their morphology, HER2^{loss} cells have lost expression of K7 and K8 with respect to HER2^{labile} cell line. This difference mirrors differences in migratory phenotype and metastatic potential between HER2^{labile} and HER2^{loss} cell lines.

Ifitm10 is a member of INF-induced membrane protein family, which is involved in proliferation and cell-cell adhesion. Recently, a read-through involving ifitm10 and CTSD (cathepsin D) was identified specifically in mammary carcinomas. Its inhibition in human mammary MCF7 cell line hampers cell proliferation (Varley et al., 2014). In our model, Ifitm10 is down-regulated in HER2^{loss} cell line: this could be interpreted as an important gene for HER2^{labile} cells proliferation, whereas HER2^{loss} cells may rely on different pathways.

Wnt7b encodes a soluble signaling factor belonging to Wnt family, which was originally uncovered as preferential integration site of mouse mammary tumor virus (MMTV), thus indicating a strong link to mammary tumors. It has been found up-regulated in human mammary triple-negative cell lines MDA-MB231 and BT-20 and in 10% of human mammary carcinomas (Huguet et al., 1994). It cooperates with TGF-B pathway in maintenance of a mesenchymal and migratory phenotype in mammary carcinoma cells (Sundqvist et al., 2018). Surprisingly, in our model this gene is down-regulated in HER2^{loss} cell line.

Postn encodes periostin, an ECM protein with anti-apoptotic, pro-angiogenic, pro-metastatic and genetic instability promoting activities which favor mammary carcinoma (Ruan et al., 2009). In triple negative tumors it appears involved in maintenance of staminal niche (Lambert et al., 2016). Unexpectedly, this gene was down-regulated in HER2^{loss} cell.

Pla2g7 is a phospholipase with a known pro-metastatic role in MDA-MB-435 and BT549 human mammary cell lines, where it also promotes EMT. It is abundantly expressed in triple negative, where it is also associated to worst prognosis (Lehtinen et al., 2017). Pla2g7 is the only up-regulated gene in HER2^{loss} and its activities well copes with its aggressiveness and mesenchymal phenotype.

To some up, differential expression of Myh14, Cdkn2b, Krt7 and Krt8 and Pla2g7 well mirrors differences in phenotype between HER2^{labile} and HER2^{loss} cell lines. In turn, we would expect Wnt7b, Postn an Ifitm10 as up-regulated in HER2^{loss}, due to their

association with aggressiveness and stemness. Their up-regulation in HER2^{labile} could represent a spy of these cells being prone to acquisition of mesenchymal characteristics or relying on different pathways for maintenance of malignant phenotype.

3.2 HER2-positive *versus* HER2-negative

All HER2-positive cell lines in our model (in green in figure 10) were compared to all cell lines which have lost HER2 expression (in red in figure 10). This analysis identified 751 differentially expressed genes; 409 of them were up-regulated in HER2-negative cell lines and 349 were down-regulated.

The gene lists were first of all analyzed through PANTHER to obtain a functional classification of transcripts. Genes down-regulated in HER2-negative cells, thus up-regulated in HER2-positive cells, 109 (45%) had a binding and 78 (31%) a catalytic molecular function. Most genes clustered in metabolic (114; 20%) and cellular processes (157;27%), this last cluster gathering together genes principally involved in cell communication (55; 67%). Other highly represented biological process (>50 genes clustered) were response to stimuli (60; 10%), biological regulation (62; 18%) and developmental processes (54; 16%). Most genes involved in developmental processes were subcategorized in cellular development (15; 29%) (fig. 11A). Among the 409 genes up-regulated in cell lines which have lost HER2 expression, 111 (39%) had a binding and 112 (39%) a catalytic molecular function. Most genes clustered in metabolic (137; 35%) and cellular processes (179;45%), this last cluster gathering together genes principally involved in cell communication (55; 31%). Highly represented biological process (>50 genes clustered) were response to stimuli (50; 13%) and biological regulation (51; 13%) Many genes involved in response to stimuli clustered again in response to toxic substances (20; 40%) (fig. 11B).

A second analysis, through STRING, was focused on interaction between gene products of gene down- and up-regulated in HER2-negative cell lines with respect to HER2-positive cells (fig. 12A and fig. 13A).

329 genes out of 349 up-regulated in HER2-positive cell lines were mutually interacting in a network (Protein Protein Interaction enrichment value p<01 e^{-16}). Some new knots emerged, such as CDH1, Stat3, Erbb2, Notch1, Kit, SPTAN1, PTPN1, STAT5A and B, JUP, ITGB3, FGFR1, PAK1, Cul1, IL5 and EFNB1 (fig. 13A). ErbB2 resulted down-regulated in HER2^{loss} cells. Indeed, many of these knots of interaction are directly linked

to HER2 iper-expression and have been reported as up-regulated in HER2-positive human breast cancers. For example, **Stat** signaling is widely reported in all breast cancer subtypes and particularly Stat3 is associated to HER2-positive breast cancer (Furth P., 2014). **PTPN1** and **PAK1** are involved in HER2 signaling at different levels. **Cul1** is involved in HER2 mediated oncogenesis, since this ubiquitin-ligase leads to p27 degradation, which is increased in HER2-positive tumors (Zhang et al., 2004). **IL5** and **EFNB1** have been reported as up-regulated specifically in HER2-positive or enriched breast cancer (Koenig et al., 2016; Fernandez-Nogueira et al., 2016), whereas **FGFR1** can be found co-amplified with HER2 in breast cancer and the co-amplification can be considered a poor prognosis indicator (Chen et al., 2018). Hence, up-regulation of PTPN1, FGFR1, PAK1, Cul1, IL5 and EFNB1, and their interactor could be expected in HER2-positive samples.

Other genes up-regulated in HER2-positive cells account for their polygonal shape and growth in a monolayer of closely interacting cells. Among these, **Cdh1** is a known marker of epithelial cells whose lost is frequently associated with EMT and is therefore up-regulated in polygonal HER2-positive cell lines (see paragraph 2.5). **JUP** encodes a part of the sub-membranous complex of intermediate junctions and desmosomes, is therefore found mostly in epithelial cells and its high expression is reported to hamper migration and invasiveness in mammary tumors. Moreover, it has been found associated to HER2 iper-expression (Silvrikoz et al., 2013). **Notch1** is activated by cell-cell contact and together with **Kit** is involved in maintenance of cell proliferation and staminal properties. Moreover, c-KIT expression is epigenetically downregulated during breast epithelium transformation and cancer development via KIT promoter hypermethylation (Janostiak et al., 2018). Achieving a mesenchymal phenotype, HER2^{loss} cells loose mutual contacts and consequently Notch1 expression. Notch1 and Kit may represent key signaling pathway for proliferation of HER2-positive cell lines, whereas HER2^{loss} cells loose addiction from these factors.

Lastly, some up-regulated genes were correlated to luminal cell differentiation. For example, **SPTAN1** encodes a fodrin involved in movement and secretion. High level of these proteins and their interactors in HER2-positive cell lines can hence indicate their luminal differentiation, which is lost in HER2 loss.

Unexpectedly, **ITGB3** was found up-regulated in HER2-positive cells. In contrast, in literature this integrin is reported as up-regulated in stressful conditions such as hypoxia and appears to promote a migratory and invasive phenotype activating EMT through Snail and TGF- (Sesè et al., 2017). It was also found up-regulated in triple negative mammary carcinomas and related to its migratory properties (Klahan et al., 2014). ITGB3 over-expression in HER2-positive cells seems in contrast with these observations.

Most genes up-regulated in HER2-negative cells were significantly mutually linked in a network (PPI enrichment value $p=1.0e^{-16}$), as well; main knots of interaction with more than 20 interactors were VEGF, MYC, FN1, VIM, PTGS2, PDGFRB, DCN, CAV1, CDKN1A, ENO2 and many more knots with at least 10 interacting genes were identified (fig. 12A).

Again, many of these genes are known to be down-regulated in HER2-positive human breast cancer or have in turn been associated with basal-like breast cancers. **FN1** has been described as down-regulated in HER2 overexpressing carcinomas (Mackay et al., 2003); hence, in our model, once HER2 expression is lost, FN1 expression is restored. Moreover, Fn1 and **VIM** (a known marker of mesenchymal cells) expression, together with CD44high/CD24low phenotype, have been found strongly associated to apocrine, basal-like and triple negative breast cancers in a population of Omani women (Lakhtakia et al., 2017). **ENO2, VEGFA** and **PTGS2** are involved in angiogenesis and directly transcriptionally regulated by HER2 (Al-Ammedine et al., 2013); their increased transcription in HER2-negative cell lines must hence be up-regulated by different mechanisms. It however copes well with increased ability of forming vascular tube *in vitro* of HER2-negative cells.

Other genes and their interaction are known for their role in promoting tumor cell aggressiveness, EMT or sustaining proliferation of mesenchymal cells. This category was the most interesting to us, because it could reveal which genes and pathway HER2-negative cells actually rely on for proliferation and maintenance of malignant phenotype. **Dcn** and **Cav1** encode a proteoglycan and a scaffold protein, respectively, which normally exert a tumor-suppressive action binding growth factor and mediating their degradation (Zhang et al., 2018). In our model, Dcn and Cav1 up-regulation could be responsible of a more intense degradation of HER receptors and may be a spy for HER2-negative cell lines relying on a different pathway for proliferation. **Cdkn1a** encodes the

inhibitor of cell cycle p21; despite being a tumor-suppressor, high levels of cytoplasmic p21 together with high levels of cyclin B and p53 have been correlated to poor prognosis in breast cancer, regardless of HER2 expression (Abbas and Dutta, 2009). In our model, p21 could hence be linked to more aggressive properties of HER2-negative cell lines. **MYC** is an oncogene whose expression is markedly high in triple negative with respect to ER-positive and HER2-positive breast carcinomas (Fallah et al., 2017). In our model, its iper-expression in lines which have lost HER2 expression reflects their affinity to triple negative breast cancer cells. Lastly, **PDGFR-** is a growth factor receptor which sustains growth and proliferation of mesenchymal cells; it is hence reliable that this receptor may sustain growth of HER2-negative cell lines as well. This hypothesis grew stronger analyzing the list of genes up-regulated in HER2-negative cells with the database ArchS4-kinase: 50 or more of these genes resulted significantly correlated to the kinase activation of PDGFR- and its isoform PDGFR- .

Through EnrichR, we looked for significant enrichments in biological processes or pathways. Up-regulated biological processes and pathways in HER2-positive cells comprising more than 10 genes were represented by positive regulation of protein modification processes, protein localization at membrane, proteoglycans in cancer and regulation of actin cytoskeleton (fig. 13B and 13C). Considering processes and pathways involving less than 10 genes, genes up-regulated in HER2-positive cells were also significantly associated to processes of cell junction assembly as well as differentiation and epithelial cell development. HER2-negative cells were instead significantly enriched for pathways or biological processes of PI3K-Akt signaling, proteoglycans in cancer, focal adhesion, protein processing in endoplasmic reticulum, lysosome, ECM organization, positive regulation of migration, angiogenesis, exocytosis, biosynthesis, PkB signaling, cellular biosynthesis processes and response to oxidative stress (fig. 12B and 12C).

To sum up, HER2-positive cells show an increased epithelial differentiation and cell-cell communication. Most knots and processes highlighted in analysis can be related to these two functions or to HER2 signaling itself. HER2-negative cell lines show indications of a lost addiction from HER2 signaling, an increased angiogenesis and migration and an expression profile which often reflects those of triple negative or basal-like breast

cancers. Myc and PDGFR-B showed up as possible oncogenes sustaining proliferation of HER2-negative cell lines.

A Down-regulated genes in HER2 negative versus HER2 positive cells
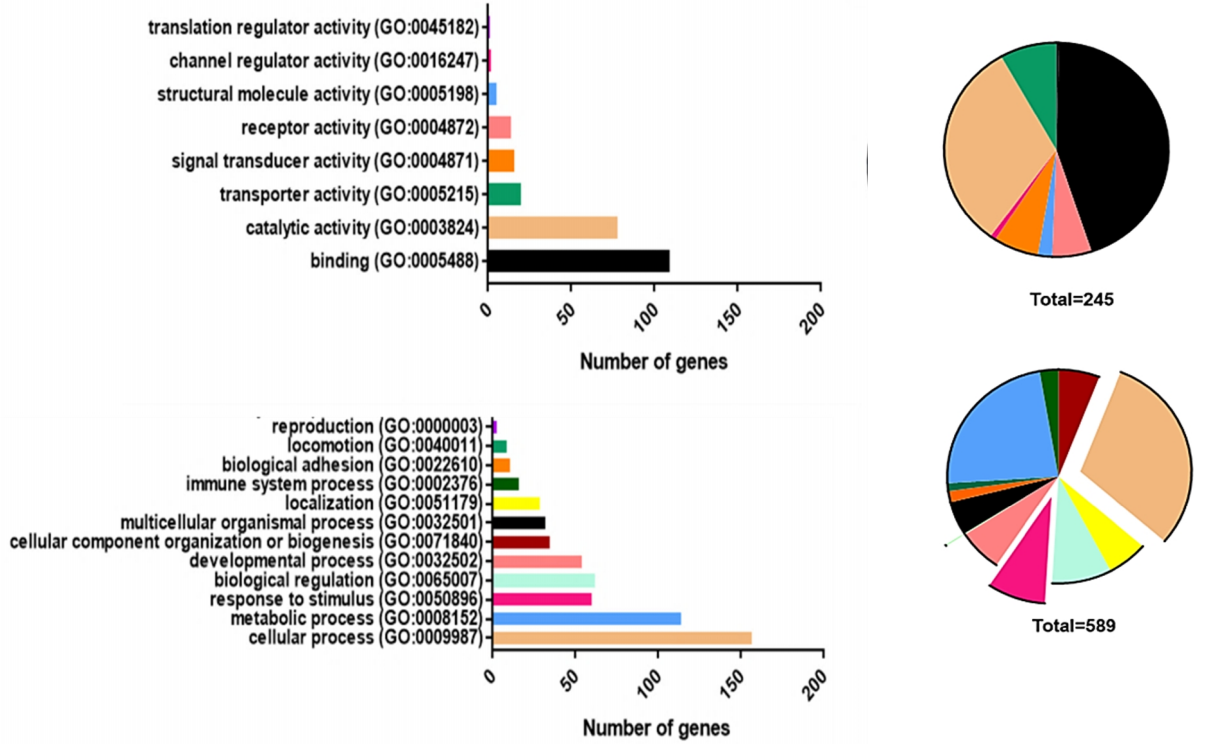
B Up-regulated genes in HER2 negative versus HER2 positive cells
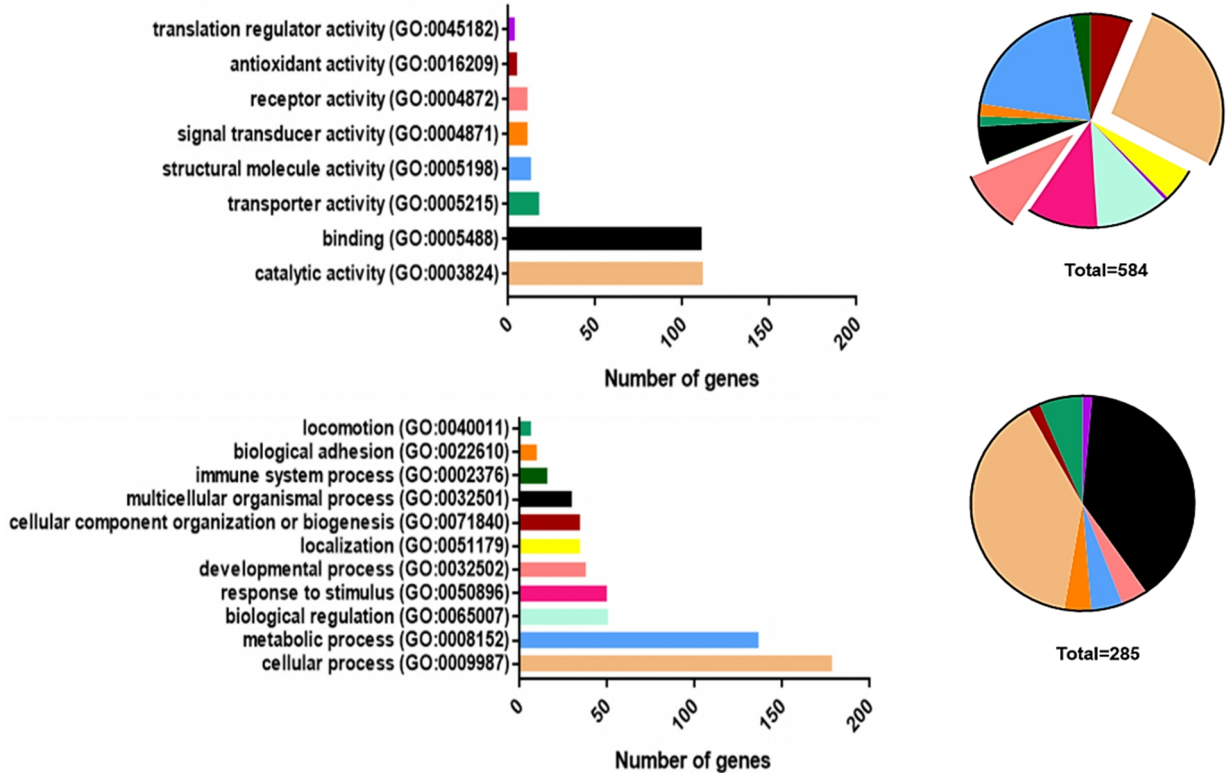
Figure 11. HER2-negative *versus* HER2-positive
Functional clustering of genes down-regulated (A) and up-regulated (B) in HER2-negative cells analyzed through PANTHER database. Upper graphs refer to molecular function, lower graphs to biological process.
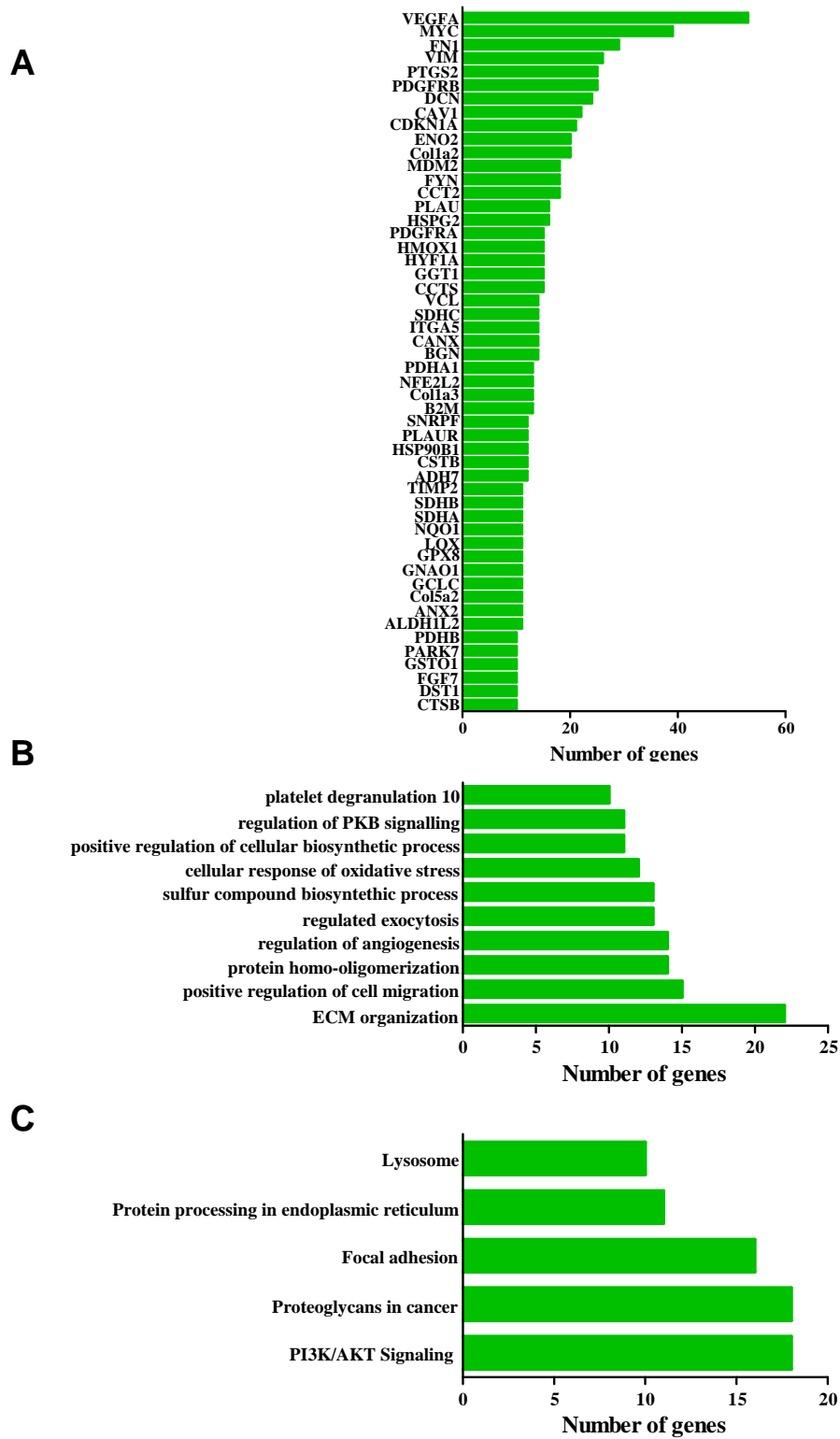
Figure 12. HER2-negative *versus* HER2-positive

Analysis of genes up-regulated in HER2-negative cells. (A) Graph bar lists gene with more than 10 molecular interactors. (B) Significantly enriched biological Processes and (C) KEGG pathways analyzed with EnrichR.

A

| Gene | Number of genes |

(Bar chart A with genes: CDH1, STAT3, ERBB2, NOTCH1, Kit, SPTAN1, PTPN1, STAT5A, JUP, ITGB3, STAT5B, FGFR1, PAK1, CUL1, IL5, EFNB1; x-axis "Number of genes" from 0 to 30)

B

(Bar chart B: protein localization to periphery, protein localization to plasma membrana, protein localization to membrane, positive regulation of protein modification process; x-axis "Number of genes" from 0 to 25)

C

(Bar chart C: Regulation of actin cytoskeleton, Proteoglycans in cancer; x-axis "Number of genes" from 0 to 15)

Figure 13. HER2-negative *versus* HER2-positive

Analysis of genes down-regulated in HER2-negative cells. (A) Graph bar lists gene with more than 10 molecular interactors. Significantly enriched biological Processes (B) e KEGG pathways (C) analyzed with EnrichR.

4. Inhibiting HER2^{loss} cells

RNASequencing analysis results indicated PDGFR-B as a possible molecule sustaining growth of HER2-negative cell lines. We therefore chose it as a target of therapy with sunitinib. Sunitinib is a small-tyrosine-kinase inhibitor approved by EMA for therapy of renal cell carcinoma and imatinib-resistant GIST (gastrointestinal stromal tumors). Sunitinib is a multi-targeted molecule which has been shown to inhibit PDGFRs, VEGFR and c-Kit. PDGFRs and VEGFA, VEGFR ligand, both resulted up-regulated in HER2^{loss} cells, so observed effects of this molecule could be due to inhibition of either target. First of all, we validated PDGFR-B expression at protein level and performed some *in vitro* experiments to assess its efficacy and mechanism of action. Lastly, we checked its efficacy *in vivo* as well, in tumors induced by HER2^{loss} cells or by HER2^{labile} cells (which give rise to HER2-negative tumors).

4.1 PDGFR-B validation in HER2^{loss} model

PDGFR-B had already been individuated as a differentially expressed molecule in HER2^{loss} cell line when compared to HER2^{stable} cell line in a previous PCR Array analyzing genes linked to EMT. Its up-regulation at RNA level has hence already been validated; PDGFR-B has been found up-regulated in HER2^{labile} cell treated with trastuzumab as well (see fig. 8). DGFR-B expression at protein level was checked by flow-cytometry. PDGFR- was detected only in HER2^{loss} cells, whereas the other cell lines were completely negative (fig. 14A). Of note, in HER2^{labile} TRT and TRNT which became spindle-like after treatment with trastuzumab, PDGFR-B expression at protein level was enhanced as well (fig. 14B).
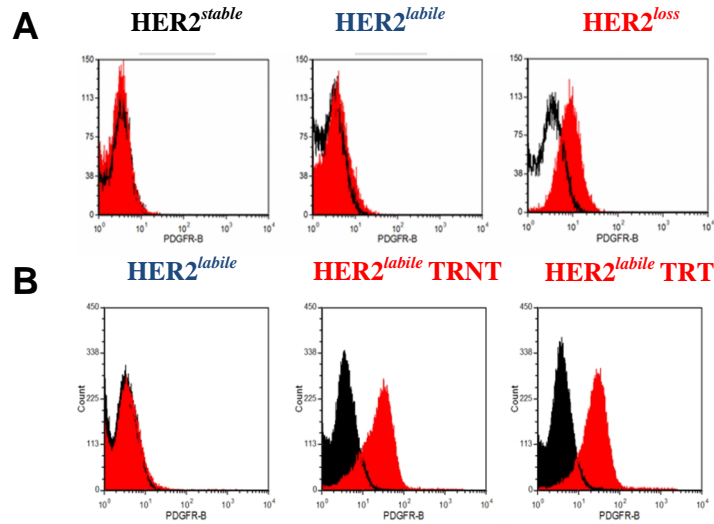
Figure 14. Expression of PDGFR-B
Figure shows PDGFR-B expression at protein level determined by FACS analysis. Black profile refers to cell incubated with secondary fluorescinated antibody only; red profile refers to cell incubated with -PDGFR-B.

4.2 Treatment with sunitinib of HER2^{loss} cells *in vitro*

We determined sunitinib efficacy in inhibiting growth of HER2^{loss} cell line both under 2D-adherent and 3D-non-adherent culture conditions.

Under 2D adherent conditions, HER2^{loss} appeared sensible to sunitinib. Sunitinib 1 µM already showed poor effects on cell growth, whereas sunitinib 10 µM completely inhibited growth of HER2^{loss} cell line. IC50 was calculated as 4.66 µM (fig. 15A).

We chose concentrations of 1 and 5 µM for further analysis under 3D-non-adherent conditions. Untreated cells formed big sprouting colonies (79±4) as well as cells treated with sunitinib's vehicle (DMSO 0.05%). Sunitinib 1µM dramatically reduced size of colonies, but colony count was reduced only of 20%. Sunitinib 5 µM was able to completely impede growth of any colonies in this setting (fig. 15B and C). Hence, HER2^{loss} cells resulted sensible to sunitinib *in vitro*.

In a different experiment, HER2^{loss} cells were seeded 8×10^4 cell/cm^2 and treated with sunitinib 5 µM (fig. 16A). Untreated cells and vehicle treated cells remained spindle-like and grew in multilayer. After 4 days of treatment, cells treated with sunitinib 5 µM acquired mostly a more polygonal shape and cells appeared to grow in a monolayer with fewer spindle-like cells on a different focus. These cells gradually lost this morphology and turned back spindle-like, but the same and more pronounced alterations in morphology were observed treating HER2^{loss} cell line with a higher dose of sunitinib (10

µM) (fig. 16B). Despite cells acquiring a more polygonal shape, HER2 expression remained negative as shown by RT-PCR analysis (fig. 16C). In this setting, sunitinib effect on cell growth appeared reduced with respect to previous experiments, maybe due to the presence in the medium of extra growth factors such as BPE and MITO^{SE}.
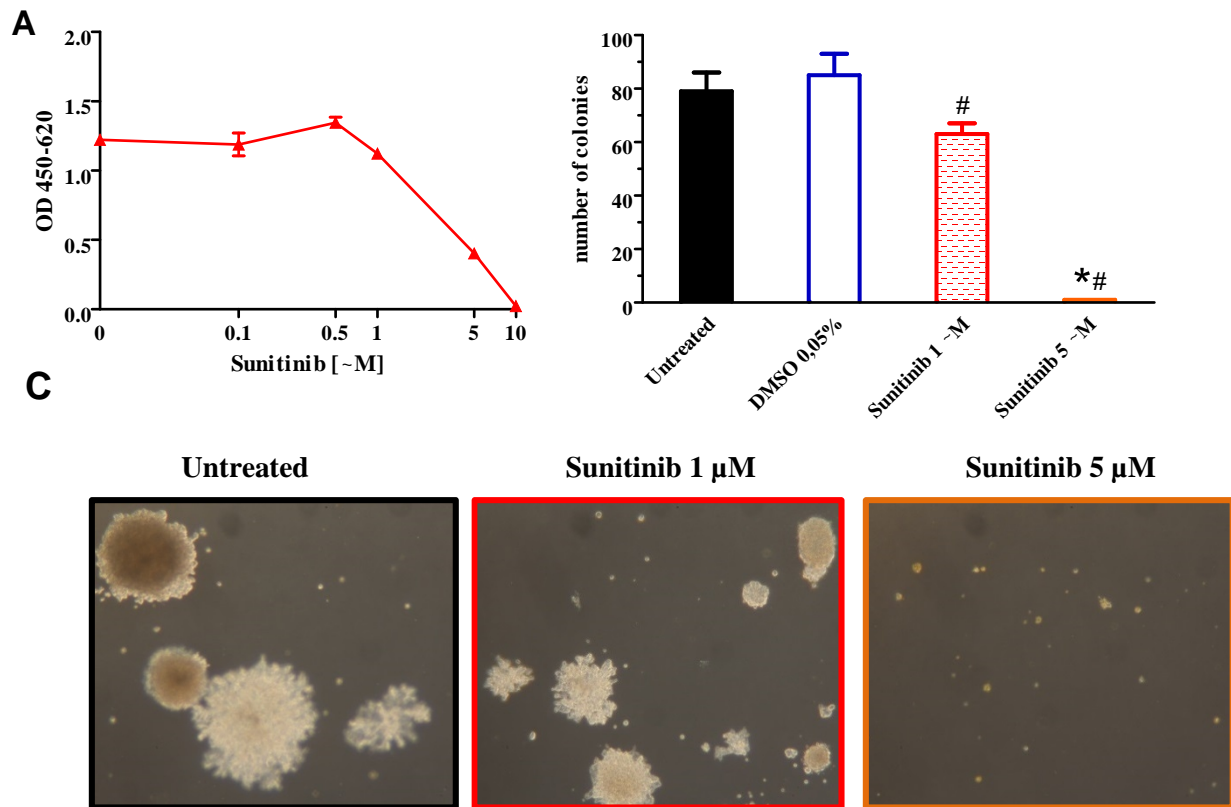
Figure 15. Sunitinib *in vitro*.
(A) Inhibition curve of HER2^{loss} cell line under 2D-adherent conditions by WST-1 analysis. (B) Bars report absolute number of colonies grown out of HER2^{loss} cells seeded in soft-agar (3D-non-adherent conditions). Statistical analysis: Student's *t* test, * and # <0.05 *versus* control or vehicle, respectively. (C) Pictures of soft-agar colonies of untreated (black outline) and cells treated with sunitinib 1 µM (pink outline) or 5 µM (orange outline). Photos were shot at Diavert microscope, 2,5× magnification.
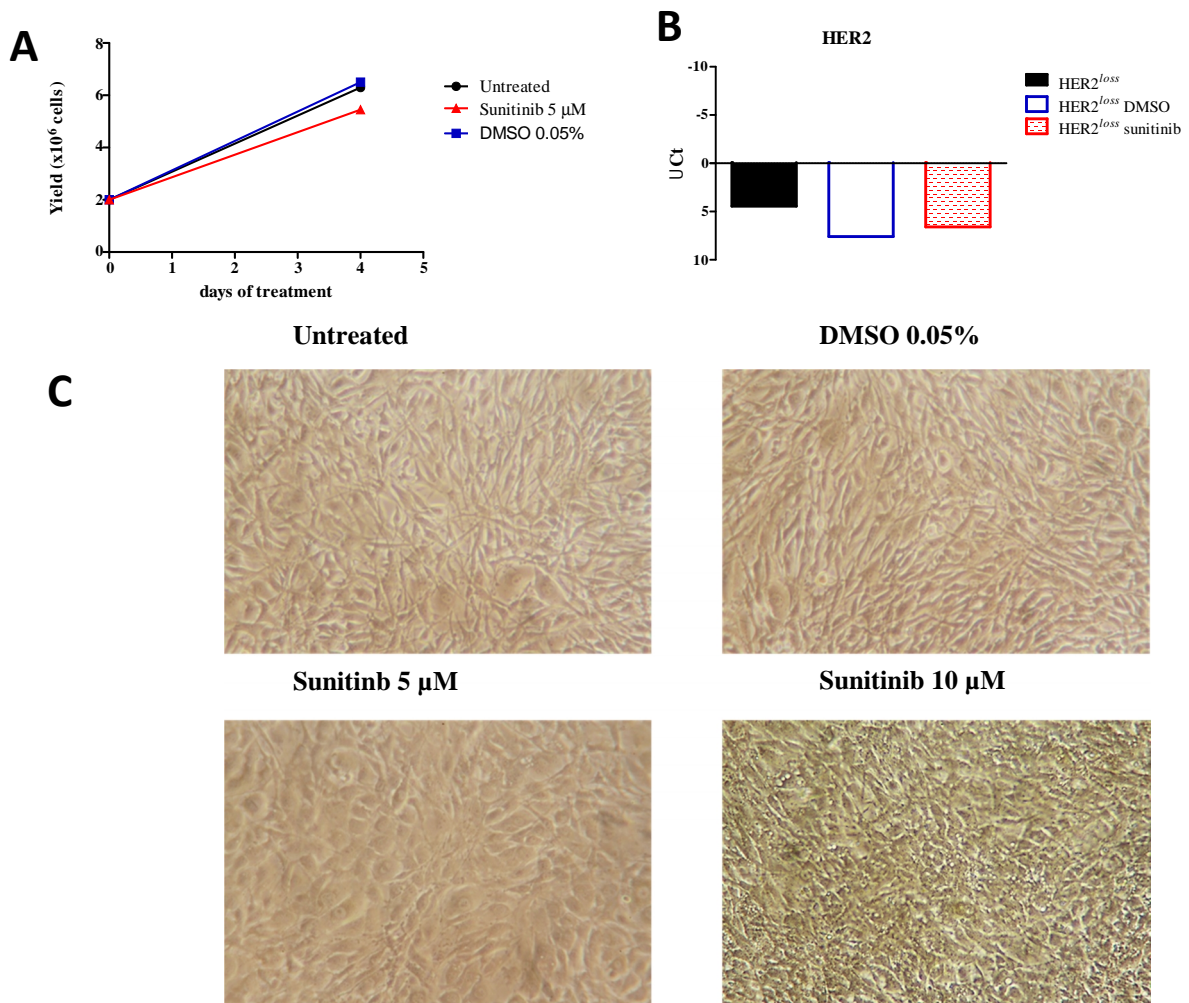
Figure 16. Sunitinib alters morphology of HER2^{loss} cells

HER2^{loss} cells (8×10^4 cells/cm^2) were treated with medium only (untreated) or DMSO 0.05% or sunitinib 5-10 µM.

    (A) Growth curve of untreated (black round) and vehicle cells (blue rectangle) and cells treated with sunitinib (red triangle).

    (B) Analysis of HER2 at mRNA level by RT-PCR analysis, normalized over TBP (total binding protein) expression (Ct=Ct$_{gene}$-Ct$_{TBP}$).

    (C) Photos were shot at Diavert microscope, 250× magnification.

4.3 Modulation of IL-6 following treatment with sunitinib

After 4 days of treatment with sunitinib, surnatants were collected from treated and untreated cells and IL-6 production was checked. IL-6 is a cytokine involved in inflammation and angiogenesis; it has been reported to induce EMT which is implicated in emergence of BCSC. High levels of this cytokine have been linked to poor clinical outcome in breast cancer patients. Lastly, its up-regulation has been reported in a model

of BT474/PTEN- treated long-term trastuzumab (LTT), which became spindle-like upon treatment: here, IL6 appeared to trigger an inflammatory loop which leads towards acquisition of a staminal, basal-like phenotype and resistance to trastuzumab (Korkaya et al., 2012). Moreover, HER2^{loss} and HER2^{labile} induced tumors show an abnormal angiogenesis *in vivo*, characterized by absence of pericytes, which could be due to an elevated production of IL-6 (Gopinathan et al., 2015). Due to this experimental observation and similarities between BT474/PTEN-/LTT and HER2^{labile} TRT cells, we decided to investigate IL-6 expression and production in our model of HER2 loss and in response to treatment with sunitinib.

IL-6 has not been found in surnatants of HER2^{labile} cells, where its concentration is inferior to 30 pg/ml. In turn, HER2^{stable} and HER2^{loss} cells produced IL-6 with mean concentrations of 316±55 pg/ml and 999±188 pg/ml, respectively. Surprisingly in our model, IL-6 was not elevated in HER2^{labile} cells treated long-term with trastuzumab (TRT) and its concentration remained almost undetectable (fig. 17A).

Treatment with sunitinb in HER2^{loss} cells managed to reduce IL-6 production (fig. 17B). We also checked activation of IL-6 down-stream pathways to IL-6, such as Stat3, by western blot analysis. We found a down-regulation of pStat3 upon treatment with sunitinib (fig. 17C).

To sum up, IL-6 production was increased in HER2^{loss} cells with respect to the other cell lines. It was almost undetectable in HER2^{labile} cells and spindle-like HER2^{labile} TRT did not start producing this cytokine. Sunitinb was able to decrease its production in HER2^{loss} treated cells as well as to inhibit down-stream pathway. We can therefore speculate an involvement of IL-6 in HER2^{loss} spindle-like morphology and basal-like features, which calls for further investigation.

4.4 Sunitinib modulates angiogenesis *in vitro*

HER2^{loss} has a greater ability than HER2^{stable} and HER2^{labile} of forming vascular tubes *in vitro*. We performed a Matrigel Tube Formation Assay on vehicle treated cells and cells treated with sunitinib.

After 24h of treatment, cells were seeded in matrigel and tube formation was observed after 16 hours. Vehicle-treated cells formed spheres sprouting out many tubes each, which were mutually interconnected. HER2^{loss} cells treated with sunitinib lost their capability of

forming tubes and cells formed only close-agglomerated spheres with no branches (fig. 17D).
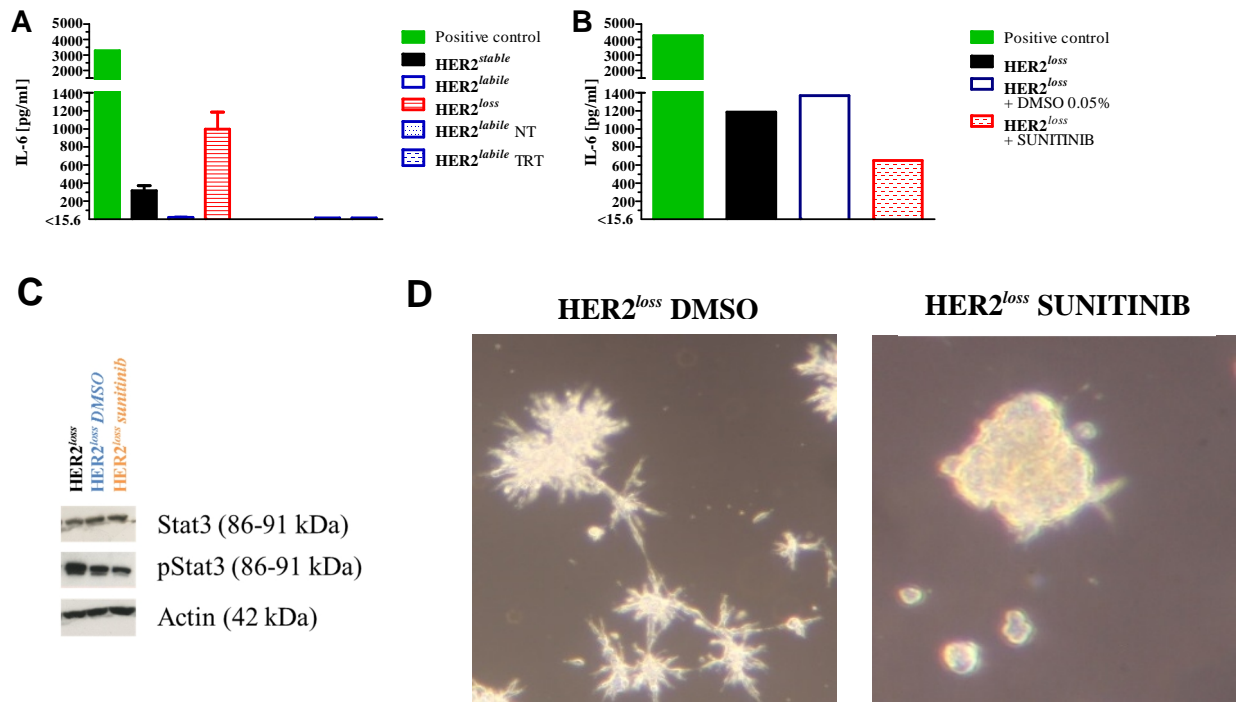
Figure 17. Sunitinib effects on IL-6 and angiogenesis

(A) and (B) Concentration of IL-6 determined by ELISA. Surnatants were collected 4 days after seeding and eventually treatment of indicated cell lines. Positive control is a murine cell-line transduced with IL-6 (TS/A-IL6).
(C) Western blot analysis of Stat3 and pStat3 in HER2^{loss} cells treated with medium only, DMSO 0.05% or sunitinib 5 µM for 4 days.
(D) Matrigel Tube Formation Assay of HER2^{loss} cells treated DMSO 0.05% or sunitinib 5 µM treated for 24 hours before seeding in Matrigel. Photos (Diavert microscope, 2,5× magnification) were shot 16 hours after seeding.

5. Sunitinib *in vivo*

Lastly, we checked sunitinib action on HER2-negative tumors induced by inoculation of HER2^{labile} and HER2^{loss} cell line in FVBhuHER2 mice *in vivo*.

HER2^{labile} cells grew *in vivo* after a long latency period. Sunitinib was able to significantly slow down tumor growth from day 37 and also significantly improved survival to 1 cm^3 tumors with respect to untreated mice (fig. 18A). Importantly, all tumors in treated as well as vehicle groups were negative for HER2 expression (data not shown). HER2^{loss} cells, even if injected at lower dose, grew much quicker with tumors tripling their volumes in just one week. In this setting, sunitinb was not able to impede tumor growth or improve survival (fig. 18B).
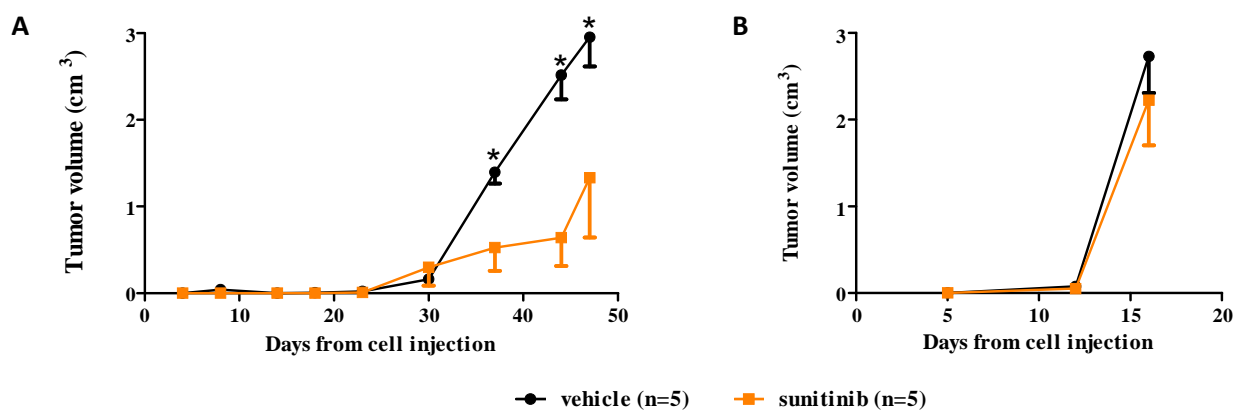
Figure 18. Sunitinib *in vivo*

(A) 10^6 HER2^{labile} cells injected in FVBhuHER2 mice treated every second day from +3; (B) 10^5 HER2^{loss} cells injected in FVBhuHER2 mice treated daily (7/7) from +1 after cell injection. Animals received METOCELL 0.5%+TWEEN80 0.4% (vehicle) or sunitinb 60 mg/kg *per os*. Each point represents the mean±s.e.m. of 5 mice. Statistical analysis of growth curve: Student's *t* test, * p< 0.05.

6. Neratinib in a mammary patient-derived-xenograft collection

6.1 Establishment of a mammary patient-derived-xenograft collection

Recently, a collection of mammary patient derived xenografts (PDX) was established at the Laboratory of Biology and Immunology of Metastasis, directed by Professor Lollini, in collaboration with the equips of Professor Foschini (Bellaria Hospital, Bologna) and Professor Taffurelli (Sant´Orsola-Malpighi Hospital, Bologna). A total of fresh 66 non-consecutive primary breast cancer specimens were received shortly after surgery and immediately implanted orthotopically in the mammary fat pad of immune-deficient mice. Table 2 describes the clinical features of tumors implanted. Most tumors were invasive ductal carcinomas (IDC) (59; 89%). Grading was generally high with half of implanted tumors scoring grade III (33; 50%). On the other hand, tumor sizes were rather small and little node invasion was noticed; indeed, approximately half samples scored T1 (33, 50%) and showed no node invasion (29; 44%). Proliferation index was evenly distributed and varied from low (27; 41%) to high (24; 36%). Most samples were hormone receptor positive (55; 83%) and only 15 (23%) showed HER2 amplification or overexpression. Altogether the characteristics of our panel of primary tumors mirrored the proportions observed in most patient populations in the clinic.

6.2 Stable PDX attainment classified by intrinsic subtypes

According to intrinsic subtypes classification, the majority of implanted specimens received were luminal A (31; 47%), nevertheless no stable PDX transplantable *in vivo* for more than 3 passages was obtained for this subtype even if one tumor actually grafted at 1st passage *in vivo*. 14 of the implanted tumors were luminal B (21%): 2 stable PDXs were obtained for this subtype. Triple positive tumors represented 15% of received samples (10); two specimens actually grafted in mice but no stable PDX was obtained for this subtype. Despite HER2-positive tumors' rarity (5; 8%) in implanted tumors, this subtype showed the highest take (4; 80%) and PDX production (2; 40%). None of the few triple negative tumors implanted (6; 9%) gave rise to a stable PDX. Table 3 summarizes rates of engraftment and stable PDX attainment by intrinsic subtype. The final collection can hence count 2 luminal B, 2 HER2-positive and 1 triple negative PDX. Overall 7.5% of the implanted tumors produced a stabilized PDX.

PARAMETER		Cases	(%)
HISTOLOGY			
	Invasive ductal carcinoma (IDC)	59	89
	Invasive lobular carcinoma (ILC)	6	9
	Invasive mucinous carcinoma (IMC)	1	2
GRADE			
	III	33	50
	II	22	33
	I	11	17
TUMOR SIZE			
	T1	33	50
	T2	29	44
	>T2	2	3
	Not evaluated	2	3
NODE INVASION			
	N0	29	44
	N1	17	26
	N2	15	23
	Not evaluated	5	7
HORMON RECEPTORS			
	ER+ and/or PR+	55	83
	ER- and PR-	11	17
HER2 EXPRESSION			
	HER2 overexpression or amplification	15	23
PROLIFERATION			
	Ki-67 high	27	41
	Ki-67 intermediate	15	23
	Ki-67 low	24	36

Table 2. Clinical features of primary tumors implanted
The table records the main clinical features of tumors received from surgery, such as histology, grading, staging (T= size and N=nodular invasion), receptor *status* (estrogen receptor, ER; progesterone receptor, PR; and HER2) and proliferation index (Ki-67).

	Luminal A	Luminal B	HER2	Triple-positive	Triple-negative
Implanted tumors	31 (47%)	14 (21%)	5 (8%)	10 (15%)	6 (9%)
Grafted tumors (1st passage)	1	2	3	2	1
Stable PDX (%) (3rd passage)	0 (0%)	2 (14%)	2 (40%)	0(0%)	1 (17%)

Table 3. PDX attainment by intrinsic subtype
The table classifies implanted tumors by intrinsic subtype according to ASCO/CAP 2015 suggestions and records how many specimens grafted (i.e. grown in mice at first passage) and how many gave rise to a stable PDX (i.e. transplantable to the third passage) in mice.

6.3 HER2 expressing PDXs: features of originating tumors

Among the 5 stable PDX models attained at our laboratory: 2 were luminal B, 2 were HER2-positive, whereas 1 was triple-negative. We chose the luminal B PDX showing some evidence of HER2 expression (PDX-SBR18) and the two HER2-positive PDX (PDX-BBR4 and PDX-SBR45) and for further analysis. The characteristics of tumors originating these PDXs are detailed in table 4.

The tumor giving rise to PDX-SBR18 was classified as luminal B. It was small and presented limited node invasion. Its proliferation index was high. The implanted specimen showed low p53, intermediate Bcl2 and no HER1 expression.

The two tumors clinically classified as HER2-positive, giving rise to PDX-BBR4 and PDX-SBR45, shared only the receptor *status* (ER-, PR-, HER2+) and the high proliferation index. All other immune-histological parameters analyzed differed greatly. The tumor originating PDX-BBR4 was little and did not show any node invasion, whereas PDX-SBR45 originated from a bigger tumor with a higher node grade. PDX-BBR4 originating tumor had a high expression of Bcl2 and p53, but showed no HER1 expression. On the contrary, PDX-SBR45 originating tumor was negative for Bcl2 and p53 but positive for HER1 expression.

	PDX-SBR18	PDX-BBR4	PDX-SBR45
Intrinsic subtype	Luminal B	HER2-positive	HER2-positive
pT	T1c	T1c	T2
pN	N1	N0 (sn -)	N2 (+9/25)
Hormone receptors	ER+ PR-	ER- PR-	ER- PR-
HER2 score	2+	2+ (amplified)	+3
Ki-67	High	High	High
Bcl2	Intermediate	Positive	Negative
P53	6	100	0
HER1	Negative	Negative	Positive

Table 4. Characteristics of tumors originating HER2 expressing PDX
The table records the major features of tumors originating PDX-SBR18, PDX-BBR4 and PDX-SBR45 detected by hysto-pathological analysis such as intrinsic subtype defined following suggestions of St. Gallen *consensus* 2015, pT (size), pN (node invasion), HER2 score according to ASCO/CAP 2013 recommendations, proliferation index (ki-67), expression scores for Bcl-2 (B cell lymphoma 2), p53 (tumor protein p53) and HER1.

6.4 HER2-expressing PDX: stability of growth parameters and hysto-pathological features

Growth and hysto-pathological characteristics of HER2-expressing PDX were followed over time in several passages *in vivo* to assess their stability.

No dramatic receptor conversion was observed over time in any of the PDX models and there were no changes in intrinsic subtypes. HER2 score in PDX-SBR18 varied randomly from score 0/1+ to 2+ over time, whereas PDX-BBR4 and PDX-SBR45 scored 3+ in any analyzed sample (Table 5).

PDX-SBR18 and PDX-SBR45 remained stably ER+PR- and ER+/PR+, respectively, over time; in turn, some PR expression was observed in PDX-BBR4 passages V-VII (1%-3%) (Table 5).

HER1 expression remained negative in PDX-SBR18 and PDX-BBR4 throughout this observation, whereas some fluctuations occurred in PDX-SBR45 around the intermediate score (Table 5).

All tumors retained a high proliferative index over time. Bcl2 and p53 expression was stable in PDX-BBR4 and PDX-SBR45, whereas in PDX-SBR18 a slight increase in these parameters was observed over time indicating a possible selection of a more aggressive subpopulation *in vivo* (Table 5).

Growth parameters such as latency and growth rate were also followed over time up to the XII passage *in vivo*. No significant alterations were observed in PDX-SBR18 latency or time to $1cm^3$ after passage II-III (fig. 19A). PDX-BBR4 showed a trend towards increased growth rate and a significantly decreased survival to $1 cm^3$ tumors in passage IV-V and later passages with respect to passages II-III (fig. 19B). PDX-SBR45 showed an increased growth rate and significantly decreased survival to $1cm^3$ tumor in late passages (VI-VII-VIII) compared to II-III and IV-V (fig. 19C).

Overt metastasis was never observed in our PDX collection from I to XII passage. Presence of disseminated tumor cells (DTCs) was checked in target organs (lung, bone marrow, brain and ovaries) by RT-PCR. In PDX-SBR18, DTCs were found in the lung of 4 out of 19 animals analyzed (21%); no other human cells were detected in any other organ. PDX-BBR4 tumor cells disseminated to lung, bone marrow and ovaries in less than 10% of analyzed animals. PDX-SBR45 rarely disseminated to the same organs. In both PDX-BBR4 and PDX-SBR45 a maximum of 1500 DTCs per organ was detected (Table 6).

Overall, histological characteristics were rather stable over serial passages *in vivo* in our PDX collection. Increased growth rates over time were observed in PDX-BBR4 and PDX-SBR45, thus indicating a smooth selection of more aggressive clones. DTCs were a seldom event in our PDX collection.

Passage in mice	Hormone receptors	Ki-67	Bcl2	p53	HER1	HER2
PDX-SBR18						
Patient	**ER+ PR–**	**High**	**Int**	**6**	**Neg**	**Sc2+**
I	ER+ PR–	High	Int	0.1	Neg	Sc0/1+
II (n=2)	ER+ PR–	High	Int	1.1-0.1	Neg	Sc2+ 20% - Sc1+
III (n=3)	ER+ PR–	High	Int/Pos	14-19	Neg	Sc2+ 70%-Sc1+
IV	ER+ PR–	High	Int	28	Neg	Sc1+/2+
V (n=3)	ER+ PR–	High	Int/Pos	13-35	Neg	Sc1+/2+- Sc2+80%
VI (n=3)	ER+ PR–	High	Int/Pos	6-26	Neg	Sc2+ 15%- Sc1+/2+
VII (n=2)	ER+ PR–	High	Int/Pos	6-21	Neg	Sc1+/2+
VIII (n=3)	ER+ PR–	High-Int	Int/Pos	15-21	Neg	Sc1+/2+- Sc2+
IX (n=2)	ER+ PR–	High	Int/Pos	10-48	Neg	Sc1+/2+
PDX-BBR4						
Patient	**ER– PR–**	**High**	**Pos**	**100**	**Neg**	**Sc 2+ (FISH Pos)**
II	ER– PR–	n.d.	Pos	98	Neg	Sc 3+ (FISH Pos)
III	ER– PR–	High	Pos	100	Neg	Sc 3+ (FISH Pos)
IV	ER– PR–	High	Pos	100	Neg	Sc 3+ (FISH Pos)
V	ER– PR 1% +	High	Pos	100	Neg	Sc 3+ (FISH Pos)
VI	ER– PR 3%+	High	Pos	100	Neg	Sc 3+ (FISH Pos)
VII	ER– PR 2% +	High	Pos	100	Neg	Sc 3+ (FISH Pos)
XII	ER–PR-	High	Pos/Int	100	Neg	Sc 3+ (FISH Pos)
XV	ER–PR-	High	Pos/Int	100	Neg	Sc 3+ (FISH Pos)
PDX-SBR45						
Patient	**ER– PR–**	**High**	**Neg**	**0**	**Pos**	**Sc3+**
I	ER– PR–	High	Neg	0	Neg	Sc3+
II (n=2)	ER– PR–	High	Neg	0	Pos/Int	Sc3+
III (n=3)	ER– PR–	High	Neg	0	Neg/Int-Pos	Sc3+
IV (n=4)	ER– PR–	High	Neg	0	Neg/Int-Int	Sc3+
V	ER– PR–	High	Neg	0	Int	Sc3+
VII	ER– PR–	High	Neg	0	Int	Sc3+

Table 5. Stability of hysto-pathological features over time in HER2 expressing PDX
The table records hysto-pathlogical features of HER2 expressing PDX in serial passages *in vivo.* If not else stated, data refer to one tumour per passage.
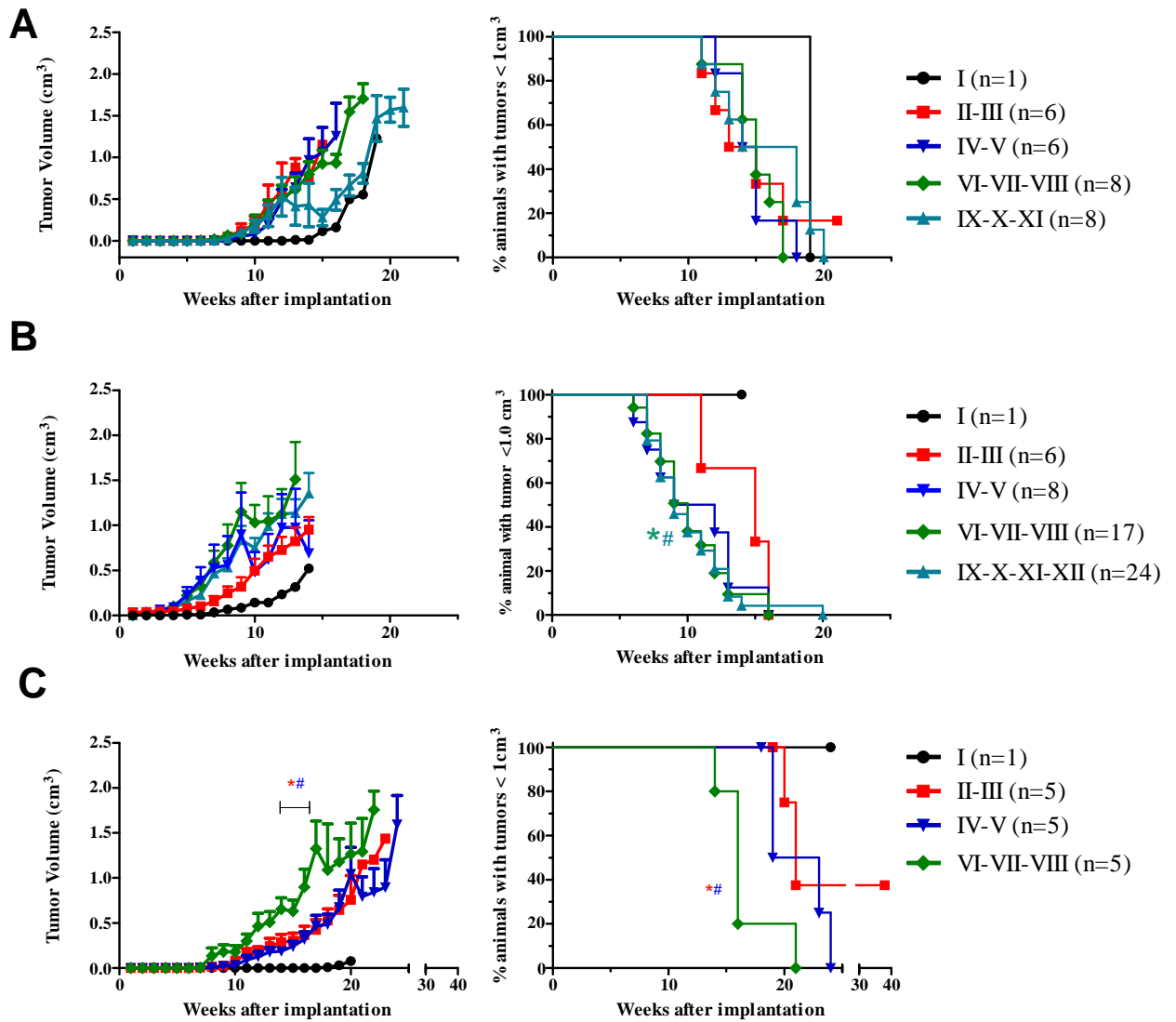
Figure 19. Stability of growth parameters and histological features in HER2 expressing PDX

The figure shows the growth curve and the percent survival to 1 cm^3 tumor over serial passages *in vivo* of PDX-SBR18 (A), PDX-BBR4 (B) and PDX-SBR45 (C). Statistical analysis of growth curve: Students' *t* test, (C) II-III versus IV-V (*) and VI-VII-VIII (#) p<0.05 weeks 14-18. Statistical analysis of survival curve: Mantel-Cox test: (B) II-III versus VI-VII-VIII (§) and IX-X-XI-XII ($) p<0.05; (C) II-III versus IV-V (*) and VI-VII-VIII (#) p<0.05.

PDX	Analysed organs							
	Lung		Bone Marrow		Brain		Ovaries	
	Incidence (%)	DTC (range)	Incidence	DTC (range)	Incidence	DTC (range)	Incidence	DTC (range)
PDX-SBR18	4/19 (21%)	0-3000	0/20	0-0	0/19	0-0	0/18	0-0
PDX-BBR4	3/33 (9%)	0-1500	2/37(5%)	0-1000	0/35	0-0	1/36(3%)	0-100
PDX-SBR45	1/13 (8%)	0-1500	1/14(7%)	0-1000	0/13	0-0	2/14(14%)	0-500

Table 6. Multiorgan dissemination ability of HER2 expressing PDX
The table records incidence and range of disseminated tumor cells (DTC) detected by RT-PCR evaluating the -satellite region of the human chromosome 17 in lung, bone marrow (right+left), brain and ovary (right+left).

6.5 Neratinib in HER2-positive PDX

Susceptibility to neratinib was evaluated in PDX-BBR4 and PDX-SBR45 *in vivo*. Treatment was carried on for 15-17 weeks.

PDX-BBR4 at XII passage *in vivo* was highly responsive to neratinib and the drug was able to withhold tumor growth in 100% of treated mice. Neratinib daily treatment (5 days per week) was withdrawn after 15-17 weeks and its effect appeared to be prolonged over time. Only one mouse (33%) slowly relapsed and its tumor reached a volume of 1.0 cm^3 after 20 weeks from treatment withdrawal. The other mice (66%) remained tumor-free for more than one year after treatment initiation (65-82 weeks) until sacrifice occurred due to tumor unrelated causes (fig. 20A and 20B).

In PDX-SBR45, Neratinib was able to halt tumor´s growth throughout treatment duration (15 weeks) and its effect was prolonged over time. Indeed, after treatment discontinuation all animals remained tumor-free for at least 15 weeks. 3 out of 5 animals (60%) relapsed and showed tumors of 1cm^3 after at least 9 months (42 weeks) from treatment initiation (fig. 20D and 20E).

6.6 Signaling alterations induced by neratinib in HER2-positive PDX
Molecular alterations induced by treatment with neratinib were investigated in mice treated for 4 continuous days starting with 1 cm^3 tumors.
Drug administration in PDX-BBR4 led to a reduction in expression of all members of ErbB family (p<0.05 HER1, HER2 and HER4) and to a significant decrease of all their phosphorylated forms, thus indicating an induced receptor down-modulation. IHC analysis reported this PDX to be negative for HER1 expression (i.e. less than 10% of cells

were positively stained), still some expression was eobserved through western blot analysis. Of note, reduction in HER3 levels was the most variable between analyzed mice, hence no statistical significance was reached. Downstream of HER2 receptors there was a significant reduction in the phosphorylated form of Akt, whereas MAPK signaling was not hampered by the treatment. Moreover, a trend towards a decreased Stat3 expression was registered in treated mice, but expression of pStat3 was not varied upon treatment (fig. 20C).

Short term treatment with neratinib in PDX-SBR45 led to a reduction in expression of all members of ErbB family except for HER4, which was not expressed in this PDX, ($p<0.05$ for HER1, HER2) and to a significant decrease of all their phosphorylated forms, thus indicating an induced receptor down-modulation. Of note, reduction in HER3 levels was the most variable between analyzed mice, hence no statistical significance was reached. Downstream effectors of this blockade were pAkt and pMAPK, which resulted both significantly down-modulated. Other alterations following neratinib treatment were represented by a decreased expression of Stat3, yet pStat3 levels were not diminished by treatment with neratinib (fig. 20F).
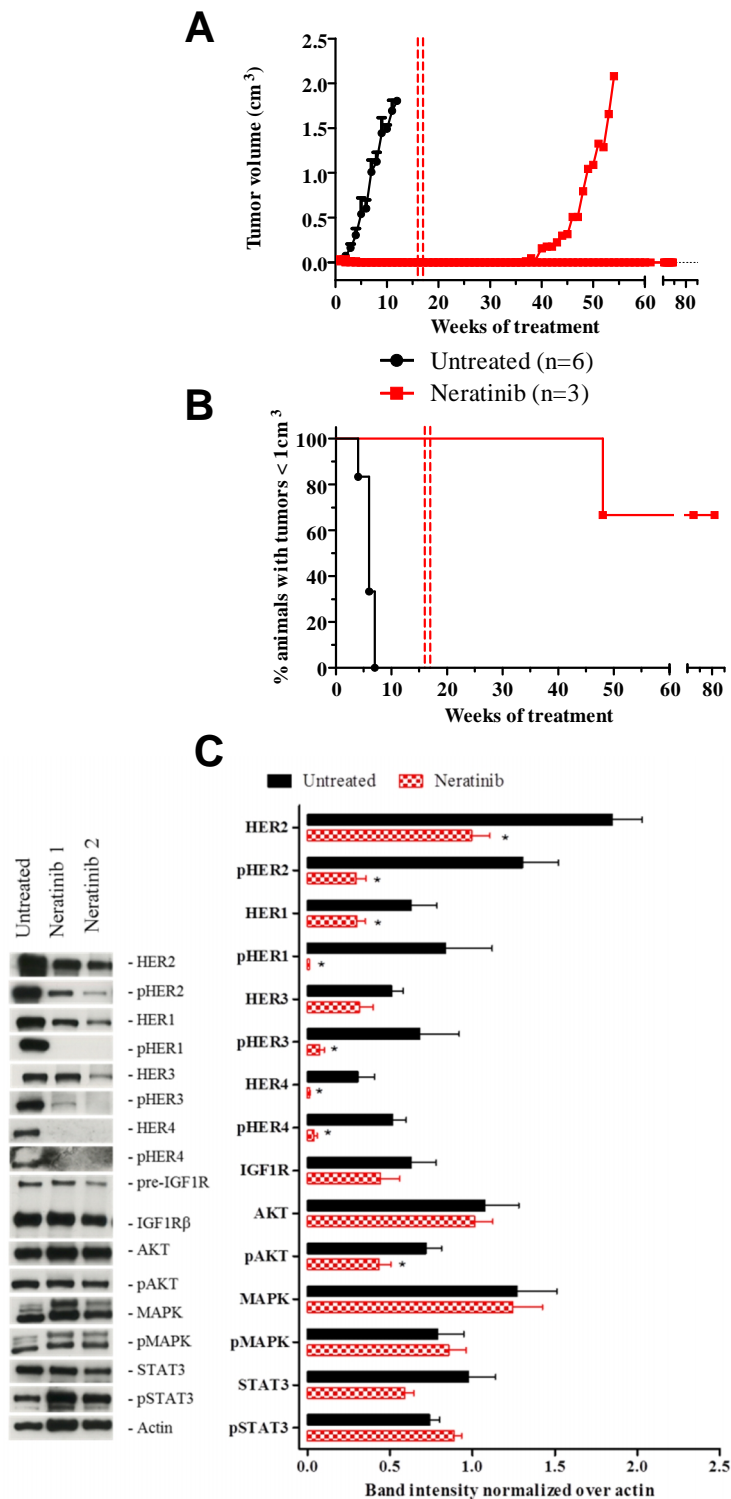
Figure 20. Neratinib susceptibility and molecular alterations in HER2-positive PDX

PDX-BBR4 was treated with neratinib *per os* 40mg/kg (red square); control mice are indicated with a black round. The red dotted lines indicate when the treatment was stopped.

(A) Tumor growth curve of PDX-BBR4 and PDX-SBR45, respectively; (B) Survival rates to 1 cm^3 tumors of PDX-BBR4 and PDX-SBR45, respectively. Statistical analysis of survival curve, Mantel-Cox test, # p< 0.05).

(C) shows a representative image of the western blot analysis of ErbB family members and downstream signaling in untreated and neratinib group (short-term treatment) of PDX-BBR4 and PDX-SBR45, respectively. The bar graphs report band intensity normalized over actin for each protein of untreated group (solid black) or neratinib (checked red). Statistical analysis: Student's *t* test, * p<0.05; ** p<0.01, *** p<0.001.
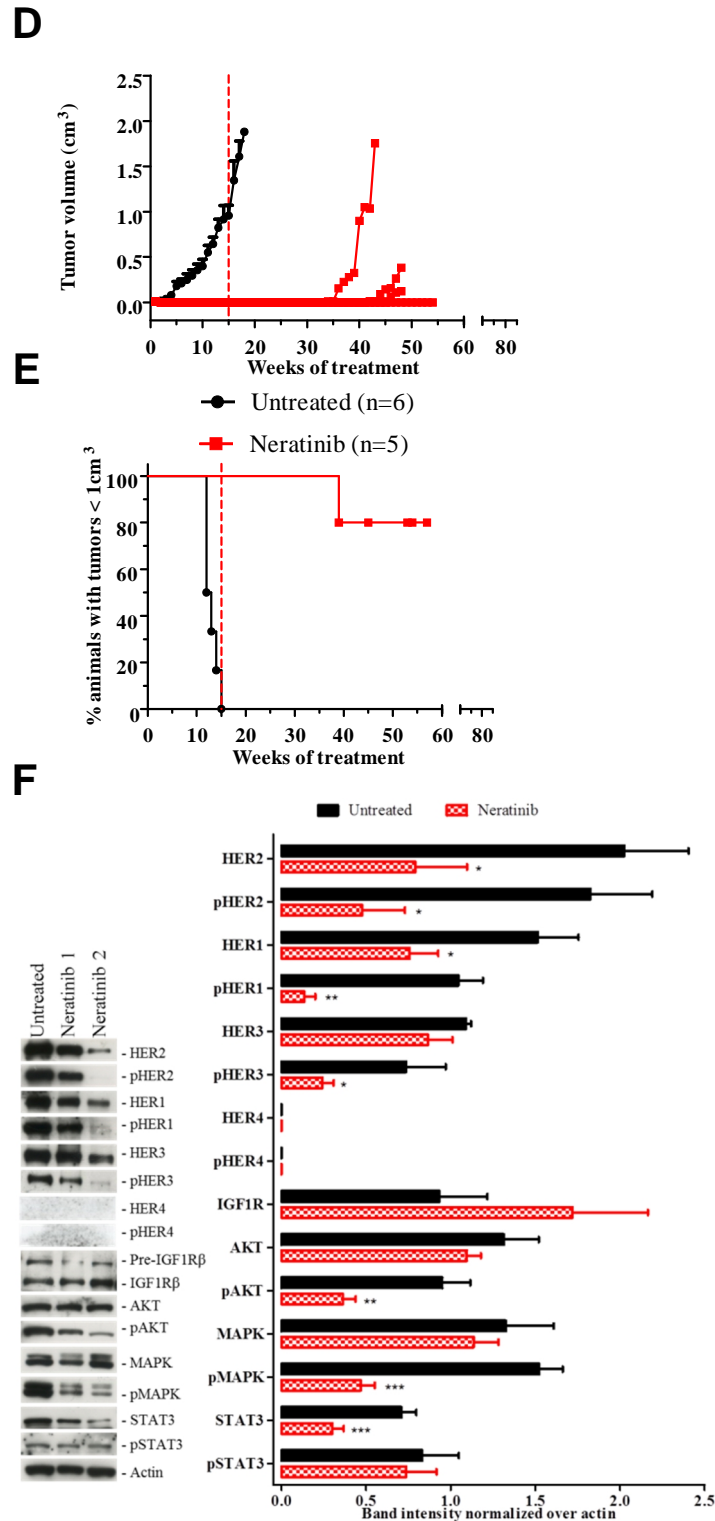
Figure 20. Neratinib susceptibility and molecular alterations in HER2-positive PDX

PDX-SBR45 was treated with neratinib *per os* 40mg/kg (red square); control mice are indicated with a black round. The red dotted lines indicate when the treatment was stopped.

(D) Tumor growth curve of PDX-BBR4 and PDX-SBR45, respectively; (E) Survival rates to 1 cm^3 tumors of PDX-BBR4 and PDX-SBR45, respectively. Statistical analysis of survival curve, Mantel-Cox test, # p< 0.05.

(F) shows a representative image of the western blot analysis of ErbB family members and downstream signaling in untreated and neratinib group (short-term treatment) of PDX-BBR4 and PDX-SBR45, respectively. The bar graphs report band intensity normalized over actin for each protein of untreated group (solid black) or neratinib (checked red). Statistical analysis: Student's *t* test, * p<0.05; ** p<0.01, *** p<0.001.

6.7 Neratinib susceptibility in luminal B PDX

Neratinib action in PDX-SBR18, a luminal B enriched with HER2 expression, was studied in comparison and concert with tamoxifen, the standard of care for luminal B tumors regardless of their HER2 *status*.

Treatment with tamoxifen alone significantly reduced tumor growth starting from week 3 of treatment and increased survival to 1 cm^3 tumor in the treated group. Despite PDX-SBR18 expressing HER2, neratinib alone had no effect neither on growth rate nor on survival and all animals bore 1 cm^3 tumors while still in treatment. Combined treatment with tamoxifen and neratinib slowed tumor growth and increased survival to 1 cm^3 tumor significantly with respect to untreated group. When compared to tamoxifen alone, neratinib addition slightly but significantly slowed growth and ameliorated survival to 1 cm^3 tumors (fig. 21A).

6.8 Molecular alterations induced by neratinib in luminal B PDX

Downstream pathway analysis was focused on determining neratinib molecular effects and could not directly show tamoxifen downstream action. Any treatment reduced HER2 and pHER2 expression with respect to untreated mice: tamoxifen alone showed a tiny effect, whereas neratinib was able to strongly down-modulate HER2 and pHER2 either alone or in combination with tamoxifen. An additive action of the two drugs was shown only with regard to pHER2. HER1 was not expressed in PDX-SBR18; HER3 and HER4 were not significantly altered by any treatment and their phosphorylated forms were not detected by western blot analysis. Downstream of HER-receptors no significant changes in expression were seen (fig. 21B).
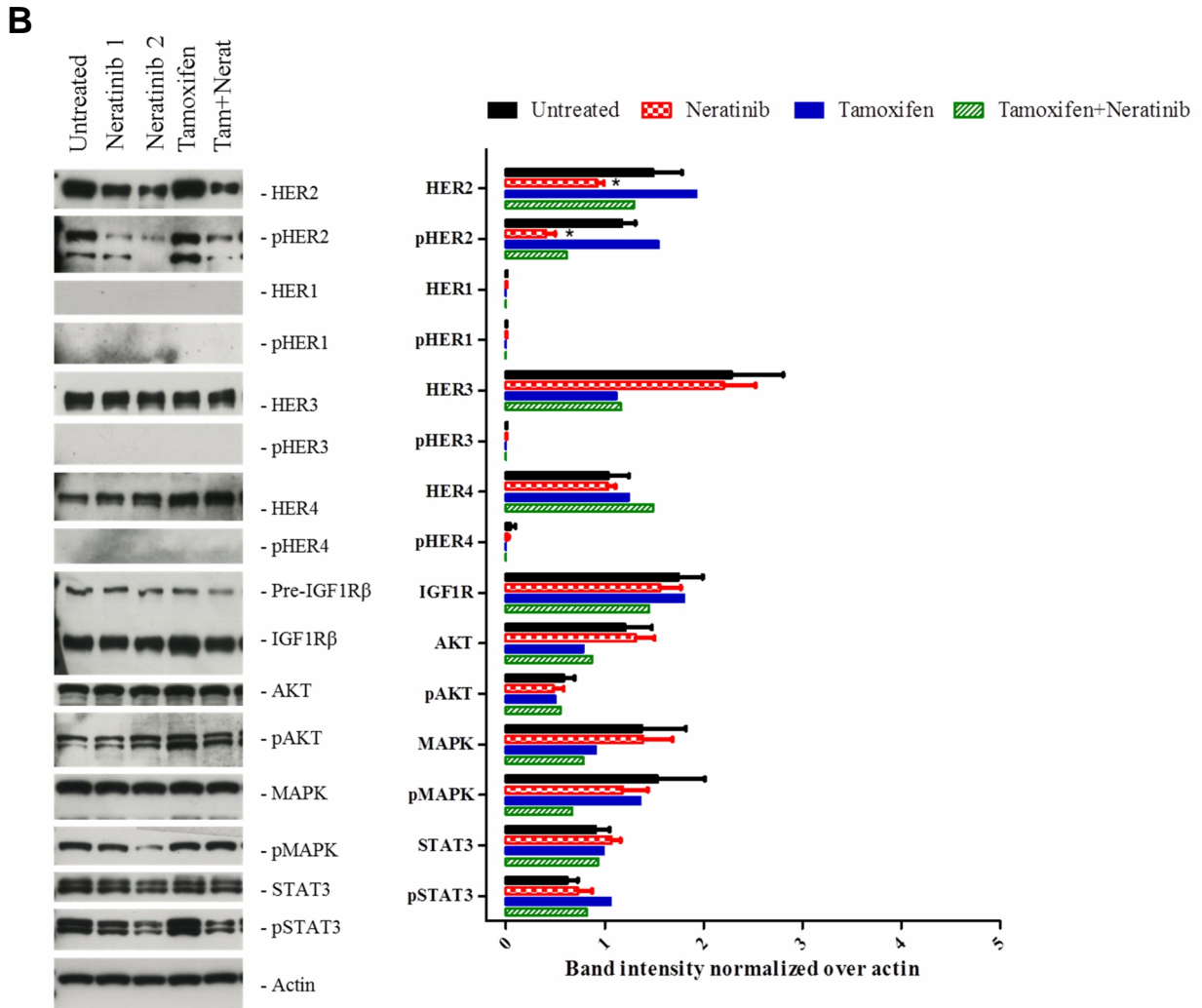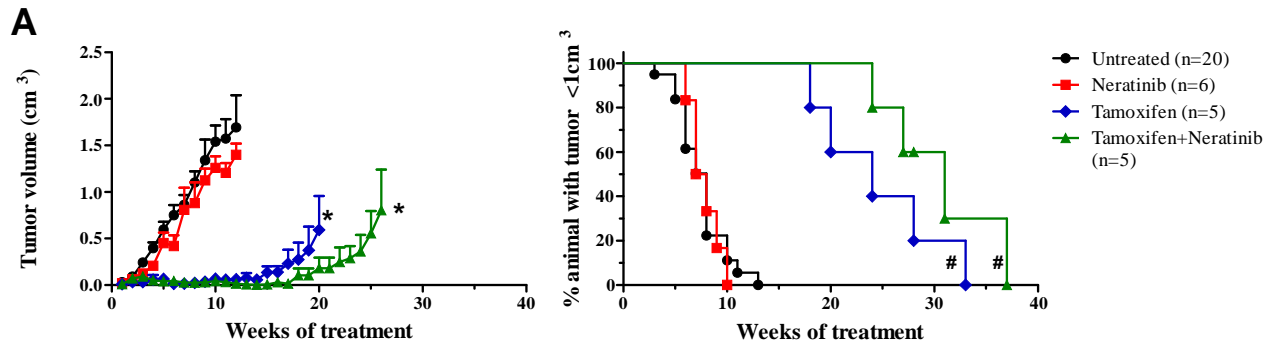
Figure 21. Neratinib susceptibility and molecular alterations in HER2-enriched PDX

(A) Growth curve and survival to 1 cm³ tumors for PDX-SBR18 untreated animals (black round) and animals treated with neratinib *per os* 40mg/kg (red square), tamoxifen (blue rhombus) or their combination (green triangle). Each point represents the mean of indicated mice. Statistical analysis of growth curve, Student's *t* test, * p<0.05. Statistical analysis of survival curve, Mantel-Cox test, # p< 0.05).

(B) Representative image and western blot analysis of ErbB family members and downstream signaling: the bar graphs report band intensity normalized over actin for each protein and group. Statistical analysis: Student's *t* test, * p<0.05.

6.9 Neratinib in trastuzumab-resistant PDX

PDX-BBR4 was initially sensitive to trastuzumab, which significantly slowed tumor growth and prolonged survival to 1 cm³ tumors with respect to the untreated controls (fig. 22A). Its action appeared limited when compared to neratinib, which halted tumor growth almost completely (see fig. 20A).

Tumors arisen in trastuzumab-treated mice were transplanted for several consequent passages *in vivo* in order to obtain a resistant model. After 6 passages, growth and survival curves of trastuzumab treated animals overlapped with the one of control mice, thus indicating that PDX-BBR4 had lost its susceptibility to trastuzumab. Transplanted once again and treated with neratinib, the tyrosine kinase inhibitor was able to arrest tumor growth in 100% of mice throughout treatment duration and significantly improve survival to 1cm³ tumors (fig. 22B).
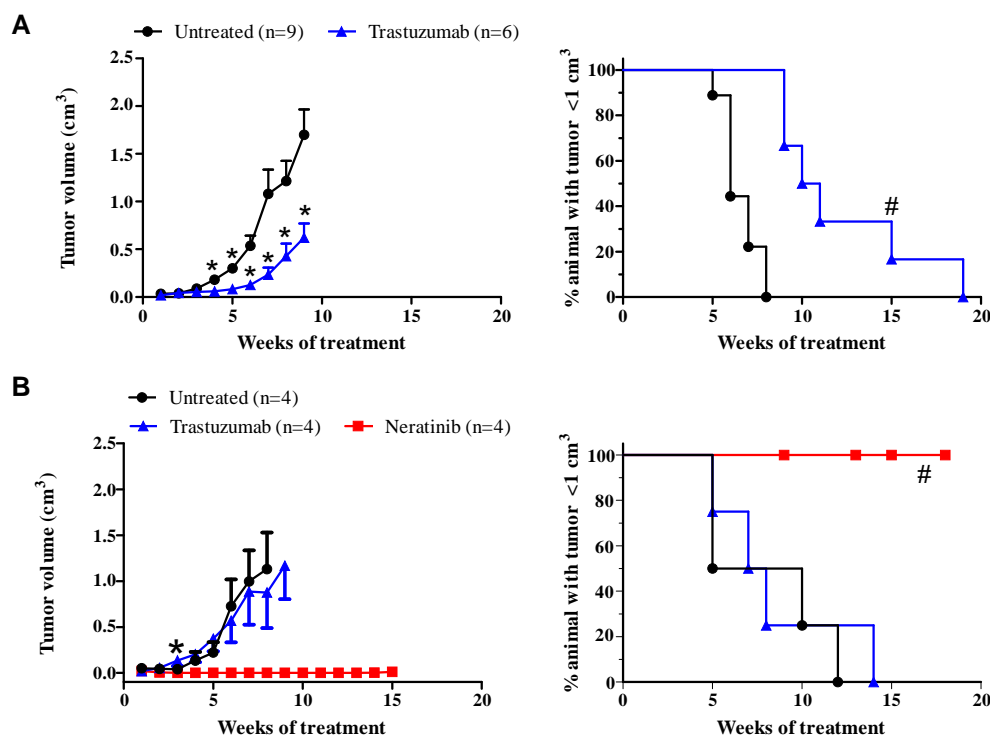
Figure 22. Neratinib in trastuzumab-resistant PDX
PDX-BBR4 was treated with trastuzumab 4 mg/kg (blue triangle) for six consecutive passages and with neratinib 40 mg/kg (red square) at next passage *in vivo*. Untreated mice are shown as solid round.
(A) Tumor growth curve and survival to 1 cm³ tumors for mice bearing PDX-BBR4 treated with trastuzumab at 1st passage. Each point represents the mean±s.e.m. of indicated mice in the tumor growth curve.
(B) Tumor growth curve and survival to 1 cm³ tumors for mice bearing BBR-4 PDX treated with trastuzumab at 6th consecutive passage or with neratinib at following passage *in vivo*. Each point represents the mean±s.e.m. of indicated mice in the tumor growth curve.
Statistical analysis of growth curve, Student's *t* test, (*) $p<0.05$ *versus* control (A) or trastuzumab (B).
Statistical analysis of survival curve, Mantel-Cox test, (#) $p< 0.05$ *versus* control (A) or trastuzumab (B).

6.10 Neratinib in a model of cancer progression

PDX-BBR4 eventually showed signs of progression *in vivo*. PDX-BBR4 at II passage had been transplanted into 3 different mice, whose tumors had been amplified in more mice, giving rise to 6 different sub-lines. Progression event had taken place in only one of the six different sub-lines at passage XIII and to a lesser extent in another sub-line. In the progressed sub-line, a statistically significant increase and decrease was respectively found comparing growth curves and survival to 1 cm^3 tumor of passages II-XII and >XIII (fig. 23A). Moreover, cells dissociated from progressed and not progressed tumors were injected intravenously to experimentally induce metastasis. Only cells derived from progressed BBR-4 PDX were able to give rise to overt lung metastasis.

In this spontaneously arisen model of progression, we set out to verify susceptibility to neratinib. The drug was still able to halt tumor growth to negligible volumes throughout treatment duration (18 weeks) and to delay significantly time to 1 cm^3 tumors with respect to control group. Nevertheless, after its discontinuation tumors rapidly relapsed and reached 1 cm^3 within 10 weeks in 100% mice (fig. 23B).
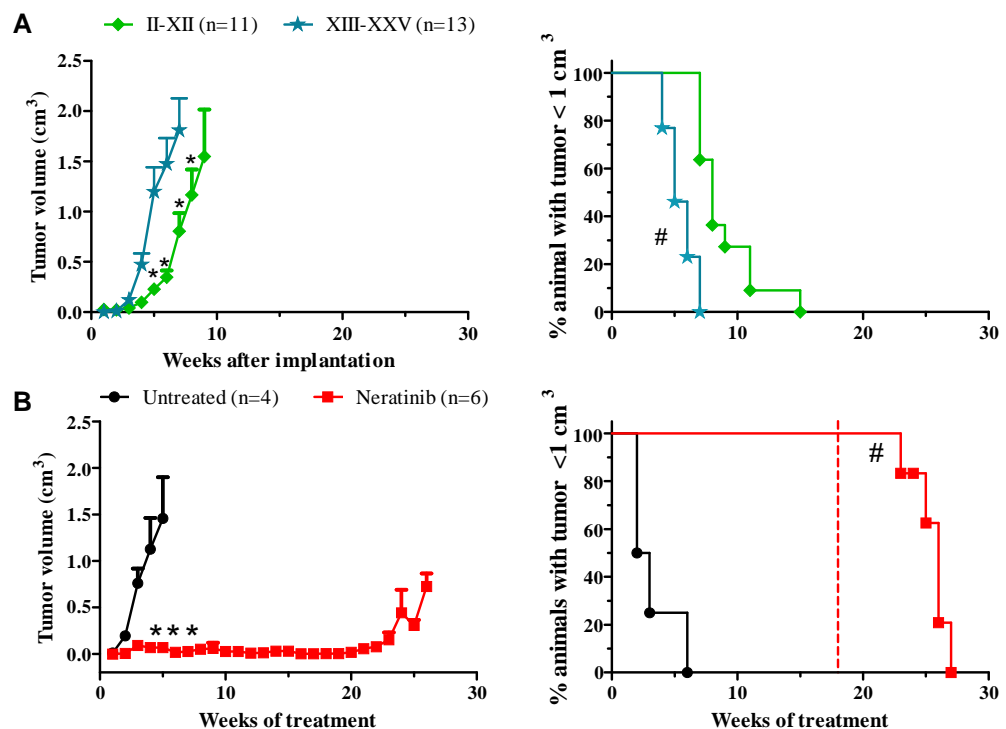
Figure 23. Neratinib in cancer progression
(A) Growth curve and survival to 1 cm^3 tumors for mice bearing a sub-line of PDX-BBR4 PDX from passages II to XII (bluish star) and for later passages (green rhombus). Each point represents the mean±s.e.m. of indicated mice in the growth curve. (B) Growth curve and survival to 1 cm^3 tumors of untreated animals (black round) and animals treated with neratinib *per os* 40mg/kg (red square). The red vertical line indicates when the treatment was stopped. Each point represents the mean±s.e.m. of indicated mice in the growth curve. Statistical analysis of growth curve, Student's *t* test, * $p<0.05$. Statistical analysis of survival curve, Mantel-Cox test, # $p< 0.05$).

6.11 Neratinib in tumors arisen after treatment with neratinib

Tumors arisen in PDX-BBR4 or PDX-SBR45 bearing mice after treatment with neratinib were transplanted in other animals and treated again with the tyrosine kinase inhibitor.

Both in PDX-BBR4 and PDX-SBR45, neratinib was again able to halt tumor growth to negligible volumes throughout treatment duration (fig. 24). Moreover, it significantly improved survival to 1 cm^3 tumors in both PDXs. Hence, susceptibility to neratinib was not lost after the first cycle of therapy and the drug was still effective on relapses.
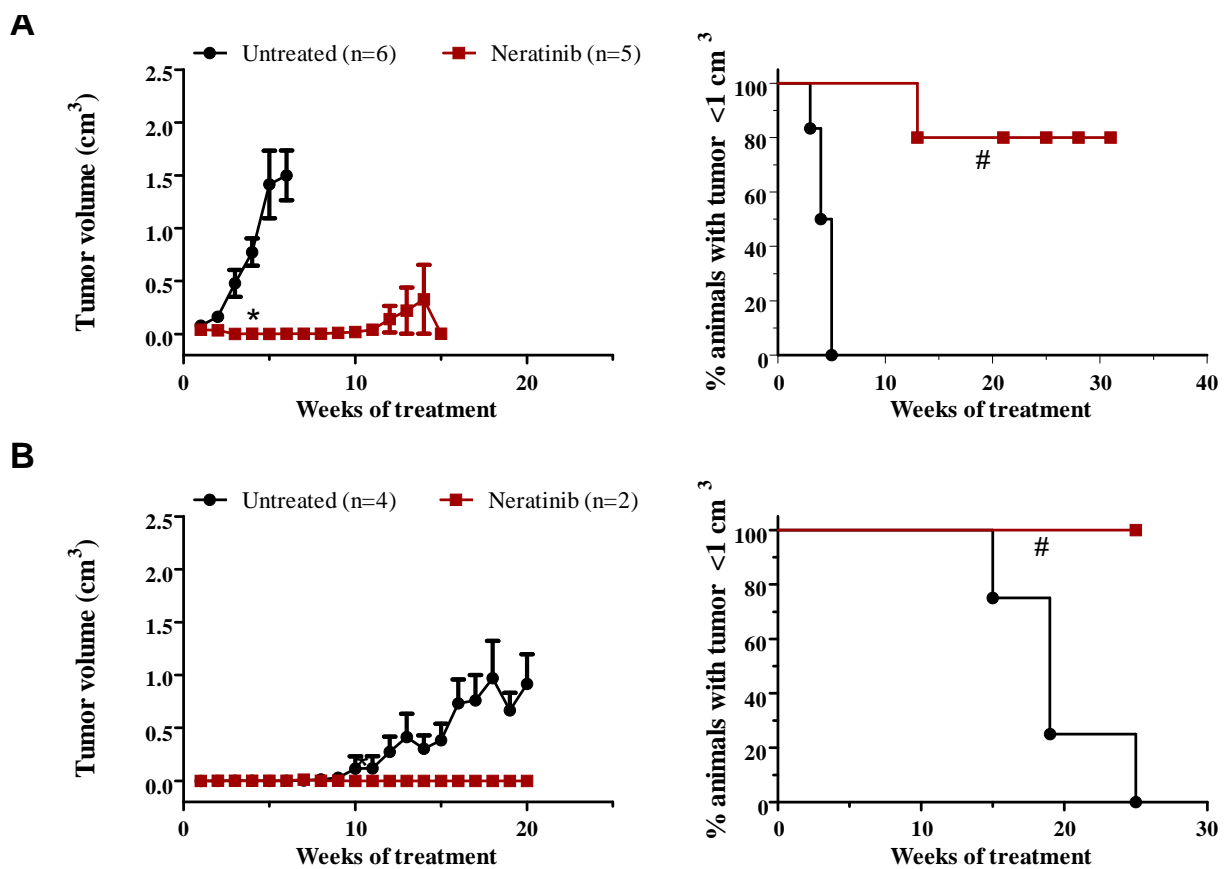
Figure 24. Neratinib in relapses
PDX-BBR4 (A) and PDX-SBR45 (B) treated with neratinib eventually relapsed. Tumors were transplanted and treated with neratinib again. Figure reports growth curve and survival to 1 cm^3 tumors of untreated mice (black round) or treated again with neratinib 4 mg/kg (brown square). Each point represents the mean±s.e.m. of indicated mice for the growth curve. Statistical analysis of growth curve, t Student's test, * $p<0.05$. Statistical analysis of survival curve, Mantel-Cox test, # $p< 0.05$).

6.12 Are PDXs a possible model for HER2 loss?

HER2 expression has been monitored by PCR, in addition to histological analysis already reported in table 4, throughout *in vivo* passages II-XII and in tumor relapses after treatment with neratinib in all three PDXs.

In PDX-SBR18, HER2 expression showed some fluctuations from passage II to passage XII, nevertheless low levels of HER2 expression were always maintained. After neratinib treatment, HER2 expression appeared to increase slightly but still significantly (fig. 25A).

PDX-BBR4 showed a slightly decreasing HER2 expression after passage II-III, which however remained unvaried in tumors grown after neratinib treatment was stopped (fig. 25B).

PDX-SBR45 had a constant HER2 expression both throughout *in vivo* passages. In 2 out of 3 tumors grown after treatment with neratinib, HER2 expression was similar to the one of untreated controls. One tumor had a much lower HER2 expression with respect to the others; yet, it was still quite high and no abrupt loss of HER2 expression was observed (fig. 25C).

Overall, despite some decrease and fluctuations, HER2 expression appeared stable and was not lost neither in passages *in vivo* nor after treatment with neratinib. Hence, further modifications and improvements of this model, i.e. through reconstitution of the immune system or huminization of the micro-environment, will be needed to render PDX useful models of HER2 loss and receptor discordance in general.
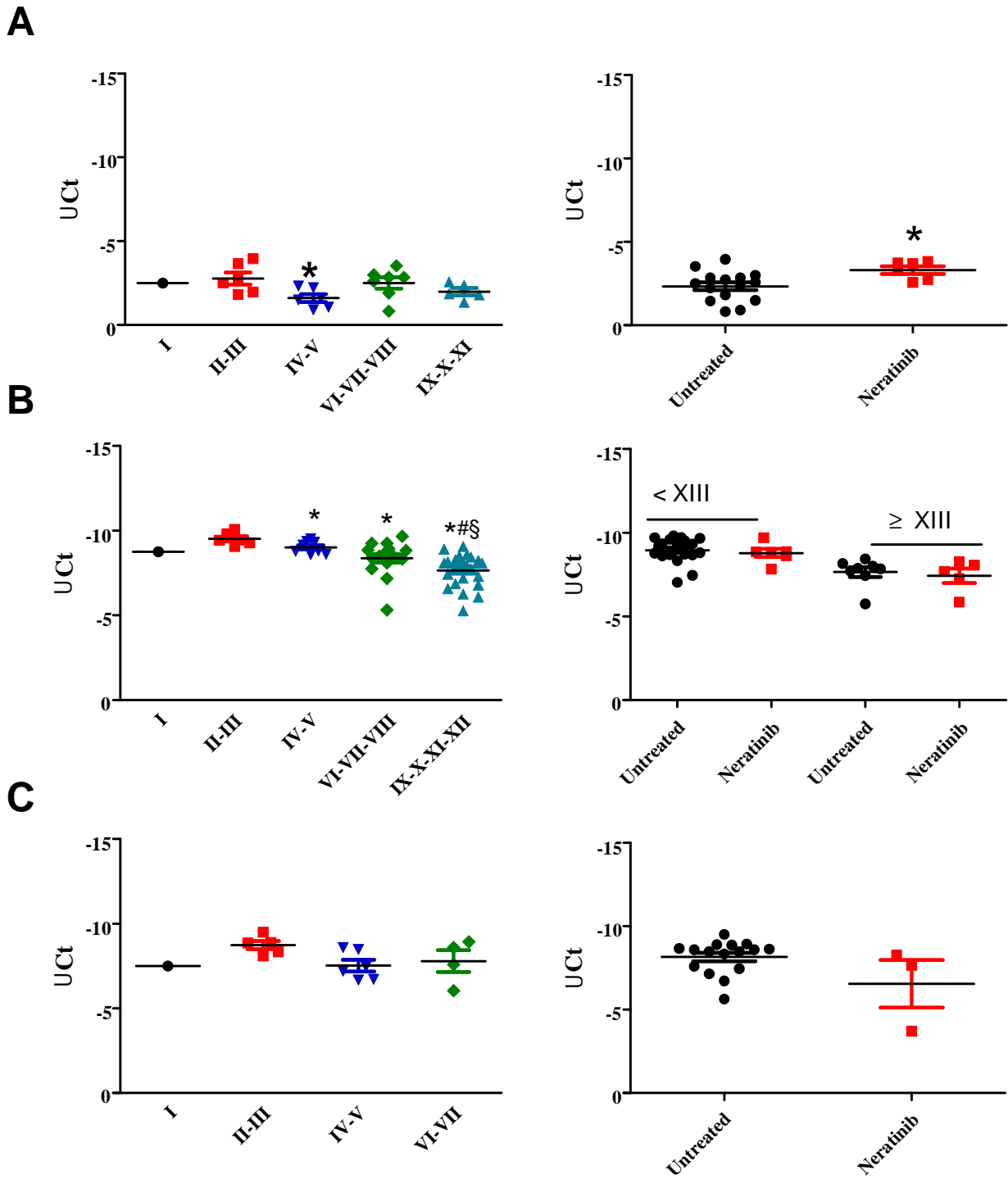
Figure 25. Stability of HER2 expression
HER2 expression was examined by RT-PCR in indicated passages and after neratinib treatment in PDX-SBR18 (A), PDX-BBR4 (B) and PDX-SBR45 (C). Expression is indicated as ΔCt ($Ct_{HER2}-Ct_{huTBP}$). Statistical analysis: Student's *t* test, p< 0.05 (*) *versus* passages II-III (left graph) or untreated (right graph), passages IV-V (#), passages VI-VII-VIII (§).

Discussion

HER2 discordance between primary tumor and metastasis is a clinical issue and occurs in a pooled meta-analysis percentage of 10.8% (Schrjiver et al., 2018). Some authors have reported models of loss of neu/HER2 expression in murine or human cell lines, respectively (Nanni et al., 2000; Song et al., 2014; Creedon et al., 2016). Recently, a murine model of HER2 loss in mammary tumors has been developed in the Laboratory of Biology and Immunology of Metastasis directed by Professor Pier-Luigi Lollini. Previous characterization indicated the association of loss of HER2 expression with spindle-like morphology, an increased stemness, an EMT profile, a greater aggressiveness *in vivo* and superior vasculogenic-like activity *in vitro*. These observations were in line with observations in other model of loss of HER2 (Song et al., 2014; Creedon et al., 2016). In this work, we sought to understand mechanisms underlying loss of HER2 expression and identify druggable targets in HER2-negative tumors.

Contrasting data are reported in literature on the effect of adjuvant therapy with trastuzumab in promoting loss of HER2 expression in metastasis (Timmer et al., 2017; Wang et al., 2017). Moreover, some authors have reported trastuzumab as well as lapatinib-resistant human mammary cell lines SkBr3 to lose HER2 expression and acquire mesenchymal phenotype and staminal properties (Korkaya et al., 2012; Creedon et al., 2016). We firstly set out to assess effect of trastuzumab in HER2^{labile} cell line, which spontaneously loses HER2 expression *in vivo*. Long-term treatment with trastuzumab accelerates emergence of a mesenchymal population out of HER2^{labile} cell line, which is mesenchymal and endorsed with staminal properties and an EMT profile of transcription. This cell line, HER2^{labile} TRT, closely resembles HER2^{loss} cells, obtained from *in vivo* injection of HER2^{labile} cell line. An acceleration of growth rate was further observed in tumors induced by HER2^{labile} cells *in vivo* upon treatment with trastuzumab. Hence, in our model trastuzumab accelerates emergence of a mesenchymal and staminal population with an EMT profile of transcription, as previously observed in literature. Of note, mesenchymal phenotype could not be reverted by trastuzumab subtraction; this is in line with observations reported in literature that once established, EMT-like phenotype is sustained by an autocrine loop (Scheel et al., 2014).

Of note, in our model loss of HER2 expression occurs also spontaneously when HER2^{labile} cells are seeded at low density ($4x10^4$ cell/cm^2). Again, in these conditions of culture cells acquire staminal properties and spindle-like morphology. Thus, density of cells seems to influence HER2 expression. Indeed, HER2^{labile} cells seem to lose HER2

whenever they are not densely packed due to low dose, treatment with anti-HER2 drugs or upon *in vivo* injection. The observation that even high doses of HER2^{labile} injected always give rise to HER2-negative tumors further supports the hypothesis that high cell density is required but not sufficient for HER2^{labile} cells to maintain HER2 expression. Cell-cell contact appears to be required, as well. A permissive environment for induction of EMT has been reported to be poor in secreted inhibitors of EMT-linked pathways, such as SFRP1, DKK1, gremlin and BMPs (Scheel et al., 2014). In our model, SFRP1 resulted up-regulated in HER2^{stable} cell line, which does not lose HER2 expression; it would be interesting to study the dynamic of expression of these inhibitors according to cell density in our model.

At this point, many questions arose about mechanisms underlying loss of HER2 expression. Experiments reported in this thesis clearly allowed us to exclude immunological selection of HER2-positive cells *in vivo*, indeed tumors arisen upon HER2^{labile} injection in immune-compromised mice were HER2-negative as well. Loss of the transgene in HER2^{loss} cells was also excluded and these cells appeared to harbor the same copy number of HER2 as HER2^{labile} cells, comparable with SkBr3 human mammary cancer cells. In our model HER2 is expressed nor at protein nor at mRNA level; hyper-methylation of promoters is frequent in cancer and leads to silencing of genes down-stream. We hence checked if this could be the mechanism underlying loss of HER2 expression in HER2^{loss} cells or silencing an EMT program latent in HER2^{labile} cells. Yet, treatment with a demethylating agent did not restore HER2 expression in HER2^{loss} cells, but an increase in the HER2-negative population was observed in HER2^{labile} cells treated with cytotoxic doses of demethylating agent. Hence, mechanism underlying loss of HER2 expression must be further investigated with different demethylating agents or down-stream in the way from gene to protein.

Recently, a possible hypothesis on the mechanism of resistance to HER2 targeted therapy involving loss of HER2 expression has also been proposed: in brief, HER2 overexpression would activate an EMT program with increased production of metalloproteinases, which would in turn cleave HER2 generating p95HER2 isoform, lacking ECD but still signaling (Nami & Wang, 2017); HER2^{labile} cells express HER2 fragments, which are not detected in HER2^{stable} cells, indeed. Moreover, expression of Mek has been reported to stabilize HER2 expression in mammary cells detached from ECM (Khan et al., 2017). These models appear not to be fully applicable in our model,

where HER2 is barely not transcribed. Nevertheless, functional studies of secreted EMT inhibitors, HER2 fragments and Mek through silencing or gene transduction will help us clarifying molecular mechanisms of HER2 loss.

A second hypothesis arose for emergence of HER2^{loss} cells: HER2^{labile} line could be representative of a tumor population harboring clones with a heterogeneous expression of HER2 and HER2^{loss} cells could represent a selected clone rather than an evolution of the initial HER2^{labile} population. This intra-tumor heterogeneity is indeed observed in 1-40% of HER2-positive tumors in the clinical practice and represents a clinical issue (Ng et al., 2015). It is of main importance for the success of HER2 targeted therapies to ensure that the vast majority of tumor cells are indeed addicted to HER2 expression for the maintenance of malignant phenotype (Escrìvia-de-Romani et al., 2018). If instead there is a sub-clone which does not express HER2, it is likely that targeted therapies will clear off HER2-positive cells but not eradicate the tumor which will relapse as HER2-negative. This could be the case in our model: in presence of anti-HER2 targeted agents or upon heavy dilution, equilibrium between the HER2-positive and HER2-negative population could be outweighed in favor of HER2-negative population. Of note, for many of their characteristics, i.e. expression of stem cell markers, migratory and metastatic properties, EMT transcription profile, HER2^{loss} cells can be likened to breast cancer stem cells, so a further hypothesis could be the selection of a pure population of breast cancer stem cells.

It is of crucial importance to identify druggable targets in HER2-negative metastasis or recurrences of HER2-positive primary tumors. Therefore, we compared the transcriptomes of all HER2-positive cell lines in our model with all the HER2-negative cells. Among HER2-positive cell lines we included, other than the HER2^{labile} cells, the HER2^{stable} cell line, which did not show any sign of loss of HER2 expression nor acquisition of mesenchymal or staminal phenotype when treated long term with trastuzumab (HER2^{stable} TR(N)T), and one of its HER2-positive clones (HER2^{stable} AG3). Among HER2-negative cell lines, other than HER2^{loss} and HER2^{labile} TR(N)T cells, we included HER2^{loss} cells treated with trastuzumab, which again did not undergo any morphological or molecular changes. Inclusion of HER2^{stable} TR(N)T cells and HER2^{loss} TR(N)T cells permitted us on the one hand to identify genes not linked to lability of HER2 expression and on the other hand to identify those whose expression is modified upon trastuzumab binding to HER2.

Direct comparison of HER2^{labile} and HER2^{loss} cells evidenced only 8 differentially expressed genes, of which 7 were down-regulated and 1 was up-regulated in HER2^{loss} cells. Differential expression of Myh14, Cdkn2b, Krt7 and Krt8 and Pla2g7 well mirrors differences in phenotype between HER2^{labile} and HER2^{loss} cell lines. In turn, we would expect Wnt7b, Postn an Ifitm10 to be up-regulated in HER2^{loss}, due to their association with aggressiveness and stemness. Their up-regulation in HER2^{labile} could represent a spy of these cells being prone to acquisition of mesenchymal characteristics or relying on different pathways for maintenance of malignant phenotype.

Comparison of transcripts of all HER2-positive and HER2-negative cells in our model revealed 751 genes differentially expressed between the two subsets. Analysis of protein-protein interaction and pathway enrichment helped us interpreting these data. Many knots of interactions emerged in protein-protein interaction analysis reflected presence or absence of expression of HER2 in the two sets of cells analyzed. Down-regulation of PTPN1, FGFR1, PAK1, Cul1, IL5 and EFNB1, and their interactors could be expected in HER2-negative samples as all of them have been reported to be involved in HER2-mediated oncogenesis or at least up-regulated in HER2 enriched tumors. In the same way, up-regulation of FN1 and VIM can be expected in HER2-negative samples. Other knots of interaction and pathways simply mirrored differences in phenotype previously observed between HER2-negative and HER2-positive cell lines. Up-regulation of cell migration and angiogenesis in HER2-negative cells is therefore not surprising. On the other hand, it should be noted that molecules involved in angiogenesis such as VEGFA and PTGS2 are reported as direct transcriptional target of HER2 (Moasser et al., 2007; Al-Ameddine et al., 2013). Hence, in HER2-negative cells their up-regulation must be driven by a different transactivation route. Some knots in protein-protein interaction and some significantly enriched pathways are linked to mesenchymal nature of HER2-negative cells. VIM itself is a known marker of mesenchymal differentiation and CDH1 in turn marks epithelial cells: accordingly, they were found up- and down-regulated in HER2^{loss} cells together with their interactors. Analogously, HER2^{loss} cells showed increased ECM organization, focal adhesions (i.e. cell-ECM contacts) as well as decreased protein localization to membrane (i.e. less molecules involved in cell-cell and cell-ECM adherence and communication) and regulation of actin cytoskeleton. In turn, HER2-positive cells presented up-regulation of epithelial/luminal differentiation, being SPTAN1 involved in secretion and Notch1 activated by cell-cell interaction. Except of

these descriptive and somewhat expected knots of interaction and enriched pathways, HER2-negative cells also showed up-regulation of PKB, response to hypoxia, biosynthesis and protein oligomerization. Most importantly, MYK and PDGFR-B interactors and PI3K/Akt pathway were found up-regulated in HER2-negative cells: these pathways are known to be involved in oncogenic transformation and could hence be the ones sustaining malignant phenotype in HER2-negative cells. Functional studies will now be required to assess the role of the above reported genes in HER2 loss and as therapeutic targets.

In this thesis, we focused on PDGFR-B as therapeutic target in HER2^{loss} cells and sunitinib was chosen as therapeutic agent. Sunitinib is a small-tyrosine-kinase inhibitor approved by EMA for therapy of renal cell carcinoma and imatinib-resistant GIST (gastrointestinal stromal tumors). It is a multi-targeted molecule which has been shown to inhibit PDGFRs, VEGFR and c-Kit. Use of this multi-targeted drug permit us to simultaneously inhibit PDGFRs and the pathway down-stream VEGFA, the ligand of VEGFR. Both genes resulted as up-regulated in HER2^{loss} cells, so use of this molecule appeared doubly indicated.

Sunitinib was effective in halting growth of HER2^{loss} cells both in 2D-adherent and 3D-non-adherent culture with an IC50 of 4.66 μM. Sunitinib induced a transient change in HER2^{loss} morphology; nevertheless, HER2 expression remained negative in treated cells. Sunitinb also reduced ability of HER2^{loss} cells of forming vascular-like tubes *in vitro*. Production of IL-6 was also evaluated. IL-6 is a cytokine involved in inflammation and angiogenesis. High levels of this cytokine have been linked to poor clinical outcome in breast cancer patients (Korkaya et al. 2012), but different roles of IL-6 have been reported in breast cancer. IL-6 is part of a pro-inflammatory autocrine loop elicited by HER2, which triggers activation of Stat3 signaling axis and is critical for tumorigenesis (Hartman et al., 2011). On the other hand, up-regulation of IL-6 has been reported in a model of BT474/PTEN- treated long-term trastuzumab (LTT). In this model, IL-6 appeared to trigger an inflammatory loop which leads towards acquisition of a staminal, basal-like phenotype and resistance to trastuzumab (Korkaya et al., 2012). Moreover, HER2^{loss} and HER2^{labile} induced tumors show an abnormal angiogenesis *in vivo*, characterized by absence of pericytes, which could be due to an elevated production of IL-6 (Gopinathan et al., 2015). In our model, IL-6 production was detected in the supernates of HER2^{stable} and HER2^{loss} but not in HER2^{labile} conditioned media; treatment with sunitinib lowered

production of IL-6 by HER2^{loss} cells. Production of IL-6 in our model appears to be paramount of the two roles identified for this cytokine in breast cancer and its pathway deserves further studies.

In vivo, sunitinib was able to significantly slow down growth of HER2-negative tumors induced by HER2^{labile} cells but resulted ineffective on the fast growth of tumors induced by HER2^{loss} cells. Altogether, these data indicate therapeutic targeting of PDGFR-B and VEGFA by sunitinib in HER2-negative cells is effective in slowing down growth of HER2-negative tumors through alteration of morphology and EMT profile as well as down-modulation of angiogenesis and production of IL-6. Nevertheless, inhibition of PDGFR-B and VEGFR by sunitinb does not eradicate the tumors, thus indicating that PDGFR-B and VEGFA signaling pathways clearly sustain growth of HER2-negative cells, but likely they do not represent key drivers of their malignant phenotype.

We took advantage of the collection of mammary *patient-derived-xenografts* recently established in the Laboratory of Biology and Immunology of Metastasis to obtain further models of progression.

Take rate in this collection (7.5%) is similar to the one reported for bigger collections (10%; Dobrolecki et al., 2017). As frequently observed, our collection is also biased towards more aggressive subtypes showing the highest rates of PDX attainment and no PDX attainment for luminal A subtype, the most benign. PDX recapitulate and stably maintain over time the characteristics of originating tumor at genomic, phenotypic, histological, molecular and metabolic level and constitute therefore a useful tool for basic and preclinical research. In our collection, histological parameters and growth rates were highly stable over serial passages *in vivo* (at least up to passage XII); yet, for some PDXs, increasing growth rates and survival to 1 cm^3 tumors were observed, thus indicating a further selection for more malignant clones *in vivo*.

HER2 expression is not always homogenous and wide-spread in every cell in a tumor. Clinically, 10% of cells overexpressing HER2 at membrane level or a HER2: CEP ratio ≥ 2 or a HER2 copy number >6 are enough to classify a breast cancer as HER2-positive (Loibl & Gianni, 2017). As a consequence, different HER2-positive tumors do not show the same level of HER2 expression and the same percentage of cells overexpressing HER2. The two HER2-positive PDX used for the experiments reported in this thesis were paramount of this inter-tumor heterogeneity. PDX-BBR4 displayed a weak staining in

10% of cells (2+) with HER2 amplification whereas PDX-SBR45 staining was more strong and complete (3+). As the originating tumors, the two PDX differed greatly also for expression of other histopathological features, such as p53, Bcl-2 and HER1 expression. Nevertheless, no major differences were observed in the sensitivity of these two PDX to neratinib. The pan-HER inhibitor was equally able to halt tumor growth almost completely throughout treatment duration (15 weeks) and no tumor growth was observed later on for a very long time (>20 weeks). Some mice remained tumor-free for more than one year. After this period, relapses were observed both in PDX-BBR4 and PDX-SBR45; tumors arisen after treatment with neratinib were not resistant to this drug, though, and treatment with neratinib of relapses, serially transplanted in other mice, was still effective in halting tumor growth almost completely. Importantly, a model of resistance to trastuzumab and a model of progression were achieved using HER2-positive PDX-BBR4 and neratinib showed up its efficacy in halting tumor growth almost completely in these more challenging models, as well.

Short term treatment with neratinib significantly decreased expression at protein level of HER1, HER2 and HER4 and their phosphorylated forms. Of note, trends towards HER3 and pHER3 inhibition was also observed underlining reliance of other HER receptors on HER3; yet, great differences were observed among different treated mice in inhibition of this receptor. As reported in literature (Canonici et al., 2013), neratinib significantly inhibited pMAPK and/or pAkt down-stream HER receptors.

PDX-BBR4 gave rise to two models of progression, displaying increased growth rate and metastatic potential or resistance to trastuzumab. In both models, neratinib was effective in halting tumor growth. Neratinib has been recently approved by FDA in patients having completed 1-year adjuvant therapy with trastuzumab. Approval by EMA was more troublesome and adverse effects were judged not to adequately counterbalance the relatively small vantage in survival provided by treatment with neratinib. EMA has therefore limited use of neratinib in triple positive tumors, where it showed a greater efficacy. Collectively, our data, obtained in ER-/PR- HER2+ PDX, strongly indicate a great and long-lasting efficacy of neratinib even in trastuzumab-resistance and after progression and call for further evaluation of neratinib in advanced clinical settings.

We also evaluated neratinib in a luminal B PDX-SBR18, as single therapy or in combination with tamoxifen, the standard of care for luminal B tumors. Tumor

originating PDX-SBR18 already showed some HER2 expression (score 0/1+) and *in vivo* a clone with slightly higher HER2 expression was selected (score 2+). As partially expected, neratinib alone was totally ineffective as a single therapy, thus indicating that this luminal B tumor expresses HER2 but this is not the key pathway sustaining its proliferation. Of note, PDX-SBR18 has no active signaling down-stream other HER receptor, as indicated by no detection of pHER forms by western blotting; this of course limited neratinib action and underscores PDX-SBR18 reliance on different pathways. In combination with tamoxifen, though, neratinib slightly slowed tumor growth and increased survival to 1 cm^3 tumors with respect to tamoxifen as single agent. This effect was small, though significant, and this observation copes well with neratinib's greater efficacy in triple positive tumors rather than in HER2-positive only. Triple-positive tumors have been reported to be most likely to resist to endocrine or targeted therapies due to the fine crosstalk existing between RTKs and hormone receptors in breast normal and cancer cells. (Iancu et al., 2017). Ample preclinical and clinical justification for combinatorial therapy targeting both estrogen and HER2 pathways concurrently already exists (Mehta et al., 2014) and the little effect of the combination of tamoxifen and neratinib reported on luminal PDX-SBR18, indicate that a dual blockade could ameliorate prognosis of patients with tumors expressing both HER2 and hormone receptors.

Original scope of this work was to verify if PDX could constitute models of HER2 loss or even patient's avatar predicting loss of HER2 expression in patient's recurrences or metastasis. The latter is of course not applicable due to low take rates, long times required for PDX generation and low metastatic rates observed. We checked HER2 expression both on serial passages *in vivo* and on tumors grown after treatment with neratinib, but no abrupt loss of HER2 expression was registered. Hence, further studies will be needed to evaluate receptor discordance in PDXs: it should be noted that effects of tumor microenvironment and immune system are difficult to evaluate. A possibility for further studies would be to reconstitute immune system of immunodeficient mice or to directly administer cytokines to evaluate their effect on receptor discordance and on stability of PDX in general.

Conclusion

Our model of mice transgenic for human HER2 expression has shown that spontaneous or trastuzumab-induced loss of HER2 expression can progress towards a more aggressive phenotype, acquisition of EMT, increased stemness and metastatic potential, increased and but altered angiogenesis as well as resistance to targeted anti-HER2 therapies. Loss of HER2 expression and worst prognosis is observed in some human HER2-positive tumors as well. In this murine model, the study of transcriptome of cell lines with different HER2 expression has permitted us to identify pathways related to the modulation of this more malignant phenotype, which could represent a therapeutic target in case of HER2 loss; in this perspective, some indications for inhibition of PDGFR-B by sunitinib emerged. Further functional analysis based on transduction or silencing of significative genes individuated by transcriptomic analysis will help identifying drivers and therapeutic targets in HER2^{loss}.

On the other hand, the study of HER2-positive breast carcinoma patient derived xenografts with different HER2 expression highlighted a different mode of increased metastasis and resistance to targeted therapies without loss of HER2 expression. Resistance to trastuzumab in this model was overcome by treatment with neratinib. This drug was also moderately effective in combination with tamoxifen in slowing down growth of a PDX HER2-expressing (score 2+) but without HER2 amplification, thus clinically diagnosed as HER2-negative luminal B.

Bibliography

Abbas T, Dutta A (2009) p21 in cancer: intricate networks and multiple activities. Nat Rev Cancer 9:400–414

Alameddine RS, Otrock ZK, Awada A, Shamseddine A (2013) Crosstalk between HER2 signaling and angiogenesis in breast cancer: molecular basis, clinical applications and challenges. Curr Opin Oncol 25:313–324.

Al-Hajj M, Wicha MS, Benito-Hernandez A, Morrison SJ, Clarke MF (2003) Prospective identification of tumorigenic breast cancer cells. Proc Natl Acad Sci U S A 100:3983–3988.

Ali HR, Rueda OM, Chin SF, Curtis C, Dunning MJ, Aparicio SA, Caldas C. (2014) Genome-driven integrated classification of breast cancer validated in over 7,500 samples. Genome Biol. 15(8):431

Ananthi S, Lakshmi CNP, Atmika P, Anbarasu K, Mahalingam S (2018) Global Quantitative Proteomics reveal Deregulation of Cytoskeletal and Apoptotic Signalling Proteins in Oral Tongue Squamous Cell Carcinoma. Sci Rep 8:1567.

Anderson WF, Rosenberg PS, Prat A, Perou CM, Sherman ME (2014) How many etiological subtypes of breast cancer: two, three, four, or more? J Natl Cancer Inst 106.

Andrechek ER, Hardy WR, Siegel PM, Rudnicki MA, Cardiff RD, Muller WJ (2000) Amplification of the neu/erbB-2 oncogene in a mouse model of mammary tumorigenesis. Proc Natl Acad Sci U S A 97:3444–3449.

Arribas J, Baselga J, Pedersen K, Parra-Palau JL (2011) p95HER2 and breast cancer. Cancer Res 71:1515–1519.

Arteaga CL, Engelman JA (2014) ERBB receptors: from oncogene discovery to basic science to mechanism-based cancer therapeutics. Cancer Cell 25:282–303

Ashaie MA, Chowdhury EH (2016) Cadherins: The Superfamily Critically Involved in Breast Cancer. Curr Pharm Des 22:616–638

Aurilio G, Disalvatore D, Pruneri G, Bagnardi V, Viale G, Curigliano G, Adamoli L, Munzone E, Sciandivasci A, Vita F de, Goldhirsch A, Nolè F (2014) A meta-analysis of oestrogen receptor, progesterone receptor and human epidermal growth factor receptor 2 discordance between primary breast cancer and metastases. Eur J Cancer 50:277–289

Baselga J, Coleman RE, Cortés J, Janni W (2017) Advances in the management of HER2-positive early breast cancer. Crit Rev Oncol Hematol 119:113–122.

Bazley LA, Gullick WJ (2005) The epidermal growth factor receptor family. Endocr Relat Cancer 12 Suppl 1: S17-27.

Bieche I, Vacher S, Vallerand D, Richon S, Hatem R, Plater L de, Dahmani A, Némati F, Angevin E, Marangoni E, Roman-Roman S, Decaudin D, Dangles-Marie V (2014) Vasculature analysis of patient derived tumor xenografts using species-specific PCR assays: evidence of tumor endothelial cells and atypical VEGFA-VEGFR1/2 signalings. BMC Cancer 14:178.

Beach JR, Hussey GS, Miller TE, Chaudhury A, Patel P, Monslow J, Zheng Q, Keri RA, Reizes O, Bresnick AR, Howe PH, Egelhoff TT (2011) Myosin II isoform switching mediates invasiveness after TGF- -induced epithelial-mesenchymal transition. Proc Natl Acad Sci U S A 108:17991–17996.

Boggio K, Di Carlo E, Rovero S, Cavallo F, Quaglino E, Lollini PL, Nanni P, Nicoletti G, Wolf S, Musiani P, Forni G. (2000) Ability of systemic interleukin-12 to hamper progressive stages of mammary carcinogenesis in HER2/neu transgenic mice. Cancer Res. 60(2):359-64.

Bose R, Kavuri SM, Searleman AC, Shen W, Shen D, Koboldt DC, Monsey J, Goel N, Aronson AB, Li S, Ma CX, Ding L, Mardis ER, Ellis MJ (2013) Activating HER2 mutations in HER2 gene amplification negative breast cancer. Cancer Discov 3:224–237.

Bray F, Ferlay J, Soerjomataram I, Siegel RL, Torre LA, Jemal A (2018) Global cancer statistics 2018: GLOBOCAN estimates of incidence and mortality worldwide for 36 cancers in 185 countries. CA Cancer J Clin

Buyru N, Altinisik J, Ozdemir F, Demokan S, Dalay N (2009) Methylation profiles in breast cancer. Cancer Invest 27:307–312.

Canonici A, Gijsen M, Mullooly M, Bennett R, Bouguern N, Pedersen K, O'Brien NA, Roxanis I, Li J-L, Bridge E, Finn R, Siamon D, McGowan P, Duffy MJ, O'Donovan N, Crown J, Kong A (2013) Neratinib overcomes trastuzumab resistance in HER2 amplified breast cancer. Oncotarget 4:1592–1605.

Castagnoli L, Ghedini GC, Koschorke A, Triulzi T, Dugo M, Gasparini P, Casalini P, Palladini A, Iezzi M, Lamolinara A, Lollini PL, Nanni P, Chiodoni C, Tagliabue E, Pupa SM. (2017). Pathobiological implications of the d16HER2 splice variant for stemness and aggressiveness of HER2-positive breast cancer. Oncogene 36(12):1721-1732.

Castiglioni F, Tagliabue E, Campiglio M, Pupa SM, Balsari A, Ménard S (2006) Role of exon-16-deleted HER2 in breast carcinomas. Endocr Relat Cancer 13:221–232.

Chang H, Liu Y, Xue M, Liu H, Du S, Zhang L, Wang P (2016) Synergistic action of master transcription factors controls epithelial-to-mesenchymal transition. Nucleic Acids Res 44:2514–2527

Chen S, Qiu Y, Guo P, Pu T, Feng Y, Bu H (2018) FGFR1 and HER1 or HER2 co-amplification in breast cancer indicate poor prognosis. Oncol Lett 15:8206–8214.

Connell CM, Doherty GJ (2017) Activating HER2 mutations as emerging targets in multiple solid cancers. ESMO Open 2.

Creedon H, Gómez-Cuadrado L, Tarnauskait Ž, Balla J, Canel M, MacLeod KG, Serrels B, Fraser C, Unciti-Broceta A, Tracey N, Le Bihan T, Klinowska T, Sims AH, Byron A, Brunton VG (2016) Identification of novel pathways linking epithelial-to-mesenchymal transition with resistance to HER2-targeted therapy. Oncotarget 7:11539–11552.

De Giovanni C, Nicoletti G, Quaglino E, Landuzzi L, Palladini A, Ianzano ML, Dall'Ora M, Grosso V, Ranieri D, Laranga R, Croci S, Amici A, Penichet ML, Iezzi M, Cavallo F, Nanni P, Lollini PL. (2014) Vaccines against human HER2 prevent mammary carcinoma in mice transgenic for human HER2. Breast Cancer Res. 23;16(1): R10

Dieci MV, Barbieri E, Piacentini F, Ficarra G, Bettelli S, Dominici M, Conte PF, Guarneri V (2013) Discordance in receptor status between primary and recurrent breast cancer has a prognostic impact: a single-institution analysis. Ann Oncol 24:101–108.

Di Carlo E1, Modesti A, Castrilli G, Landuzzi L, Allione A, de Giovanni C, Musso T, Musiani P. (1997) Interleukin 6 gene-transfected mouse mammary adenocarcinoma: tumour cell growth and metastatic potential. J Pathol. 182(1):76-85.

Dobrolecki LE, Airhart SD, Alferez DG, Aparicio S, Behbod F, Bentires-Alj M, Brisken C, Bult CJ, Cai S, Clarke RB, Dowst H, Ellis MJ, Gonzalez-Suarez E, Iggo RD, Kabos P,

Li S, Lindeman GJ, Marangoni E, McCoy A, Meric-Bernstam F, Piwnica-Worms H, Poupon M-F, Reis-Filho J, Sartorius CA, Scabia V, Sflomos G, Tu Y, Vaillant F, Visvader JE, Welm A, Wicha MS, Lewis MT (2016) Patient-derived xenograft (PDX) models in basic and translational breast cancer research. Cancer Metastasis Rev 35:547–573.

Duru N, Candas D, Jiang G, Li JJ (2013) Breast cancer adaptive resistance: HER2 and cancer stem cell repopulation in a heterogeneous tumor society. J Cancer Res Clin Oncol 140:1–14.

Eccles SA (2011) The epidermal growth factor receptor/Erb-B/HER family in normal and malignant breast biology. Int J Dev Biol 55:685–696.

El-Rehim HAA, El-Arnaouty MB (2004) Properties and biocompatibility of polypropylene graft copolymer films. J Biomed Mater Res Part B Appl Biomater 68:209–215.

Emde A, Köstler WJ, Yarden Y (2012) Therapeutic strategies and mechanisms of tumorigenesis of HER2-overexpressing breast cancer. Crit Rev Oncol Hematol 84 Suppl 1:e49-57.

Escrivá-de-Romaní S, Arumí M, Bellet M, Saura C (2018) HER2-positive breast cancer: Current and new therapeutic strategies. Breast 39:80–88.

Fallah Y, Brundage J, Allegakoen P, Shajahan-Haq AN (2017) MYC-Driven Pathways in Breast Cancer Subtypes. Biomolecules 7.

Fernández-Nogueira P, Bragado P, Almendro V, Ametller E, Rios J, Choudhury S, Mancino M, Gascón P (2016) Differential expression of neurogenes among breast cancer subtypes identifies high risk patients. Oncotarget 7:5313–5326.

Finkle D, Quan ZR, Asghari V, Kloss J, Ghaboosi N, Mai E, Wong WL, Hollingshead P, Schwall R, Koeppen H, Erickson S (2004) HER2-targeted therapy reduces incidence and progression of midlife mammary tumors in female murine mammary tumor virus huHER2-transgenic mice. Clin Cancer Res 10:2499–2511

Freudenberg JA, Wang Q, Katsumata M, Drebin J, Nagatomo I, Greene MI (2009) The role of HER2 in early breast cancer metastasis and the origins of resistance to HER2-targeted therapies. Exp Mol Pathol 87:1–11.

Furth PA (2014) STAT signaling in different breast cancer sub-types. Mol Cell Endocrinol 382:612–615

Garrett JT, Arteaga CL (2011) Resistance to HER2-directed antibodies and tyrosine kinase inhibitors: mechanisms and clinical implications. Cancer Biol Ther 11:793–800

Gopinathan G, Milagre C, Pearce OMT, Reynolds LE, Hodivala-Dilke K, Leinster DA, Zhong H, Hollingsworth RE, Thompson R, Whiteford JR, Balkwill F (2015) Interleukin-6 Stimulates Defective Angiogenesis. Cancer Res 75:3098–3107.

Guen VJ, Chavarria TE, Kröger C, Ye X, Weinberg RA, Lees JA (2017) EMT programs promote basal mammary stem cell and tumor-initiating cell stemness by inducing primary ciliogenesis and Hedgehog signaling. Proc Natl Acad Sci U S A 114:E10532-E10539

Guy CT, Webster MA, Schaller M, Parsons TJ, Cardiff RD, Muller WJ (1992) Expression of the neu protooncogene in the mammary epithelium of transgenic mice induces metastatic disease. Proc Natl Acad Sci U S A 89:10578–10582

Harari D, Yarden Y (2000) Molecular mechanisms underlying ErbB2/HER2 action in breast cancer. Oncogene 19:6102–6114.

Hoadley KA, Yau C, Wolf DM, Cherniack AD, Tamborero D, Ng S, Leiserson MDM, Niu B, McLellan MD, Uzunangelov V, Zhang J, Kandoth C, Akbani R, Shen H, Omberg L, Chu A, Margolin AA, Van't Veer LJ, Lopez-Bigas N, Laird PW, Raphael BJ, Ding L, Robertson AG, Byers LA, Mills GB, Weinstein JN, van Waes C, Chen Z, Collisson EA, Benz CC, Perou CM, Stuart JM (2014) Multiplatform analysis of 12 cancer types reveals molecular classification within and across tissues of origin. Cell 158:929–944.

Holen I, Speirs V, Morrissey B, Blyth K (2017) *In vivo* models in breast cancer research: progress, challenges and future directions. Dis Model Mech 10:359–371.

Hosper NA, van den Berg PP, Rond S de, Popa ER, Wilmer MJ, Masereeuw R, Bank RA (2013) Epithelial-to-mesenchymal transition in fibrosis: collagen type I expression is

highly upregulated after EMT, but does not contribute to collagen deposition. Exp Cell Res 319:3000–3009

Hsu JL, Hung M-C (2016) The role of HER2, EGFR, and other receptor tyrosine kinases in breast cancer. Cancer Metastasis Rev 35:575–588.

Huguet EL, McMahon JA, McMahon AP, Bicknell R, Harris AL (1994) Differential expression of human Wnt genes 2, 3, 4, and 7B in human breast cell lines and normal and disease states of human breast tissue. Cancer Res 54:2615–2621

Hurvitz SA, Gelmon KA, Tolaney SM (2017) Optimal Management of Early and Advanced HER2 Breast Cancer. Am Soc Clin Oncol Educ Book 37:76–92.

Hynes NE, MacDonald G (2009) ErbB receptors and signaling pathways in cancer. Curr Opin Cell Biol 21:177–184.

Iancu G, Vasile D, Iancu RC, Davi oiu DV (2017) "Triple positive" breast cancer - a novel category? Rom J Morphol Embryol 58:21–26.

Iyer SV, Dange PP, Alam H, Sawant SS, Ingle AD, Borges AM, Shirsat NV, Dalal SN, Vaidya MM (2013) Understanding the role of keratins 8 and 18 in neoplastic potential of breast cancer derived cell lines. PLoS ONE 8:e53532.

Kalluri R, Weinberg RA (2009) The basics of epithelial-mesenchymal transition. J Clin Invest 119:1420–1428

Kennecke H, Yerushalmi R, Woods R, Cheang MCU, Voduc D, Speers CH, Nielsen TO, Gelmon K (2010) Metastatic behavior of breast cancer subtypes. J Clin Oncol 28:3271–3277.

Khan IA, Yoo BH, Rak J, Rosen KV (2017) Mek activity is required for ErbB2 expression in breast cancer cells detached from the extracellular matrix. Oncotarget 8:105383–105396.

Klahan S, Wu M-S, Hsi E, Huang C-C, Hou M-F, Chang W-C (2014) Computational analysis of mRNA expression profiles identifies the ITG family and PIK3R3 as crucial genes for regulating triple negative breast cancer cell migration. Biomed Res Int 2014:536591.

Korkaya H, Kim G-I, Davis A, Malik F, Henry NL, Ithimakin S, Quraishi AA, Tawakkol N, D'Angelo R, Paulson AK, Chung S, Luther T, Paholak HJ, Liu S, Hassan KA, Zen Q, Clouthier SG, Wicha MS (2012) Activation of an IL6 inflammatory loop mediates trastuzumab resistance in HER2+ breast cancer by expanding the cancer stem cell population. Mol Cell 47:570–584.

Kotiyal S, Bhattacharya S (2014) Breast cancer stem cells, EMT and therapeutic targets. Biochem Biophys Res Commun 453:112–116.

Loibl S, Gianni L (2017) HER2-positive breast cancer. The Lancet 389:2415–2429.

König A, Vilsmaier T, Rack B, Friese K, Janni W, Jeschke U, Andergassen U, Trapp E, Jückstock J, Jäger B, Alunni-Fabbroni M, Friedl T, Weissenbacher T (2016) Determination of Interleukin-4, -5, -6, -8 and -13 in Serum of Patients with Breast Cancer Before Treatment and its Correlation to Circulating Tumor Cells. Anticancer Res 36:3123–3130

Lakhtakia R, Aljarrah A, Furrukh M, Ganguly SS (2017) Epithelial Mesenchymal Transition (EMT) in Metastatic Breast Cancer in Omani Women. Cancer Microenviron 10:25–37.

Lambert AW, Wong CK, Ozturk S, Papageorgis P, Raghunathan R, Alekseyev Y, Gower AC, Reinhard BM, Abdolmaleky HM, Thiagalingam S (2016) Tumor Cell-Derived Periostin Regulates Cytokines That Maintain Breast Cancer Stem Cells. Mol Cancer Res 14:103–113.

Lehtinen L, Vainio P, Wikman H, Huhtala H, Mueller V, Kallioniemi A, Pantel K, Kronqvist P, Kallioniemi O, Carpèn O, Iljin K (2017) PLA2G7 associates with hormone receptor negativity in clinical breast cancer samples and regulates epithelial-mesenchymal transition in cultured breast cancer cells. J Pathol Clin Res 3:123–138.

Marchini C, Gabrielli F, Iezzi M, Zenobi S, Montani M, Pietrella L, Kalogris C, Rossini A, Ciravolo V, Castagnoli L, Tagliabue E, Pupa SM, Musiani P, Monaci P, Menard S, Amici A (2011) The human splice variant 16HER2 induces rapid tumor onset in a reporter transgenic mouse. PLoS ONE 6:e18727.

Mackay A, Jones C, Dexter T, Silva RLA, Bulmer K, Jones A, Simpson P, Harris RA, Jat PS, Neville AM, Reis LFL, Lakhani SR, O'Hare MJ (2003) cDNA microarray analysis of

genes associated with ERBB2 (HER2/neu) overexpression in human mammary luminal epithelial cells. Oncogene 22:2680–2688.

Mehta A, Tripathy D (2014) Co-targeting estrogen receptor and HER2 pathways in breast cancer. Breast 23:2–9.

Ménard S, Casalini P, Campiglio M, Pupa SM, Tagliabue E (2004) Role of HER2/neu in tumor progression and therapy. Cell Mol Life Sci 61:2965–2978.

Moasser MM (2007) Targeting the function of the HER2 oncogene in human cancer therapeutics. Oncogene 26:6577–6592.

Moasser MM (2007) The oncogene HER2: its signaling and transforming functions and its role in human cancer pathogenesis. Oncogene 26:6469–6487.

Morel A-P, Lièvre M, Thomas C, Hinkal G, Ansieau S, Puisieux A (2008) Generation of breast cancer stem cells through epithelial-mesenchymal transition. PLoS ONE 3:e2888

Mujoo K, Choi B-K, Huang Z, Zhang N, An Z (2014) Regulation of ERBB3/HER3 signaling in cancer. Oncotarget 5:10222–10236.

Muller WJ, Sinn E, Pattengale PK, Wallace R, Leder P (1988) Single-step induction of mammary adenocarcinoma in transgenic mice bearing the activated c-neu oncogene. Cell 54:105–115

Murria R, Palanca S, Juan I de, Egoavil C, Alenda C, García-Casado Z, Juan MJ, Sánchez AB, Santaballa A, Chirivella I, Segura Á, Hervás D, Llop M, Barragán E, Bolufer P (2015) Methylation of tumor suppressor genes is related with copy number aberrations in breast cancer. Am J Cancer Res 5:375–385

Nami B, Wang Z (2017) HER2 in Breast Cancer Stemness: A Negative Feedback Loop towards Trastuzumab Resistance. Cancers (Basel) 9.

Nanni P1, Pupa SM, Nicoletti G, De Giovanni C, Landuzzi L, Rossi I, Astolfi A, Ricci C, De Vecchi R, Invernizzi AM, Di Carlo E, Musiani P, Forni G, Menard S, Lollini PL. (2000) p185(neu) protein is required for tumor and anchorage-independent growth, not for cell proliferation of transgenic mammary carcinoma. Int J Cancer. 87(2):186-94.

Nanni P, Nicoletti G, Palladini A, Croci S, Murgo A, Ianzano ML, Grosso V, Stivani V, Antognoli A, Lamolinara A, Landuzzi L, di Tomaso E, Iezzi M, De Giovanni C, Lollini PL. (2012) Multiorgan metastasis of human HER-2+ breast cancer in Rag2-/-;Il2rg-/- mice and treatment with PI3K inhibitor. PLoS One. 7(6):e39626

Ng CKY, Martelotto LG, Gauthier A, Wen H-C, Piscuoglio S, Lim RS, Cowell CF, Wilkerson PM, Wai P, Rodrigues DN, Arnould L, Geyer FC, Bromberg SE, Lacroix-Triki M, Penault-Llorca F, Giard S, Sastre-Garau X, Natrajan R, Norton L, Cottu PH, Weigelt B, Vincent-Salomon A, Reis-Filho JS (2015) Intra-tumor genetic heterogeneity and alternative driver genetic alterations in breast cancers with heterogeneous HER2 gene amplification. Genome Biol 16:107.

Nigam A (2013) Breast cancer stem cells, pathways and therapeutic perspectives 2011. Indian J Surg 75:170–180.

Niikura N, Liu J, Hayashi N, Mittendorf EA, Gong Y, Palla SL, Tokuda Y, Gonzalez-Angulo AM, Hortobagyi GN, Ueno NT (2012) Loss of human epidermal growth factor receptor 2 (HER2) expression in metastatic sites of HER2-overexpressing primary breast tumors. J Clin Oncol 30:593–599.

Nuciforo P, Radosevic-Robin N, Ng T, Scaltriti M (2015) Quantification of HER family receptors in breast cancer. Breast Cancer Res 17:53.

Ochoa AE, Choi W, Su X, Siefker-Radtke A, Czerniak B, Dinney C, McConkey DJ (2016) Specific micro-RNA expression patterns distinguish the basal and luminal subtypes of muscle-invasive bladder cancer. Oncotarget 7:80164–80174

Palladini A, Nicoletti G, Lamolinara A, Dall'Ora M, Balboni T, Ianzano ML, Laranga R, Landuzzi L, Giusti V, Ceccarelli C, Santini D, Taffurelli M, Di Oto E, Asioli S, Amici A, Pupa SM, Giovanni C de, Tagliabue E, Iezzi M, Nanni P, Lollini P-L (2017) HER2 isoforms co-expression differently tunes mammary tumor phenotypes affecting onset, vasculature and therapeutic response. Oncotarget 8:54444–54458.

Pang H, Rowan BG, Al-Dhaheri M, Faber LE (2004) Epidermal growth factor suppresses induction by progestin of the adhesion protein desmoplakin in T47D breast cancer cells. Breast Cancer Res 6:R239-45.

Prat A, Pineda E, Adamo B, Galván P, Fernández A, Gaba L, Díez M, Viladot M, Arance A, Muñoz M (2015) Clinical implications of the intrinsic molecular subtypes of breast cancer. Breast 24 Suppl 2:S26-35.

Praveen Kumar VR, Sehgal P, Thota B, Patil S, Santosh V, Kondaiah P (2014) Insulin like growth factor binding protein 4 promotes GBM progression and regulates key factors involved in EMT and invasion. J Neurooncol 116:455–464

Prenzel T, Begus-Nahrmann Y, Kramer F, Hennion M, Hsu C, Gorsler T, Hintermair C, Eick D, Kremmer E, Simons M, Beissbarth T, Johnsen SA (2011) Estrogen-dependent gene transcription in human breast cancer cells relies upon proteasome-dependent monoubiquitination of histone H2B. Cancer Res 71:5739–5753.

Prieto-García E, Díaz-García CV, García-Ruiz I, Agulló-Ortuño MT (2017) Epithelial-to-mesenchymal transition in tumor progression. Med Oncol 34:122.

Prieto-García E, Díaz-García CV, García-Ruiz I, Agulló-Ortuño MT (2017) Epithelial-to-mesenchymal transition in tumor progression. Med Oncol 34:122

Rexer BN, Arteaga CL (2012) Intrinsic and acquired resistance to HER2-targeted therapies in HER2 gene-amplified breast cancer: mechanisms and clinical implications. Crit Rev Oncog 17:1–16

Roskoski R (2014) The ErbB/HER family of protein-tyrosine kinases and cancer. Pharmacol Res 79:34–74.

Ruan K, Bao S, Ouyang G (2009) The multifaceted role of periostin in tumorigenesis. Cell Mol Life Sci 66:2219–2230.

Ruiz I, Vicario R, Morancho B, Morales C.B., Arenas E. J:, Herter S., Freimoser-Grundschober A., Somadin J., Sam J., Ast O., Barriocanal A.M., Luque A., Escorihuela M., Varela I., Cuartas I., Nuciforo P., Fasani R., Peg V., Rubio I., Cortes J., Serra V., Escrivia-de-Romani S., Sperinde J., Chenna A., Huang W., Winslow J., Albanell J., Seoane J., Scaltriti M., Baselga J., Tabernero J., Umana P., Bacac M.,S C., Klein C., Arribas J. (2018) p95HER2-T cell bispecific antibody for breast cancer treatment Sci. Transl. Med. 10

Sangaletti S, Tripodo C, Santangelo A, Castioni N, Portararo P, Gulino A, Botti L, Parenza M, Cappetti B, Orlandi R, Tagliabue E, Chiodoni C, Colombo MP (2016) Mesenchymal Transition of High-Grade Breast Carcinomas Depends on Extracellular Matrix Control of Myeloid Suppressor Cell Activity. Cell Rep 17:233–248

Sanguinetti A, Santini D, Bonafè M, Taffurelli M, Avenia N (2015) Interleukin-6 and pro inflammatory status in the breast tumor microenvironment. World J Surg Oncol 13:129.

Scheel C, Eaton EN, Li SH-J, Chaffer CL, Reinhardt F, Kah K-J, Bell G, Guo W, Rubin J, Richardson AL, Weinberg RA (2011) Paracrine and autocrine signals induce and maintain mesenchymal and stem cell states in the breast. Cell 145:926–940.

Schmidt M, Thomssen C, Untch M (2016) Intrinsic Subtypes of Primary Breast Cancer--Gene Expression Analysis. Oncol Res Treat 39:102–110.

Schrijver WAME, Suijkerbuijk KPM, van Gils CH, van der Wall E, Moelans CB, van Diest PJ (2018) Receptor Conversion in Distant Breast Cancer Metastases: A Systematic Review and Meta-analysis. J Natl Cancer Inst 110:568–580 Sergina NV, Moasser MM (2007) The HER family and cancer: emerging molecular mechanisms and therapeutic targets. Trends Mol Med 13:527–534.

Sesé M, Fuentes P, Esteve-Codina A, Béjar E, McGrail K, Thomas G, Aasen T, Ramón Y Cajal S (2017) Hypoxia-mediated translational activation of ITGB3 in breast cancer cells enhances TGF- signaling and malignant features *in vitro* and *in vivo*. Oncotarget 8:114856–114876

Shi J-W, Liu W, Zhang T-T, Wang S-C, Lin X-L, Li J, Jia J-S, Sheng H-F, Yao Z-F, Zhao W-T, Zhao Z-L, Xie R-Y, Yang S, Gao F, Fan Q-R, Zhang M-Y, Yue M, Yuan J, Gu W-W, Yao K-T, Xiao D (2013) The enforced expression of c-Myc in pig fibroblasts triggers mesenchymal-epithelial transition (MET) via F-actin reorganization and RhoA/Rock pathway inactivation. Cell Cycle 12:1119–1127.

Siegel RL, Miller KD, Jemal A (2017) Cancer Statistics, 2017

Sinn H-P, Kreipe H (2013) A Brief Overview of the WHO Classification of Breast Tumors, 4th Edition, Focusing on Issues and Updates from the 3rd Edition. Breast Care (Basel) 8:149–154.

Sivrikoz ON, Doganay L, Sivrikoz UK, Karaarslan S, Sanal SM (2013) Distribution of CXCR4 and -catenin expression pattern in breast cancer subtypes and their relationship to axillary nodal involvement. Pol J Pathol 64:253–259

Slamon DJ, Clark GM, Wong SG, Levin WJ, Ullrich A, McGuire WL (1987) Human breast cancer: correlation of relapse and survival with amplification of the HER-2/neu oncogene. Science 235:177–182

Slattery ML, Herrick JS, Torres-Mejia G, John EM, Giuliano AR, Hines LM, Stern MC, Baumgartner KB, Presson AP, Wolff RK (2014) Genetic variants in interleukin genes are associated with breast cancer risk and survival in a genetically admixed population: the Breast Cancer Health Disparities Study. Carcinogenesis 35:1750–1759.

Sørlie T, Perou CM, Tibshirani R, Aas T, Geisler S, Johnsen H, Hastie T, Eisen MB, van de Rijn M, Jeffrey SS, Thorsen T, Quist H, Matese JC, Brown PO, Botstein D, Lønning PE, Børresen-Dale AL (2001) Gene expression patterns of breast carcinomas distinguish tumor subclasses with clinical implications. Proc Natl Acad Sci U S A 98:10869–10874.

Sperinde J, Jin X, Banerjee J, Penuel E, Saha A, Diedrich G, Huang W, Leitzel K, Weidler J, Ali SM, Fuchs E-M, Singer CF, Köstler WJ, Bates M, Parry G, Winslow J, Lipton A (2010) Quantitation of p95HER2 in paraffin sections by using a p95-specific antibody and correlation with outcome in a cohort of trastuzumab-treated breast cancer patients. Clin Cancer Res 16:4226–4235.

Stern DF (2008) ERBB3/HER3 and ERBB2/HER2 duet in mammary development and breast cancer. J Mammary Gland Biol Neoplasia 13:215–223.

Sundqvist A, Morikawa M, Ren J, Vasilaki E, Kawasaki N, Kobayashi M, Koinuma D, Aburatani H, Miyazono K, Heldin C-H, van Dam H, Dijke P ten (2018) JUNB governs a feed-forward network of TGF signaling that aggravates breast cancer invasion. Nucleic Acids Res 46:1180–1195.

Tassi E, Al-Attar A, Aigner A, Swift MR, McDonnell K, Karavanov A, Wellstein A (2001) Enhancement of fibroblast growth factor (FGF) activity by an FGF-binding protein. J Biol Chem 276:40247–40253

Timmer M, Werner J-M, Röhn G, Ortmann M, Blau T, Cramer C, Stavrinou P, Krischek B, Mallman P, Goldbrunner R (2017) Discordance and Conversion Rates of

Progesterone-, Estrogen-, and HER2/neu-Receptor Status in Primary Breast Cancer and Brain Metastasis Mainly Triggered by Hormone Therapy. Anticancer Res 37:4859–4865.

Unni N, Sudhan DR, Arteaga CL (2018) Neratinib: Inching Up on the Cure Rate of HER2+ Breast Cancer Clin Cancer Res 24:3483–3485.

Varley KE, Gertz J, Roberts BS, Davis NS, Bowling KM, Kirby MK, Nesmith AS, Oliver PG, Grizzle WE, Forero A, Buchsbaum DJ, LoBuglio AF, Myers RM (2014) Recurrent read-through fusion transcripts in breast cancer. Breast Cancer Res Treat 146:287–297.

Velasco-Velázquez MA, Homsi N, La Fuente M de, Pestell RG (2012) Breast cancer stem cells. Int J Biochem Cell Biol 44:573–577.

Veronica Giusti (2015) Perdita di HER2 e resistenza alle terapie mirate nel carcinoma mammario HER2 positivo, Master degree thesis

Wang R-X, Chen S, Jin X, Chen C-M, Shao Z-M (2017) Weekly paclitaxel plus carboplatin with or without trastuzumab as neoadjuvant chemotherapy for HER2-positive breast cancer: loss of HER2 amplification and its impact on response and prognosis. Breast Cancer Res Treat 161:259–267.

Weigand A, Boos AM, Tasbihi K, Beier JP, Dalton PD, Schrauder M, Horch RE, Beckmann MW, Strissel PL, Strick R (2016) Selective isolation and characterization of primary cells from normal breast and tumors reveal plasticity of adipose derived stem cells. Breast Cancer Res 18:32.

Weinstein IB, Joe A (2008) Oncogene addiction. Cancer Res 68:3077-80; discussion 3080. doi: 10.1158/0008-5472.CAN-07-3293

Weinstein EJ, Kitsberg DI, Leder P (2000) A mouse model for breast cancer induced by amplification and overexpression of the neu promoter and transgene. Mol Med 6:4–16

Wong AL, Lee SC. (2012) Mechanisms of Resistance to Trastuzumab and Novel Therapeutic Strategies in HER2-Positive Breast Cancer. Int J Breast Cancer. 2012:415170

Wong SHM, Fang CM, Chuah L-H, Leong CO, Ngai SC (2018) E-cadherin: Its dysregulation in carcinogenesis and clinical implications. Crit Rev Oncol Hematol 121:11–22

Xie J, Yang Y, Sun J, Jiao Z, Zhang H, Chen J (2018) STEAP1 Inhibits Breast Cancer Metastasis and Is Associated With Epithelial-Mesenchymal Transition Procession. Clin Breast Cancer

Yan M, Parker BA, Schwab R, Kurzrock R (2014) HER2 aberrations in cancer: implications for therapy. Cancer Treat Rev 40:770–780.

Yarden Y (2001) Biology of HER2 and its importance in breast cancer. Oncology 61 Suppl 2:1–13.

Yarden Y, Sliwkowski MX (2001) Untangling the ErbB signalling network. Nat Rev Mol Cell Biol 2:127–137.

Yersal O, Barutca S (2014) Biological subtypes of breast cancer: Prognostic and therapeutic implications. World J Clin Oncol 5:412–424.

Zhang W, Ge Y, Cheng Q, Zhang Q, Fang L, Zheng J (2018) Decorin is a pivotal effector in the extracellular matrix and tumour microenvironment. Oncotarget 9:5480–5491

Zhang Y, Zou X, Qian W, Weng X, Zhang L, Zhang L, Wang S, Cao X, Ma L, Wei G, Wu Y, Hou Z (2018) Enhanced PAPSS2/VCAN sulfation axis is essential for Snail-mediated breast cancer cell migration and metastasis. Cell Death Differ

Zhang Y, Yang H-Y, Zhang X-C, Yang H, Tsai M, Lee M-H (2004) Tumor suppressor ARF inhibits HER-2/neu-mediated oncogenic growth. Oncogene 23:7132–7143.

Zhang Y, Zhang G, Li J, Tao Q, Tang W (2010) The expression analysis of periostin in human breast cancer. J Surg Res 160:102–106